

MUSIC VS NOISE: A COMPARISON OF LOUDNESS ESTIMATES

A. MIŚKIEWICZ and A. RAKOWSKI

Chopin Academy of Music
(00-368 Warszawa, Okólnik 2)

The aim of this study was to examine whether loudness estimates of music are performed according to the same principles as loudness judgements of non-musical sounds. For this purpose loudness estimates of short musical passages were compared with those of noise signals. Spectral energy distribution of noise was matched to that of music. The results show that loudness judgements of music and noise agree reasonably well. This finding suggests that loudness of musical tones may also be determined by means of objective methods for loudness calculation, which are employed in measurements of non-musical sounds.

1. Introduction

Variations of loudness in music are indicated by dynamic marks or levels (*pianissimo*, *piano*, *mezzoforte*, *forte* etc.). It has been demonstrated in a number of studies that, in most instruments, tones played at different dynamic levels – from “very soft” to “very loud” – differ not only in sound pressure, but also in spectral envelope [1, 2, 6, 8, 11]. When a tone is played louder, the amplitude of its higher-frequency partials increases relative to that of the lower frequency partials. Changes of the spectral envelope due to dynamic gradations are greatest in woodwinds and brass instruments. An example of sound spectra measured at different playing levels is given in Fig. 1. The higher harmonics of a French horn tone played *pianissimo* are very weak. As the dynamic level increases, so too does the sound level of the higher harmonics relative to that of the fundamental.

The musical dynamic marks do not specify loudness directly as a psychoacoustical magnitude. In common usage, *pianissimo* means “very soft”, *piano* “soft”, *mezzoforte* “moderately loud”, and so on. In fact, the level of loudness corresponding to a given dynamic mark varies with respect to the instrument played [9, 10].

REINECKE [11] pointed out that spectral changes of sound associated with changes in playing level provide a cue for recognizing the dynamic level at which music is performed. This may be easily demonstrated by means of musical recordings. A musically

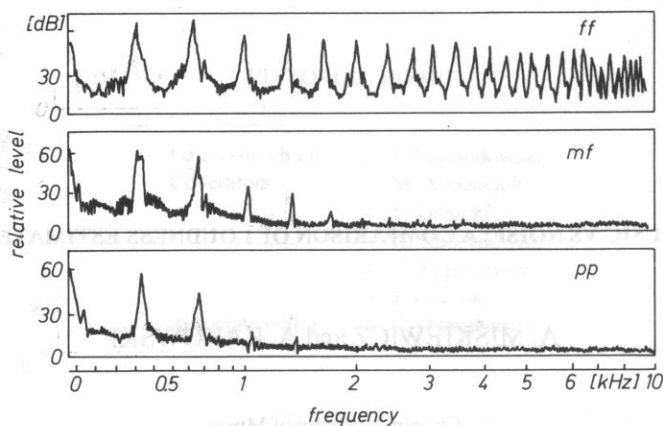


Fig. 1. Sound spectra of a horn at different playing levels, played note: F4, (from [8]).

competent listener is able to recognize the dynamic levels of music regardless the loudness level at which a recording is played back.

A great deal of research work has been carried out to examine the relationship between physical characteristics of sound and the magnitude of loudness. Investigations of loudness published so far have been carried out with non-musical stimuli. In the case of musical sounds, uncertainty arises as to whether loudness estimates of musical tones follow the same principles as loudness judgements of non-musical sounds. The difference between loudness evaluation of musical and non-musical sounds might be cognitive in origin, connected with the specific way in which the dynamic relations of music are perceived. When a musician is asked to judge the loudness of a passage of music, his responses might be influenced not only by the one-dimensional sensation of loudness, but also by implied musical dynamic levels.

The present experiment was conducted to examine whether any systematic differences occur between loudness judgments of musical and non-musical sounds. For this purpose loudness estimates of short musical passages were compared with loudness estimates of noise stimuli.



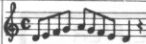


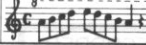
Loudness may be estimated from physical sound parameters. The validity of loudness calculation methods has not yet been tested for musical sounds. The present study provides data on the question of whether, or to what extent, methods for determining the loudness of noise may be applied to the tones of musical instruments.

2. Experimental procedure

Thirty music students estimated the loudness of short musical passages, wide-band noise with various spectral envelopes, and 1/3-octave band noise centered at 1 kHz. All stimuli were recorded on tape.

The musical passages were scale segments (see Table 1) played in various pitch registers on a viola, a clarinet and a trumpet. Three dynamic marks were used: pianis-

Table 1. Sound pressure levels of musical passages played back through a loudspeaker in the listening room.

scale segments		sound pressure level [dB SPL]								
		viola			clarinet			trumpet		
		pp	mf	ff	pp	mf	ff	pp	mf	ff
D ₃		63.7	71.6	74.9						
A ₃		66.0	74.2	77.0				65.4	77.8	84.5
D ₄		60.5	69.4	72.0	67.3	74.1	78.2	68.4	78.3	85.2
A ₄		58.1	65.1	67.3	66.9	74.7	79.6	70.9	81.5	87.3
D ₅					74.9	80.0	82.7	72.6	83.0	88.4
A ₅					74.5	78.5	82.1			

simo, mezzoforte and fortissimo. Recordings of musical examples were made in a live studio (reverberation time: 0.9–1.1 s in the range 250–4000 Hz), with a Studer A 810 tape machine. The cardioid condenser microphone (Neumann KM 84) used for recording was placed at a distance of 1.5 m from the performer.

The spectral energy distribution of the musical signals was analysed by means of apparatus shown in Fig. 2. The analysis involved measuring the sound pressure levels in 1/3-octave bands.

Next, wide-band noises were recorded, whose spectral energy distribution (sound pressure level in 1/3 octave bands) was matched to that of musical stimuli. A Brüel & Kjaer 5537 spectrum shaper was used for this purpose. Each noise matched one of the musical examples. The corresponding musical and noise signals had the same duration (approximately 4 seconds).

The experiment was carried out in individual listening sessions, by 30 subjects. The listeners judged loudness by the method of absolute magnitude estimation [4, 16], assigning to each of the stimuli a number which indicated the subjective magnitude of loudness. There was no limitation on the range of numbers: any positive number that seemed to be appropriate could be used. Subjects were told to concentrate on each judgment individually and not to be concerned with numbers assigned to preceding tones. Listeners had only 5 seconds between trials during which they wrote down the number on a prepared form. A relatively short time was chosen to minimize the probability of listeners judging stimuli relative to each other.

The stimuli were played back through a loudspeaker in a listening room. At the beginning of each listening session, prior to the main experiment, a preliminary test was presented in order to investigate whether the listeners performed loudness judgments in a similar way as reported in the literature. The test comprised eleven 1-second stimuli (1/3-octave band noises centered at 1 kHz), presented at sound pressure levels covering the range 50–90 dB SPL in 4-dB steps. The sequence of sound pressure levels was random and different for each listener.

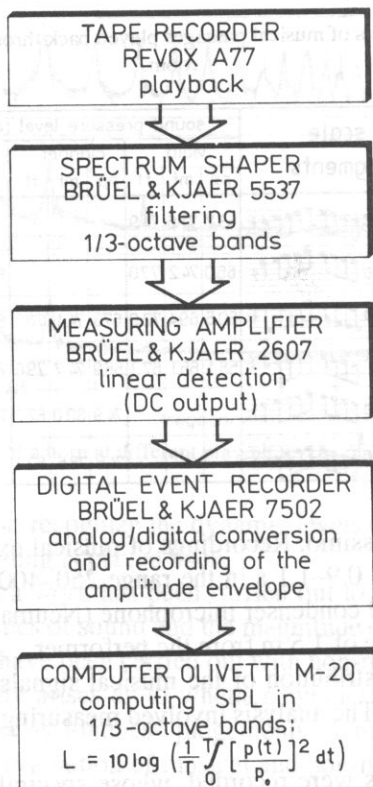


Fig. 2. Block diagram of apparatus used for measuring sound spectra of musical recordings.

The main test consisted of 3 series (viola, clarinet and trumpet) of 12 scale segments (4 pitch registers at 3 dynamic levels) and 3 series of the corresponding noise signals. The order of scale segments in each musical series was random (different for each listener) as was the order of series in each listening session.

It has been demonstrated in the literature that loudness estimates are susceptible to serial effects [e.g. 3, 5, 15]. In order to eliminate this source of bias, the sequence of noise signals within a series always replicated that of the corresponding musical stimuli. The whole test was presented to subjects only once and a listening session lasted about 25 minutes.

Table 1 specifies the sound pressure levels of stimuli presented in all six series. The sound pressure levels measured in 1/3-octave bands are shown in Figs. 3–5.

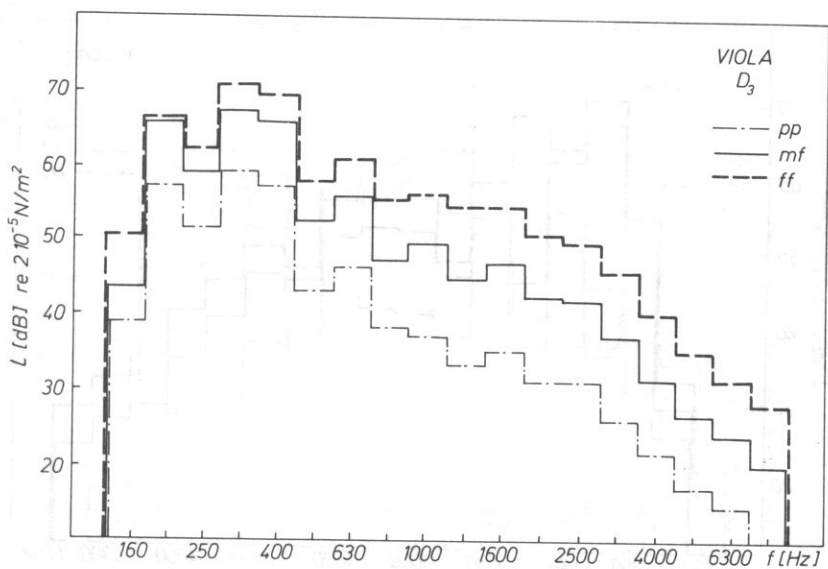


Fig. 3a. Sound pressure levels of scale segments D_3 played on a viola, measured in 1/3-octave bands.

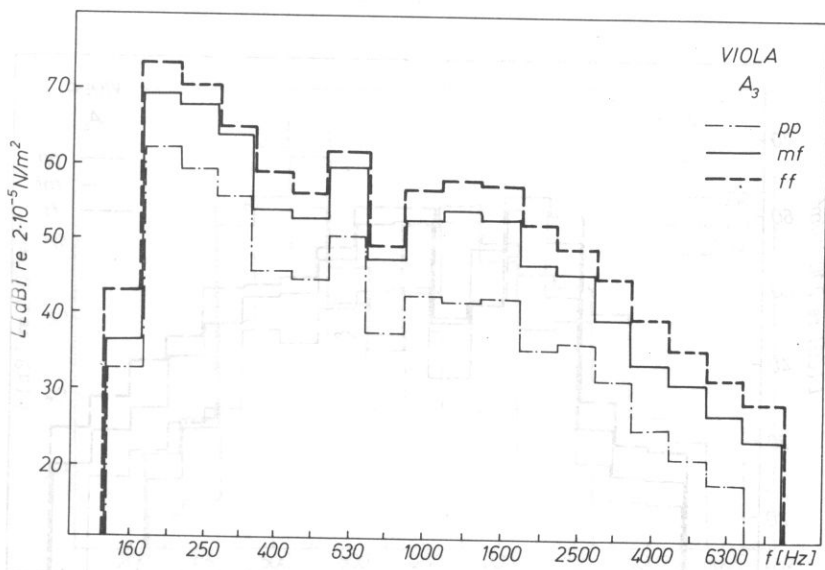


Fig. 3b. Sound pressure levels of scale segments A_3 played on a viola, measured in 1/3-octave bands.

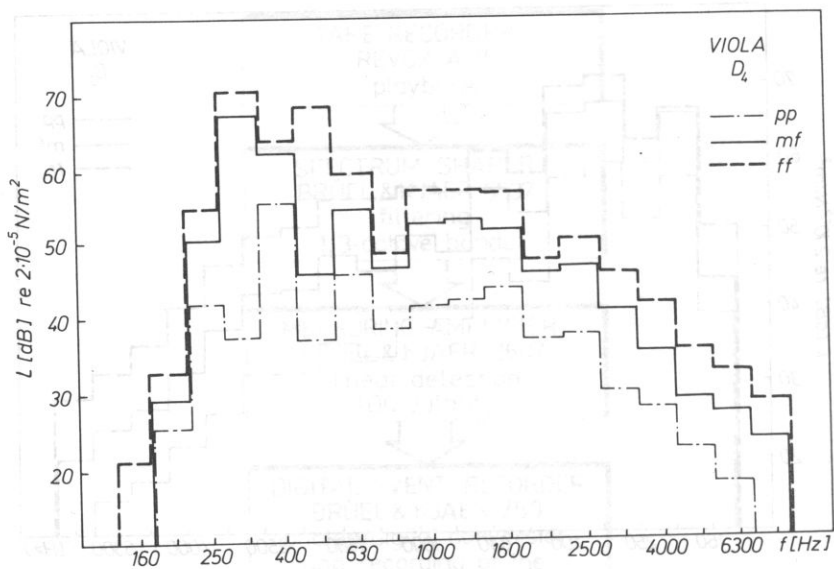


Fig. 3c. Sound pressure levels of scale segments D4 played on a viola, measured in 1/3-octave bands.

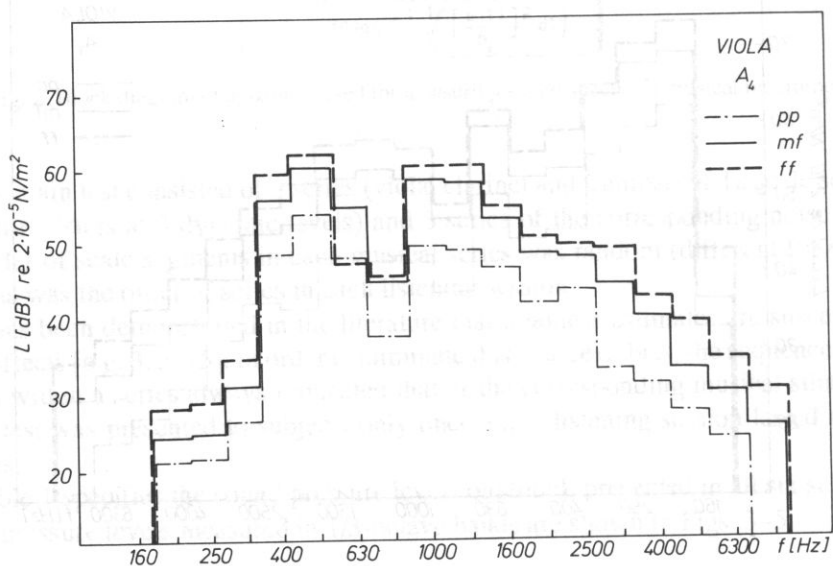


Fig. 3d. Sound pressure levels of scale segments A4 played on a viola, measured in 1/3-octave bands.

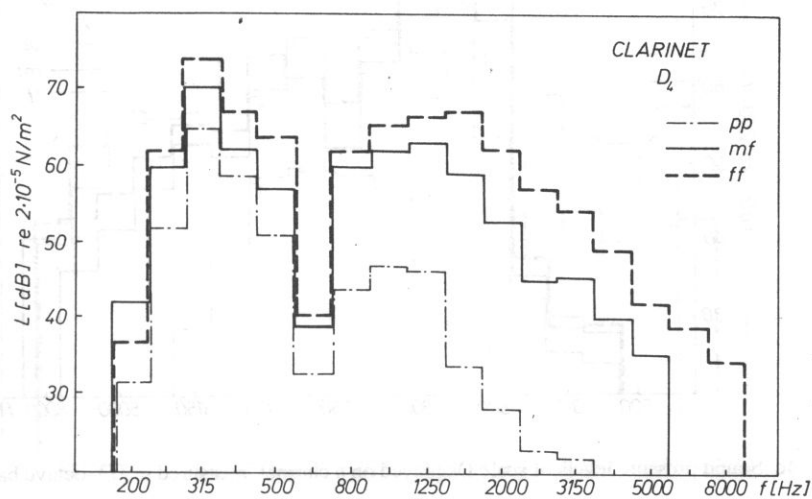


Fig. 4a. Sound pressure levels of scale segments D_4 played on a clarinet, measured in 1/3-octave bands.

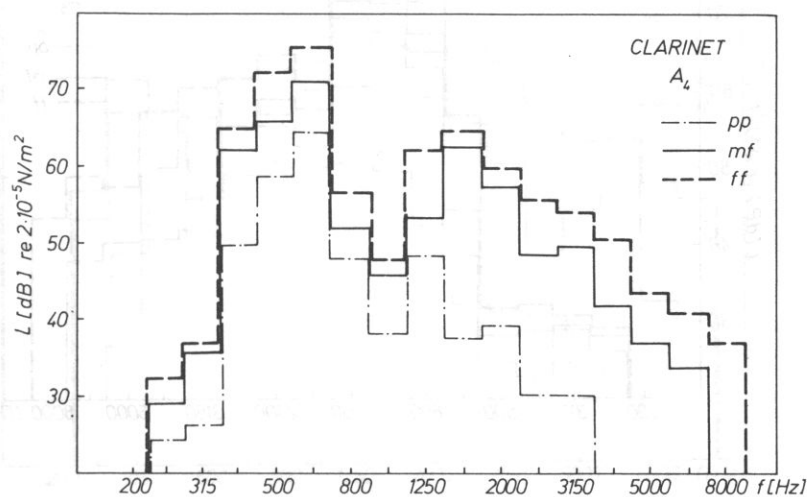


Fig. 4b. Sound pressure levels of scale segments A_4 played on a viola, measured in 1/3-octave bands.

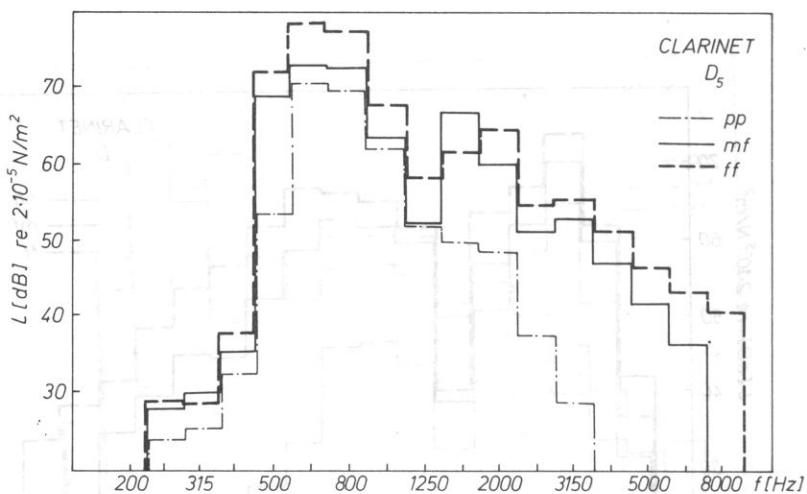


Fig. 4c. Sound pressure levels of scale D_5 played on a clarinet, measured in 1/3-octave bands.

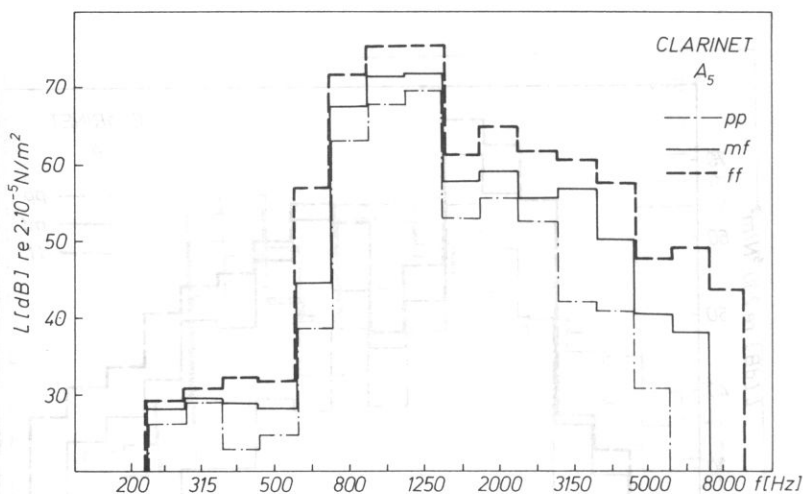


Fig. 4d. Sound pressure levels of scale segments played on a clarinet, measured in 1/3-octave bands.

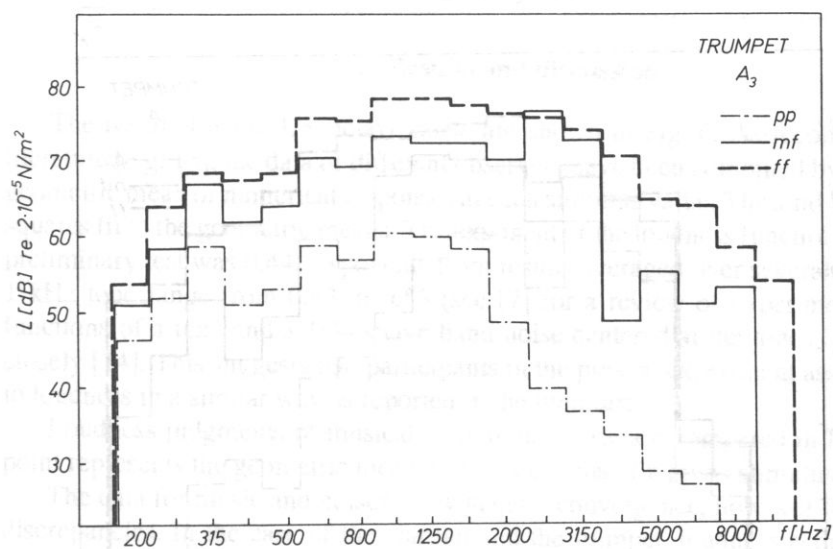


Fig. 5a. Sound pressure levels of scale A₃ played on a trumpet, measured in 1/3-octave bands.

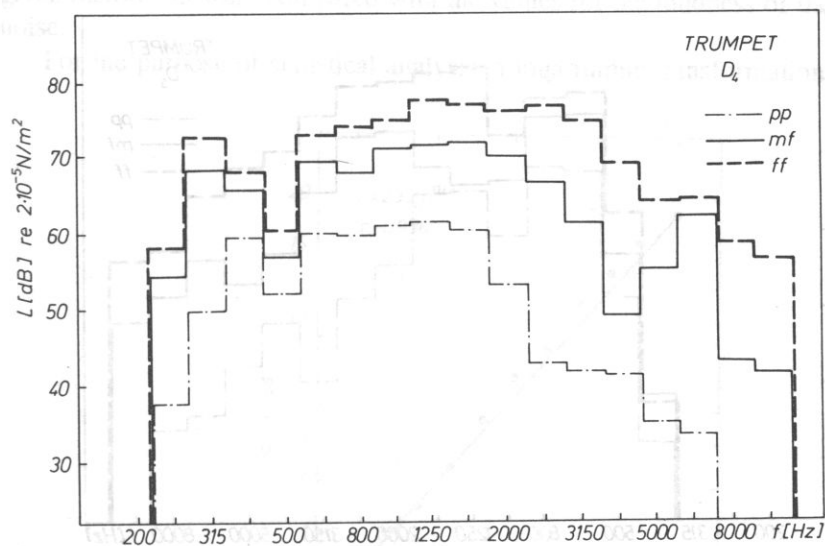


Fig. 5b. Sound pressure levels of scale D₄ played on a trumpet, measured in 1/3-octave bands.

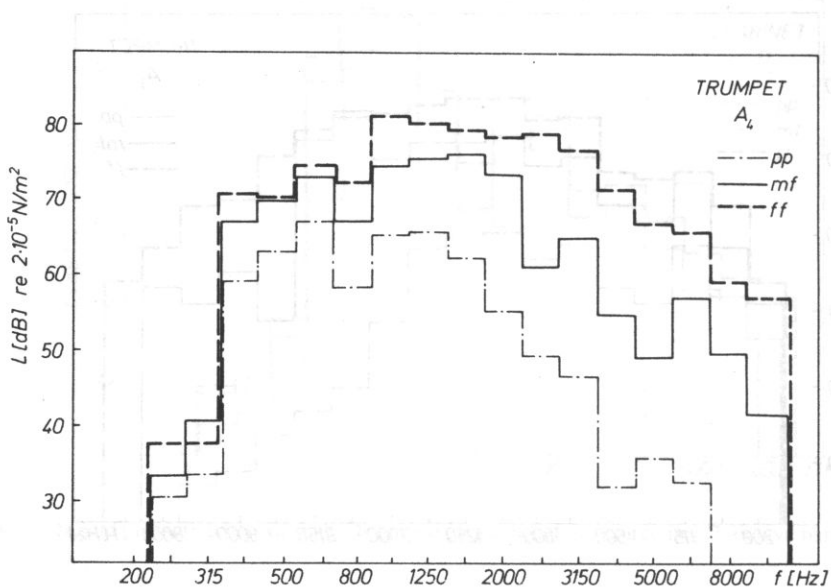


Fig. 5c. Sound pressure levels of scale segments A4 played on a trumpet, measured in 1/3-octave bands.

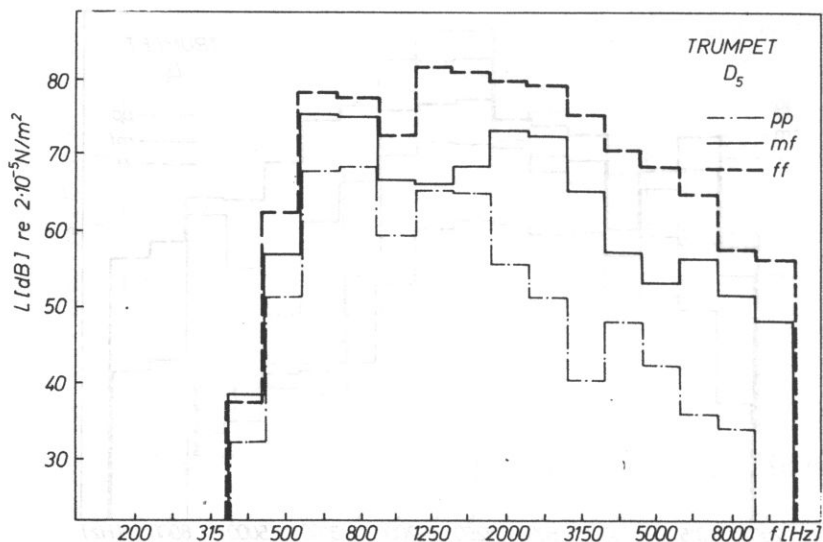


Fig. 5d. Sound pressure levels of scale segments D5 played on a trumpet, measured in 1/3-octave bands.

3. Results and discussion

The results for the 1/3-octave noise are shown in Fig. 6. As recommended in the literature [e.g. 13], the data of different observers have been combined by computing the geometric mean of numerical responses at each stimulus value. The straight line is a least squares fit to the geometric means. The exponent of the loudness function obtained in the preliminary test was 0.44. Exponents from results averaged over several observers for a 1 kHz tone range from 0.43 to 0.55 (see [7] for a review of experiments). Loudness functions of a tone and a 1/3-octave band noise centered at the tones frequency agree closely [14]. This suggests that participants in the present experiment assigned numbers to loudness in a similar way as reported in the literature.

Loudness judgments of musical stimuli and noise are compared in Figs. 7–9. Each point represents the geometric mean of 30 judgments of a given stimulus.

The data for music and noises show general convergence, however there are certain discrepancies. In the case of the clarinet and the trumpet, loudness estimates of music and noise agree fairly well (Figs. 8 and 9). The data for the viola and for noise are less convergent (Fig. 7).

In order to examine whether discrepancies between loudness estimates of music and noise are systematic and statistically significant, a *t*-test analysis was carried out. The geometric means of loudness estimates for each of the 12 musical passages played on a given instrument were compared with the values for the loudness of the corresponding noise.

For the purpose of statistical analysis, a logarithmic transformation was applied to

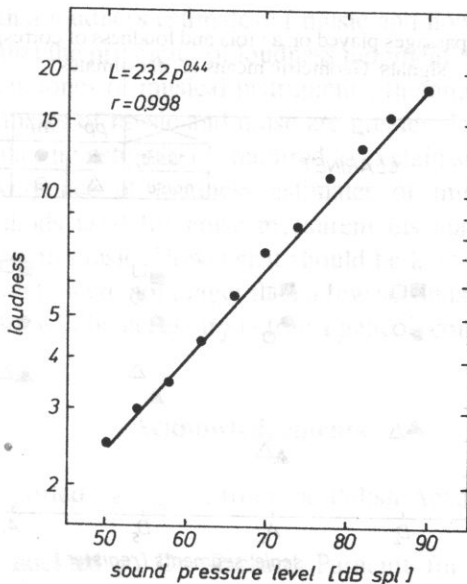


Fig. 6. Loudness of the 1/3-octave noise centered at 1000 Hz. Geometric means of 30 estimates.

the data. This made the distribution of numerical judgments approximately normal. The t -values were then computed on the transformed variable.

In case of viola and clarinet, the discrepancies between loudness estimates of music and noise were not statistically significant ($p < 0.25$). In case of the trumpet, most of the 12 noise signals were judged louder than the musical passages. The differences between loudness judgments of trumpet and noise were significant at a level of $p < 0.01$. The discrepancies between loudness estimates of trumpet and noise were nevertheless very small in magnitude (Fig. 9).

Differences between loudness estimates of music and noise were larger for some pairs of stimuli than for others. It may be assumed that those discrepancies result from differences in spectral structure between particular music and noise stimuli. Equally loud

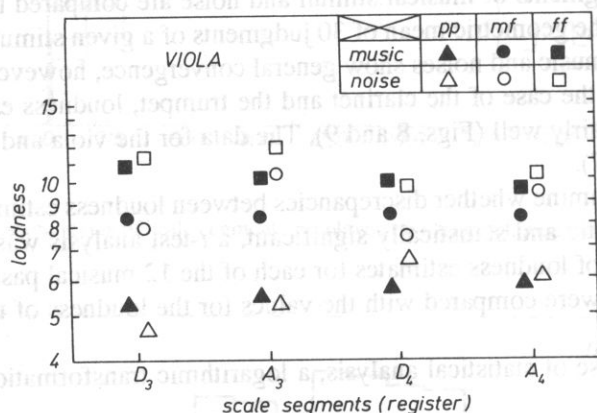


Fig. 7. Loudness of musical passages played on a viola and loudness of corresponding wide-band noise signals. Geometric means of 30 estimates.

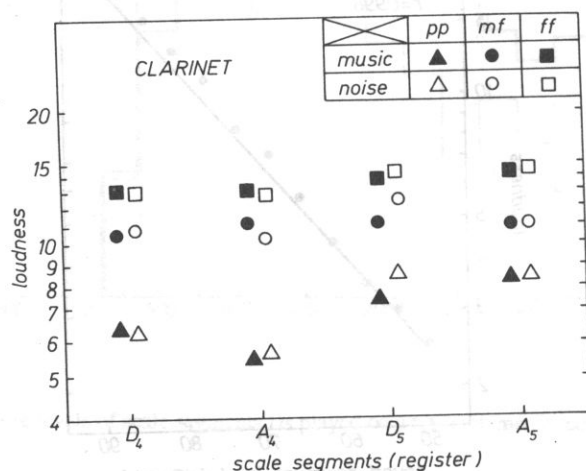


Fig. 8. Loudness of musical passages played on a clarinet and loudness of corresponding wide-band noise signals. Geometric means of 30 estimates.

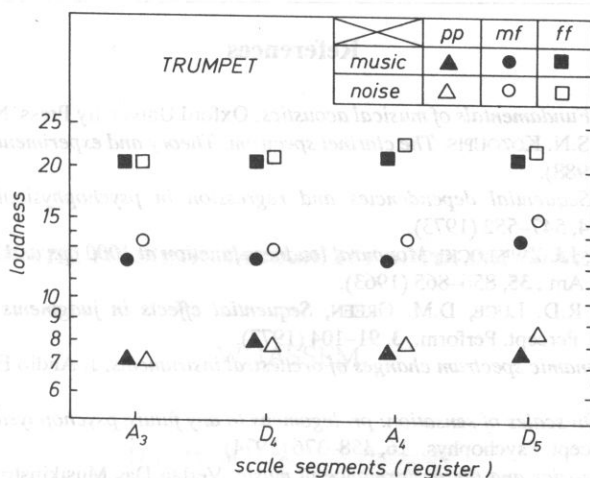


Fig. 9. Loudness of musical passages played on a trumpet and loudness of corresponding wide-band noise signals. Geometric means of 30 estimates.

sounds having different spectral structure differ in other subjective attributes. As a result, subjects' responses may be biased by other perceptual dimensions [12].

4. Conclusions

The results show that loudness estimates of music and noise agree reasonably well. This finding suggests that the principles of loudness judgment derived from non-musical stimuli also apply to the tones of musical instruments. In some cases the discrepancies between loudness estimates of music and noise are greater. This appears to depend on spectral structure. Further investigation is required to explain such differences.

The general convergence of loudness estimates of musical and noise stimuli demonstrates that methods used for noise measurements may give a reasonable approximation of loudness in music. However it should be kept in mind that the musical stimuli in the present study were not longer than a few seconds. Experiments with more complex musical stimuli will be necessary before a general conclusion can be drawn.

Acknowledgements

This work was supported by a grant from the Polish Academy of Sciences (CPBP 02.02.7.9).

The authors are indebted to Dr. Richard Parncutt for critical reading of the manuscript.

References

- [1] A.H. BENADE, *Fundamentals of musical acoustics*, Oxford University Press, New York 1976.
- [2] A.H. BENADE, S.N. KOZOUPI, *The clarinet spectrum: Theory and experiment*, J. Acoust. Soc. Am., **83**, 292–304 (1988).
- [3] D.V. CROSS, *Sequential dependencies and regression in psychophysical judgments*, Percept. Psychophys., **14**, 547–552 (1973).
- [4] R.P. HELLMAN, J.J. ZWISLOCKI, *Monaural loudness function at 1000 cps and interaural summation*, J. Acoust. Soc. Am., **35**, 856–865 (1963).
- [5] W. JESTEADT, R.D. LUCE, D.M. GREEN, *Sequential effects in judgments of loudness*, J. Exp. Psychol., Hum. Percept. Perform., **3**, 91–104 (1977).
- [6] D.A. LUCE, *Dynamic spectrum changes of orchestral instruments*, J. Audio Eng. Soc., **23**, 565–568 (1975).
- [7] L.E. MARKS, *On scales of sensation: prolegomens to any future psychophysics that will come forth as science*, Percept. Psychophys., **16**, 358–376 (1974).
- [8] J. MEYER, *Acoustics and the performance of music*, Verlag Das Musikinstrument, Frankfurt/Main 1978.
- [9] J. MEYER, *Zur Dynamik und Schalleinstung von Orchesterinstrumenten*, Acustica, **71**, 277–286 (1990).
- [10] A. MIŚKIEWICZ, A. RAKOWSKI, *The range of sound pressure level and the range of loudness in musical instruments*. Proceedings of the International Symposium on Subjective and Objective Evaluation of Sound - Poznań, Poland, pp. 172–182, E. Ozimek (Ed.), World Scientific, Singapore (1990).
- [11] H.P. REINECKE, *Über den doppelten Sinn des Lautheitsbegriffes beim musikalischen Hören*, Dissertation, Univ. Hamburg 1953.
- [12] B. SCHARF, *Loudness*, in: Handbook of perception, vol. IV, E.C. Carterette, M.P. Friedman (Eds.), Academic Press, New York 1974.
- [13] S.S. STEVENS, *Issues in psychophysical measurement*, Psychol. Rev., **78**, 426–450 (1971).
- [14] S.S. STEVENS, *Perceived level of noise by Mark VII and decibels (E)*, J. Acoust. Soc. Am., **51**, 575–601 (1972).
- [15] L.M. WARD, *Repeated magnitude estimates with a variable standard: sequential effects and other properties*, Percept. Psychophys., **13**, 193–200 (1973).
- [16] J.J. ZWISLOCKI, D.A. GOODMAN, *Absolute scaling of sensory magnitudes: a validation*. Percept. Psychophys., **28**, 28–38 (1980).

Received on August 10, 1990

ACOUSTIC-PHONETIC VARIABILITY OF POLISH VOWELS

W. JASSEM

Department of Acoustic Phonetics
Institute of Fundamental Technological Research
Polish Academy of Sciences
61-704 Poznań, Noskowskiego 10

Since the early 1960's speech sounds have been described at three levels of abstraction: intrinsic-allophonic, extrinsic-allophonic and phonemic. The acoustic features of Polish vowels have been investigated at the first and the last of these levels by acoustic-phonetic personally techniques, but extrinsic allophony has so far been largely ignored. Phonemic distinctions have been investigated in terms of format frequencies and it has been found that F_1 and F_2 are sufficient to distinguish between all the 7 Polish vowel phonemes. They are also distinctive, though less strongly both in isolation and in running speech. In the latter case the formant frequencies vary with time even within a single vocalic segment, but advanced statistical methods permit their identification on the basis of trajectories in an $F_1 - F_2$ plane. There are interactions between segmental and suprasegmental factors. Thus, speech tempo affects the formant trajectories. Otherwise, such interactions have not been extensively studied and one of the open problems is the effect of F_0 on the vowel formants. Studies of the relations between vowel-formant frequencies and speaker gender and age have, in the case of Polish speech, only just been started.

1. The acoustic and the linguistic descriptions. Allophony.

The fundamental and the most general difference between an acoustic-phonetic and a linguistic-phonetic description of a sample of spoken language is that the former is *quantitative* whilst the latter is (essentially) *qualitative*. The collection and the representation of speech data in an acoustical analysis is determined by the methodology of the exact and the technological sciences. It is therefore based on *measurements*. The methods of collecting and representing linguistic-phonetic data are quite far from being unambiguously defined.

Within a unified theory of scientific observation, acoustic-phonetic data may be described as extending on a ratio and/or difference scale whilst linguistic-phonetic data lie on a rank and/or nominal scale (ASHBY [1]). It may be assumed that the distinct lin-

guistic-phonetic categories refer to intersubjective prototypes (*ibid.*). But the criteria for the distinction of the prototypes are unclear.

Until about 1880 the phonetic description – so far only linguistic – was given on *one* level. For each of the different languages, a finite number of categorial elements called “speech sounds” (French *sons de la parole*, German *Sprachlaute*) was postulated, and every different “sound” was graphically represented by one character. A speech sample was recorded as a sequence of such distinctive characters, and the sequence was termed *phonetic transcription*.

Since about 1880, the linguistic-phonetic description began to appear at *two levels*. Now, a distinction was made between a “narrow” and a “broad” transcription (French *transcription étroite* and *transcription large*; German *enge Umschrift* and *weite Umschrift*). This distinction, observed even today, is related to the introduction into linguistics of the notion of the *phoneme* as a higher-order unit, more abstractional and, in some sense, more general than the “speech sound”. The literature on the subject of the nature of the phoneme and its relation to the lower-order phonetic unit (whatever it is called) is very rich. The relevant information may be found in monographs like JONES [26], KRÁMSKÝ [29] or FISCHER-JØRGENSEN [6]. In connection with research into the nature of the phoneme, the terms *phone* and *allophone* were introduced in the 1940’s to replace the former poorly defined “speech sound”.

Rather than engaging into a discussion of the details of the relations (allo)phone: phoneme (but see, e.g., JASSEM [14], p. 70 ff., JASSEM [16], JASSEM & DEMENKO [20]), we shall here limit ourselves to the observation that the theoretical and methodological bases of an *allophonic transcription* have yet to be formulated. In the individual languages some phonemes are described as including some “allophonic variants”, i.e. as aggregates of (normally just a few) allophones, whilst other phonemes are represented as including no allophones. For example, the (British) English phoneme /a/ is described as comprising no (qualitative) allophones whilst two or more allophones are distinguished within other monophthongs (see, e.g. ROACH [43], GIMSON [9]). In the phonology of Polish, /a/ and /e/ are described as subject to more allophonic variation than /i/ or /ɨ/ (see, e.g., WIERZCHOWSKA [50], [51]; STEFFEN-BATOGOWA [47]).

Even today there is a marked weakness of theoretical footing for the differentiation of allophones. For instance, in Spanish, the phoneme /a/ is represented by only one phone according to DALBOR [51]), two allophones according to NAVARRO-TOMÁS [38]) or four allophones according to BAZYLKO [2]), and the same sources describe Spanish /o/ as including, respectively, one, two or three (allo)phone(s).

LADEFOGED (e.g. [32]) is one of the very few specialists who attempt to formulate a criterion for allophonic distinctiveness. It is based on the possibility of differentiating languages: “... all and only the features which mark the sounds as being different from the sounds of other languages” (LADEFOGED [32], p. 9). This criterion is too general and not sufficiently precise, however. It does not break the circularity pointed out, e.g., by LINDBLOM, [33]. Languages are different phonetically *because* they use different phones. So, as emphasized by LINDBLOM (*ibid.*), the classification of and, concomitantly, the differentiation between (allo)phones must be based on some independent criteria. It should

be noted that LADEFOGED is not unaware that his premises may not be fully adequate (*op. cit.*).

Linguistic-phonetic research in the field of non-regional "standard" Polish has most aptly been summarized by STEFFEN-BATOGOWA [47]). No substantively new finding has since been made in this area. STEFFEN-BATOGOWA (*ibid.*) presents a list of phonemes in Standard Polish together with the allophones of each (pp. 46-47), which is in keeping with the position taken by the majority of Polish phonologists. The number of (allo)phones per phoneme varies here between one, e.g. for /j/, /ɛ/, and eight in the single cases of /n/. This is an analysis of the south-western variety of Standard Polish, in which only three nasal consonantal phonemes are posited: /m, n/ and /ɲ/. In the north-eastern Standard there is also /ŋ/, and then some of the allophones of south-western /n/ have to be assigned to /ŋ/. Apart from this case, the maximum number of allophones per phoneme in Steffen-Batogowa is four. Just as anywhere else, we are not told why the particular number of variants have been distinguished. Assuming *some* non-arbitrary phonemic system for a specified language, even a not-particularly-accurate recording-and-measurement device like the now outdated (but extremely useful in its time) analog Sona-Graph was quite able to show that the variability among the representations of a given phoneme is very considerably greater than an allophonic differentiation would suggest, and that much of this variability is quite *systematic*. We shall have more to say about the systematic sources of variability further on but at this point we should like briefly to consider one, viz. *coarticulation*.

The problem of coarticulation is inherently bound to the apparent double paradox which arises when an acoustic description of the speech signal is confronted with its linguistic interpretation, viz. that of *continuity vs. discreteness* and that of *variability vs. invariance*. This paradox has recently been pointed out by many authors, and an approach to its solution has been suggested in JASSEM [19], where it is maintained that the speech signal is *segmentable* in character, i.e., that it can be presented by *technical* methods as a linear sequence of acoustic-phonetic elements. Such segmental elements stand in a simple numerical relation to the respective *linguistic-phonetic* elements, such as allophones and/or phonemes in this sense, that every successive acoustic-phonetic segment is assigned to exactly one successive allophone (or phoneme) taken from a finite ensemble of allophones (or phonemes) posited for the given language. Various technical methods for the segmentation of the speech signal have been developed (the most recent description of one of them is ROACH *et al.* [44]) though the problem of variability vs. invariance still remains largely unresolved. An important step on the way to a solution is the introduction of a differentiation at another level of observation, related to the distinction between *intrinsic* and *extrinsic* allophones. According to FISCHER-JØRGENSEN ([6], p. 216), the distinction was first submitted in 1961. It is very largely a result of spectrographic visualization of the speech signal and phonetic investigations using the speech spectrograph.

When a given acoustic-phonetic segment has been assigned to a linguistically specified allophone or phoneme, its acoustic features predominantly reflect that particular allophone or phoneme, but, to a certain (probably lesser) extent it also reflects the

neighbouring allophones (or phonemes), the effect being strongest with respect to the *immediate* neighbourhood. This interaction has varying degrees of strength and gradually fades out with increasing distance between the interacting segments, usually becoming insignificant, or indiscernible, in the second-next or third-next segment. This effect of *coarticulation* is largely due to physiological constraints, such as inertia of the speech organs. Neuro-psychological origins of coarticulation have also been studied recently (e.g. Whalen [49]). There is a large measure of agreement between specialists that *intrinsic allophony* is due to coarticulation whilst *extrinsic allophony* is *conventional* in nature (see, e.g. KELLY & LOCAL [27], OHALA [39], BLADON & ALBAMERNI [3], SCHOUTEN and POLS [46]). A slightly different description of intrinsic and extrinsic allophony is given by WELLS [48], p. 41–44. That source of acoustic-phonetic variability which is due to intrinsic allophony is *universal*, whilst extrinsic allophony is *language-specific*. Typical examples of intrinsic allophony are formant transitions in the initial and final fragments of vocalic segments due to interactions with neighbouring consonants. Examples of extrinsic allophony are the two main varieties of English lateral consonants – the “clear” and the “dark” /l/, [ɫ] and [X] representing the French phoneme /r/, or Polish [e] in, e.g., *wieś* as compared with [ɛ] in *wesz* (both representing the phoneme /e/). Note that intrinsic as well as extrinsic allophony represent *contextual* effects, i.e. both reflect interdependencies between *neighbouring* segments.

The present-day knowledge of intrinsic and extrinsic allophony is far from complete and urgently requires further study. A general, strongly suggestive hypothesis that is worth testing is that differences between intrinsic allophones of a phoneme are *not perceptible* in normal conditions of listening to speech whilst extrinsic allophones are, or may be, perceptible in such conditions given the necessary attention. If extrinsic allophony is by definition conventional, then it must have been learned in the early stages of first-language acquisition. Also, if extrinsic allophony is perceptible, it should be taught and learned in second-language acquisition.

A “narrow” phonetic transcription reflects extrinsic allophony. This kind of transcription is now generally termed *allophonic transcription*.

Both extrinsic and intrinsic allophony is a matter of no little import in synchronic and diachronic phonology (see, e.g., OHALA [39]) as well as in the practical area of foreign language teaching. But it is also crucial for the solution of the apparent variability-invariance paradox and, consequently, for bridging the still existing, though evidently narrowing gap between acoustic and linguistic phonetics. In *speech technology* it has considerable significance for *electronic speech synthesis*. The principles of intrinsic allophony could be contained in the *general (universal)* part of the software, whilst extrinsic allophony could be taken care of in the specific part of the program provided for the individual language.

Thus, at the present moment, it is desirable or, in some cases, quite necessary to produce phonetic descriptions of the acoustic speech signal at *three* levels: (a) intrinsic-allophonic, (b) extrinsic-allophonic, and (c) phonemic.

There are at present many different methods of processing the acoustical speech signal, some of them disregarding phonetic segmentation and others including it in the

analysis (see, e.g. SAITO & NAKATA [45], chaps. 1–8; O'SHAUGHNESSY [40] chaps. 6–8). Many of these methods extract from the signal certain parameters representable as slow-varying time functions which stand in relatively simple relations to the speech production process (articulation), such as the frequencies of the local maxima in the dynamic spectrum, i.e., the time-varying *formant frequencies*.

The material presented below is an overview of the research into the variability of Polish vowels in terms of their acoustic parameters, especially their formant frequencies, performed to date. It has been based on measurements carried out by means of spectrographic and oscillographic analysis, as well as (to a limited extent) on perceptual experimentation with synthetic material. One of the motives for undertaking such a review is the transition, in recent years, from analog to digital analysis methods. It seems to us that the planning of further research in the field of acoustic phonetics and speech technology, with entirely new facilities, requires a summary of past experience in this specific area.

2. Classification of the variability sources

The description of vowels refers principally to their *spectral* features and – in the case of actual utterances – to their *duration*. Since, in normal Polish speech (i.e. excluding whisper and some pathological cases) Polish vowels are voiced and are represented acoustically by quasi-periodic events, *fundamental frequency* is a third descriptive parameter. Differences in the temporal *amplitude envelope* between vocalic segments are of minor importance for the fundamental problems of acoustic phonetics.

From another viewpoint, differences between concrete vocalic segments or their classes may be *linguistic*, *paralinguistic* or *extralinguistic*. The first ones belong to the phonetic, phonological and phonotactic specification of the given language. The second ones fulfill certain *semantic functions*, but are *not systemic*. For instance, to express certain attitudinal or emotional states, a sequence of segments in an utterance, or a whole utterance, may be spoken with some lip-rounding so that all the vowels within that (part of an) utterance are labialized, which is reflected in specific formant frequencies. Some of the most important extralinguistic distinctions reflect differences between *voices*.

From yet another standpoint, differences between vowels may be *segmental* or *suprasegmental*. The domain of the former are individual vocalic segments in the speech chain. That of the latter includes fragments of utterances of *at least syllabic extent*. Mostly, such fragments are *accentual units* – rhythmical or tonal – or *intonational units*.

The most serious methodological difficulties in acoustic-phonetic investigations stem from the *simultaneous effect – the interaction* – of those various variability sources in actual, natural utterances, some or most of such effects being *a priori* unknown. This necessitates an initial *selection* of experimental material and a *simplification of experimental design* which would permit an exclusion, or at least a minimization of (some of) the unknown effects.

The research reviewed below was carried out using relatively modern analog

laboratory equipment. Its inception dates back to about 1965. We shall therefore take no account of earlier work though (like, e.g., JASSEM [11]) it may be regarded as the foundation of later studies.

The Polish language does not make use of duration as a phonemically distinctive attribute of vowels (as does, e.g., Czech or, partially, German) or nasalization (as does, e.g., French). Further, Polish vowels are only minimally constrained phonotactically (unlike, e.g., English vowels). All Polish vowels may be naturally used in isolation, which they actually are, as names of the six letters of the alphabet, i.e., *i, y, e, a, o, u*. These were favourable conditions for the basic acoustic analyses.

3. Phonemic and inter-speaker variability

JASSEM's paper [12] presents the formant frequencies of the Polish vowels spoken five times each by 10 subjects – 8 male and 2 female (the latter with a rather low voice register), as the result of analyses performed with the Sona-Graph. In this experiment, only two systematic variability sources were active, viz. the phonemic distinctness and individual voice features. In this simple design, it was possible to examine both effects. The proper object of this investigation was actually the interpersonal effect. But the presentation of the frequencies of all the four formants for all the vowels (with just a few missing data) was, at the time, the fullest account of the acoustical properties of Polish vowels. Table 1 below sums up the detailed data presented in that paper. It only contains the rounded figures for the two lowest formants.

Table 1.

vowel	F ₁	F ₂
i	190 270	2100 2200
ĩ	260 370	1700 2300
e	520 630	1600 2200
a	630 1000	1100 1600
o	490 680	790 1100
u	240 340	560 780

The data in Table 1 permit, on the basis of known general relations between F_1 and F_2 on the one hand and the articulatory-perceptual linguistic description on the other, the following classification of the Polish phonemes:

	front	central	back
close	i	ĩ	u
open	e	a	o

Close vowels have a low value of F_1 , whilst open vowels have a high F_1 . Front, central and back vowels have respectively high, mid and low values of F_2 .

In terms of binary distinctive features, the results lead to the following classification of the Polish vowel phonemes (cf. also JASSEM [14], 134–139):

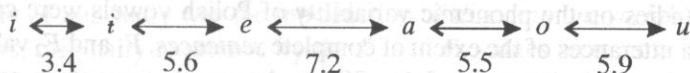
	compact	acute	low-tone
/i/	0	1	
/i̯/	0	0	0
/e/	1	1	
/a/	1	0	0
/o/	1	0	1
/u/	0	0	1

It was shown in the JASSEM [12] paper that the values of F_1 and F_2 are also quite effective in differentiating voices. The tables of Mahalanobis distances obtained for all voices separately for every phoneme, were, in a vast majority of cases, significant at $\alpha = .05$. The paper also presents the measured values of F_3 and F_4 , but only those for F_1 and F_2 were treated statistically (i.e. the sample spaces were two-dimensional).

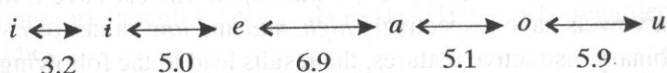
CALIŃSKI, JASSEM & KACZMAREK [4] is an extension of the paper reviewed above. It took into account the values of all four formant frequencies in a tetra-valued analysis of variance, with principal components using Wilks' criterion. The inclusion of F_3 and F_4 resulted in a distinct improvement in the discrimination of voices. For the four variables, most of the values of the F test were significant at the $\alpha = .001$ level. An examination of the relative contribution of the formants to speaker identification showed that F_2 and F_4 are more strongly discriminant than F_3 , whilst F_1 is the weakest.

The interphonemic variability of Polish vowels was studied in JASSEM, KRZYŚKO & DYCZKOWSKI, [22], where three statistical models, viz. the Bayesian, the minimax and the sequential model. The training set included isolated vowels spoken five times by each of 16 subjects (all male). The test set consisted of 10 replications of each phoneme spoken at a later date by two of voices in the training set. The possibility of identifying the vowel token as representing one of the six Polish vocalic phonemes /i, i̯, e, a, o, u/ with 2, 3 and 4 variables – again the formant frequencies – were investigated, within each of the three models. The combination of F_1 and F_2 turned out – not unexpectedly – to be the most strongly discriminant. In the minimax method the inclusion of all four formants lead to 100-% correct identification.

From a linguistic point of view, the study of the statistical distances between the phonemes was of special interest. In a 2-D space with F_1 and F_2 , the following diagram of minimal statistical distances was obtained:



and in the 4-D space, with F_1, F_2, F_3 and F_4 :



The above diagrams show that the effect of including F_3 and F_4 is negligible. An intriguing feature of the above diagrams is the *sequence* of the vowels. It reflects perfectly their placement on the articulatory-perceptual vowel quadrilateral proceeding anticlockwise from the upper-left to the upper-right (see, e.g. JASSEM [13]). It is also noteworthy that the minimal-distance relations correspond ideally to the results obtained in a totally independent and methodologically entirely different perceptual experiment performed by ŁOBACZ & DEMENKO [36]).

Steady-state vowels were also studied for their phonemic distinctiveness using synthetic speech. The earliest experiments were carried out by MAJEWSKI & HOLLIEN [37], who used 69 different stimuli with variable formant frequency values, with 14 listeners. Similar experiments were subsequently conducted by KUDELA [30, 31] with 1702 different stimuli and 20 listeners. Kudela's studies also contain statistical analyses of the experimental results. The optimal values for the representations of the individual phonemes are, according to KUDELA-DOBROGOWSKA [31] as follows (all values in Hz):

	F_1	F_2	F_3	F_4
i	240	2280	2420	3250
ĩ	350	1560	2420	3250
e	570	1560	2200	3250
a	840	1170	2660	3500
o	570	800	2200	3250
u	320	600	2660	3500

The above values may perhaps be regarded as something like a neutral standard for a male voice.

Inter-speaker differences are particularly striking when three general classes of voices are compared, viz. male, female and children's. These differences have engaged the efforts of a number of speech specialists, and most of the data available in the literature are concerned with the English language. Without entering into details, we will here limit ourselves to the general statement that typical formant frequency values for female voices cannot be obtained from those for male voices by applying a simple ratio factor. Data for female voices are scarce in the case of Polish, and those for childrens' voices are probably non-existent.

Further studies on the phonemic variability of Polish vowels were concerned with their tokens in utterances of the extent of complete *sentences*. F_1 and F_2 values were read from sonagrams at time intervals of $\Delta t = 20$ ms. As vowel segments in natural phonetic contexts usually are not stationary events, they may be mapped as trajectories in an (F_1 ,

F_2) classification plane divided into subplanes corresponding to the individual phonemes by quadratic or linear discriminant functions. In the analyses reported in JASSEM, DYCZKOWSKI & SZYBISTA [21], 11 male voices were involved.

The classification of the trajectories was based on the observation of how the trajectories passed through the individual subplanes. In the first experiment, the subspaces were determined from pooled data coming from 10 voices *different* from the one under the identification test. In the second experiment, the phonemic subspaces were determined separately for each of two voices under the test. The joint experiment therefore simulates two situations: an identification of the vowels *with* and *without tuning* to the speaker's voice. The difference due to the application of two statistical models (quadratic and linear discriminant functions, DFs) was not very striking. The accuracy of identifying the individual vowel tokens as representing particular phonemes varied between 60% for /e/ and 88% for /i/ with quadratic DFs and between 64% for /i/ and 97% for /i/ with linear DFs. These figures refer to the "no tuning" case. That part of the experiment which simulated identification "with tuning" yielded distinctly better results: /i, i̇, a, u/ were 100% correctly identified with quadratic DFs. Linear DFs gave 100% accuracy for /i/ and /u/. Tokens representing /e/ were the most difficult to identify. In part 2 of the experiment, /e/ was identified correctly 78% and 86% of the time with linear and quadratic DFs respectively.

It is noteworthy that the trajectory identification algorithm permitted an accurate identification (i.e. the assignment to the expected phoneme) even if the trajectory passed through two or three different subspaces, which was indeed the case in by far most of the cases. The intrinsic-allophonic variability resulting from the various phonetic contexts is such that within some time intervals the spectrum of a given vowel may be characteristic for a *different* phoneme from the one the vowel is representing.

In the above experiment, which concerned vowels in *natural context*, an important simplification was made. It was assumed that the dispersion of the two-element vectors representing a phoneme is *random* and is distributed *normally*. The experiment *did not* take account of the *systematic* variation due to *intrinsic* or *extrinsic allophony*.

In JASSEM [15], a classification of Polish fricatives was performed using features of the energy spectrum. We mention this paper here only because it contained results of two designs of classification: The same material was classified once with the assumption of *phonemic* classes, and then according to *intrinsic allophones*. The classification results were significantly better when intrinsic allophones were taken account of. This strongly suggests that an investigation of allophonic variation of the Polish vowels, both intrinsic and extrinsic, is now an urgent task.

As previously indicated, the actual vowel formant frequencies result from the *simultaneous* operation of at least two variability sources: phonemic and interpersonal. The interaction of those two variability sources was studied by JASSEM [18]. The methodological novelty of this study was the introduction of *discriminant variables*. The two-element vectors, originally expressed by the F_1 and F_2 values were now situated in a *new* plane whose co-ordinates, the discriminant variables, were *decorrelated* with within-class covariance matrices transformed to *unit matrices*. This is achieved by *linear trans-*

formation of the relations between the original variables. The distances between the mean vectors in the new feature space are *true statistical distances between the mean vectors*.

For the six Polish vowel phonemes /i, i̇, e, a, o, u/ ($i = 1, \dots, 6$) and four male voices: AM, WJ, PD, RC ($j = 1, \dots, 4$) the following null hypotheses were formulated:

$$\mu_{1j} = \mu_{2j} = \mu_{3j} = \mu_{4j} = \mu_{5j} = \mu_{6j} \quad (1)$$

$$\mu_{1.} = \mu_{2.} = \mu_{3.} = \mu_{4.} = \mu_{5.} = \mu_{6.} \quad (2)$$

$$\mu_{i1} = \mu_{i2} = \mu_{i3} = \mu_{i4} \quad (3)$$

$$\mu_{.1} = \mu_{.2} = \mu_{.3} = \mu_{.4} \quad (4)$$

The experimental material in this study consisted of 40 different real or pseudo CVC words. Within phonotactic constraints, the numerical distribution of the contextual consonant phonemes was approximately equal. Each word was spoken once by each of the four subjects. Again, F_1 and F_2 were measured at $\Delta t = 20$ ms intervals. On the basis of these measurements, all the mean vectors in the expressions (1)...(4) above were calculated, their positions in the discriminant-variables plane were defined within all designs, and the statistical significance of all the distances between the means in all designs was determined.

As in the other studies in which the vowels were investigated in utterances of at least syllabic extension, intrinsic allophonic variation was ignored and a simplifying assumption was made that the joint dispersion of the variables was normal. Each vowel was represented by one extrinsic allophone, viz. the most context-independent one.

The most essential results of this study may be summarized as follows:

(1) When each of the four voices was considered separately, all the statistical distances between all the six mean vectors for the 6 phonemes were significant at $\alpha = 0.05$ in WJ and AM. In RC and PD one of the 15 distances, viz. $D(/i, e/)$ did not reach that level.

(2) When the data were collapsed for all the four voices, separately for each phoneme, six mean vectors were obtained, each representing one phoneme. In this case, again only one of the 15 distances, viz. $D(/i, e/)$ was below the $\alpha = 0.5$ level.

(3) Within each phoneme, the significance of the 6 statistical distances between the four voices was as follows: for /i, i̇, o, u/ all the distances were significant at $\alpha = 0.05$. For /e/ and /a/ one of the six distances was not significant.

(4) When all the data were pooled over all the six phonemes, separately for each speaker, four mean vectors were obtained with 6 distances between them. Out of these, two, viz. d (AM, WJ) and d (RC, WJ) were below the $\alpha = 0.05$ significance level.

Detailed results of the statistical analysis of the data in this experiment are given in JASSEM, KRZYŚKO & STOLARSKI [23], but one observation of a general character should be made here: Overall, the differences between the voices were smaller than those between the phonemes. But, in any case, the study showed that when the Polish vowels are characterized by no more than two quantitative features, it is possible to classify them both from a linguistic, viz. a phonemic point of view and from one paralinguistic standpoint, viz. that of speaker specification, at least when the number of speakers is small.

4. Intrinsic contextual allophony

The only study of the effect of intrinsic allophony on the acoustical variability of vowels in Polish published to date is FRĄCKOWIAK-RICHTER [7], which deals with the time courses of the vowel formant frequencies as affected by all the phonotactically admissible neighbouring plosives, especially their place of articulation. The formant which is the most strongly affected is F_2 . *Vis-à-vis* the "locus" and the "substrate" theories prevalent at that time, an explanation in terms of "locus frequency ranges" is offered. "The Locus Frequency Range can...be described as follows: The upper limit of the *LFR* is the highest frequency which, in the vicinity of the given consonant, any neighbouring vowel's positive transition reaches as its terminal frequency. The lower limit of the *LFR* is the lowest frequency which, in the vicinity of the given consonant, any neighbouring vowel's negative transition reaches as its terminal frequency." (*loc. cit.* p. 99). In accord with the terminology prevalent at that time, a transition is termed "negative" if the target frequency of the formant in the vowel is lower than its frequency at the border with the consonant and "positive" if the target frequency is higher. The F_2 locus frequency ranges for the different Polish stop consonants order themselves, from low to high, as follows: /p,b/, /k,g/, /t,d/, /c, ʃ/ (*ibid.* p. 107). The concrete figures are given in Tables, but they are based on just two voices. Since the vowel formant frequencies vary individual voices, it can safely be assumed that there is also speaker-dependency in the case of the absolute values of the *LFRs*.

5. Durational intrinsic-allophonic variation. Interaction between the duration and the spectral features of vowels

Durational differences between vocalic segments in natural utterances may be due to the following variability sources:

- (1) Phonemic (e.g. in Czech and, partially, in German).
- (2) Quasi-phonemic (e.g., in English).
- (3) Non-distinctive, related to the degree of openness.
- (4) Contextual extrinsic (e.g. in English and Present-Day French).
- (5) Contextual intrinsic (e.g. in Polish)
- (6) Accentual (e.g. in Russian).
- (7) Rhythmical (e.g. in English and – more weakly – in Polish)
- (8) Tempo-induced (universal).

So far as is known at present, Polish exhibits durational variations of the type (3), (5), (7) and (8). The first three have been investigated by Richter.

In FRĄCKOWIAK-RICHTER [8], the following effects are studied: (1) the vowel's articulation, (2) voicedness *vs.* voicelessness in the following consonant, (3) the duration of the rhythm unit (only partially), (4) the "place of articulation" of the following consonant, (5) the distinctive feature of the following consonant traditionally (though im-

properly) called "manner of articulation". A detailed Analysis of Variance was performed, followed by numerous Student's and Duncan's tests. Mono- and disyllabic non-sense words were analyzed, spoken by 10 subjects.

The most significant results of this study are as follows:

The effect of the presence/absence of the quasi-periodic component in the following consonantal segment was studied separately in the monosyllables and disyllables.

Both in the monosyllabic and the disyllabic "words", the relations obtained were: $t(i) < t(\dot{i}) < t(e) < t(a) > t(o) > t(u)$ (t denoting duration). For the monosyllables, the mean lables, the t values were smaller by about 20...40 ms. These relations ideally reflect the description of Polish vowels in terms of relative openness. A two-way Analysis of Variance gave:

for the vocalic phonemes $F(5,45) = 17.74^{***}$
 for the voices $F(9,45) = 54.53^{***}$

Both the differences between the vowel phonemes and the voices were, thus, very highly significant.

Taking the mean duration before a phonologically (distinctively) voiced consonant as unity, the relative duration of the vowels before the corresponding voiceless consonant was, in the individual consonant pairs.

b:p0.908	v:f0.817
d:t0.851	z:s0.813
ʃ:c0.881	ʒ:ʃ0.756
g:k0.796	ʒ:ʒ0.814
dz:ts 0.841	
dʒ:ʦ ... 0.871	

In a two-way Analysis of Variance (with speaker as the other factor) the durational differences were found to be significant at $\alpha = 0.001$ in the pairs /g:k, v:f, s:z, ʃ:ʒ, ʒ:ʒ/ and /dz:ts/, at $\alpha = 0.01$ in the pairs /d:t, c:ʃ, dʒ:ʦ/, and at $\alpha = 0.05$ in /b:p/. Thus, all differences were statistically significant, most of them (very) highly significant.

The effects of the "place" and the "manner" of articulation of the following consonant on the duration of the vowels were also studied, but were found to be weak or negligible, so we shall not consider them here. We also leave out other, detailed results obtained in the study.

The variability of vocalic duration due to the placement of accent and rhythm were studied by Richter in her papers [41] and [42]. In the former, a model was tested which is defined by the following expression:

$$V = \frac{D}{(mn)^\alpha}, \quad (5)$$

where V is the duration of the vowel, D the maximum duration of the vowel in the given text, n is the number of syllables in the rhythm unit and m is the number of syllables including the accented syllable and the remaining following syllables in the rhythm unit. α is an empirical value which is constant for the given text (assuming constant tempo). The data were found to fit the model satisfactorily.

In the other study, several regressive models were tested. Of these, the most detailed one is of the form

$$\frac{d - \bar{d}}{\bar{p}} = a + b \frac{\tilde{d} - \bar{\tilde{d}}}{\bar{p}} + c(n - \bar{n}), \quad (6)$$

where d is the cumulated duration of all segments in the rhythm unit, n is the number of segments in the rhythm unit, and $p = \frac{d}{n}$.

The absolute duration of the vowels is given by the regression equation and a Table of intrinsic durations of classes of phonemes. The regressive model was also found to be highly explanatory.

Several works by ŁOBACZ were devoted to the *interaction* between *vocalic duration* and the *vowel spectrum*, e.g., [34] and [35]. In the earlier, the author investigated the effect of speech *tempo* expressed as the number of syllables per minute on the time courses of F_1 , F_2 and F_3 in the vowels /e, a, o/ in the bilateral context of the palatal consonant /ɕ/. The time course of the formant frequency curves was divided into subsegments having definite direction of change. Using a correlation-and-regression analysis, the effect of tempo on the frequencies of the formants at subsegment boundaries was studied. The main results of this investigation were as follows:

(1) The frequencies of all formants, especially those of F_2 , in the final spectrum of the vowel are only negligibly dependent on the duration of the vowel, whilst strongly correlating with the target frequencies of the vowel and the formant frequencies of the neighbouring constant.

(2) The temporal changes of F_2 in the initial part of the vowel depend on the spectrum of the precesing consonant, the target frequency of the vowel and the vowel duration.

(3) The temporal changes of F_3 can be relatively simply expressed by the effect of the total vowel duration on the number of subsegments.

(4) The effect of duration is particularly strong and consistent in the case of F_{im} , i.e., the target frequencies of the vowel (denoted by the index m), particularly F_{2m} .

(5) Up to a critical value of about 250 ms, the total duration of the vowel has a strong effect on the durations of the subsegments. Above that value, the duration and the time courses of the formant frequencies in the initial and final fragments of the vowel become stable whilst the duration of the steady-state vowel target systematically increases.

(6) The temporal changes of F_4 and F_5 strongly tend to be speaker-dependent.

In [35] ŁOBACZ investigated the effect of speech *tempo* on the dynamic spectrum of the Polish vowels. The experimental material included complete utterances of the extent of sentences produced by 3 male voices. The formant frequencies were measured at

$\Delta t = 20$ ms. Using the statistical methods applied by JASSEM *et al.* in the works reviewed above, the (F_1, F_2) plane was divided into identification subplanes by second-order curves for each of the six phonemes, separately for *slow*, *normal* and *fast* speech. Traces of the two-element vectors in the respective planes were drawn through the subplanes and, using a simple recognition algorithm, were identified as representing the individual phonemes. The shapes and the positions of the subplanes as well as the locations and courses of the traces very strongly depended on the tempo. The overall accuracy of recognition was 98% for slow, 95% for normal and 90% for fast speech. It should be emphasized that this relatively high accuracy was due to the definition of *separate* identification spaces for each tempo. The duration of the vowel naturally depended on the tempo. The experiment can thus be seen as one form of a description of the effect of *suprasegmental vowel duration* on the temporal changes of the vowel spectrum.

6. Interaction between F_0 and the spectral features of vowels

It is generally assumed in audioacoustics that the *quality* of a (quasi) periodic sound depends on its energy-spectrum envelope and is (at least in the first approximation) independent of the *fundamental frequency*. The sounds of speech are, however, perceived by humans in a specific way in connection with interpersonal differences between voices and the interrelations of these differences with the frequency of the excitation source.

KOSIEL [28] calculated the correlation coefficients between F_0 and F_1, F_2, F_3 and F_4 . The experimental material included all the Polish vowel phonemes spoken in isolation by 10 voices on four different pitches, the distance between $F_{0\min}$ and $F_{0\max}$ being approx. one octave. Student's t test was used to test the null hypothesis of no correlation between the respective pairs of variables (F_0 and F_1, F_0 and F_2 , etc.). Only in a few isolated cases did the value of t exceed the critical value for $\alpha = 0.05$. Though the experiment was somewhat tentative, it gave no grounds for rejecting the traditional view that the speaker's control of the supraglottal organs responsible for the vowel resonances is independent from his control of F_0 .

On the other hand, there is rich literature, mainly relating to the English language, devoted to the effect of differences between male, female and childrens' voices on formant frequencies. It is common knowledge that these broad classes of voices mainly differ with respect to fundamental frequency. Two of the most recent papers dealing with this problem are JOHNSON [24] and [25]. For Polish, the problem has recently been attacked by IMIOŁCZYK [10]. On the basis of perceptual experiments with synthetic steady-state vowels, IMIOŁCZYK found that lacking any other cues, the listener judges the sex and age of the speaker from fundamental frequency, but for an impression of optimal linguistic vowel quality for a given phoneme, the formant frequencies have to be modified according as the voice is perceived as one of a woman, a man or a child.

Among the many problems concerning the variability of vowels in general, and the Polish vowels in particular, that require further research is that of the relation between F_0 and the features of the power spectrum.

7. Concluding remarks

The acoustic variability of Polish vowels has, over the last twenty five years or so, been the object of a fair number of studies, the most significant of which have been reviewed here. Though the accumulated knowledge is substantial, several aspects of the problem have not been investigated at all or require further study, such as intrinsic and extrinsic allophony or the relation between fundamental frequency and formant frequency. Such additional knowledge is urgently needed for automatic recognition and high-quality digital synthesis of Polish speech.

References

- [1] M. ASHBY, *Prototype categories in phonetics*, Speech, Hearing and language. Work in Progress. Department of Phonetics and Linguistics, vol. 4, 2128, 1990.
- [2] S. BAZYŁKO, *Elementos de fonética del español para los alumnos de estudios ibéricos*, Ed. de la Univ. de Varsovia, 1979.
- [3] R.A. BLADON and A. AL-BAMERNI, *Coarticulation resistance in English /l/*, Journal of Phonetics, 4, 2, 137-150 (1976).
- [4] T. CALIŃSKI, W. JASSEM and Z. KACZMAREK, *Investigation of vowel formant frequencies as personal voice characteristics by means of multivariate analysis of variance*, in: Speech Analysis and Synthesis, vol. 2, PWN, Warszawa 1970, pp. 739.
- [5] J.B. DALBOR, *Spanish pronunciation: theory and practice*, Holt, Rinehart and Winston, New York 1969.
- [6] E. FISCHER-JORGENSEN, *Trends in phonological theory*, Akademisk Forlag, Copenhagen 1975.
- [7] L. FRĄCKOWIAK-RICHTER, *Vowel formant transitions at stop-consonant boundaries in Polish*, in: Speech Analysis and Synthesis, vol. 2, PWN, Warszawa 1970 pp. 95-118.
- [8] L. FRĄCKOWIAK-RICHTER, *The duration of Polish vowels*, in: Speech Analysis and Synthesis, vol. 3 PWN, Warszawa 1973 pp. 87-115.
- [9] A.C. GIMSON, *An introduction to the pronunciation of English*, 4th ed. rev. by S. Ramsaran, E. Arnold, London 1989.
- [10] J. IMIOLCZYK, *Defining the perceptual borders between male, female and children's voices in isolated Polish vowels*, (in Polish), IFTR Reports, 5 (1990).
- [11] W. JASSEM, *The formants of sustained Polish vowels*, in: The study of sounds, Tokyo 1957 pp. 335-345.
- [12] W. JASSEM, *Vowel formant frequencies as cues to speaker discrimination*, in: Speech Analysis and Synthesis, vol. 1, PWN, Warszawa 1968 pp. 9-41.
- [13] W. JASSEM, *Bases of acoustic phonetics*, (in Polish) PWN, Warszawa 1973.
- [14] W. JASSEM, *Speech and communication science*, (in Polish), PWN Warszawa 1974.
- [15] W. JASSEM, *Classification of fricative spectra using statistical discriminant functions*, in: Frontiers of speech communication (B. Lindblom and S. Ohman, Eds), Academic Press, London 1979, pp. 77-91.
- [16] W. JASSEM, *The phonology of modern English*, PWN, Warszawa 1983.
- [17] W. JASSEM, *Preliminaries to an acoustical theory of the phoneme* (in Polish), XXXII Otwarte Seminarium z Akustyki OSA-85, 1985, pp. 61-64.
- [18] W. JASSEM, *Vowel-formant frequencies as linguistic and speaker-specific features of the speech signal*, in: Language in global perspective (Ed. B.J. Elson), Summer Institute of Linguistics, Dallas Texas 1988.

- [19] W. JASSEM, *Preliminaries to an acoustical definition of the phoneme*, Neue Tendenzen in der angewandten Phonetik II, Beiträge zur Phonetik u. Linguistik, Buske Verl., Hamburg 1987.
- [20] W. JASSEM, G. DEMENKO, *Phonetic transcription for speech acoustics and its implementation using a dot-matrix printer*, (in Polish), IFTR Reports, Warszawa 1988.
- [21] W. JASSEM, A. DYCZKOWSKI and D. SZYBISTA, *Semi-automatic classification and identification of vowels in typical phrases*, in: Speech Analysis and Synthesis, vol. 4, PWN, Warszawa 1976, pp. 135–145.
- [22] W. JASSEM, W. KRZYŚKO and A. DYCZKOWSKI, *Identification of isolated Polish vowels*, in: Speech Analysis and Synthesis, vol. 4, PWN, Warszawa 1976, pp. 106–133.
- [23] W. JASSEM, M. KRZYŚKO, P. STOLARSKI, *Formant frequencies as phonemic and speaker-specific features in the light of a statistical discriminant analysis*, IFTR Reports 27 (1984).
- [24] K. JOHNSON, *Intonational context and F₀ normalization*, in: Research on Speech Perception, Progress Report No. 14, Bloomington, Indiana 1988, pp. 81–108.
- [25] K. JOHNSON, *F₀ normalization and adjusting to talker*, in: Research on Speech Perception, Progress Report No. 15, Bloomington, Indiana, 1988. 237–257.
- [26] D. JONES, *The phoneme. Its nature and use*, Heffer, Cambridge 1950.
- [27] J. KELLY and S. LOCAL, *Long-domain resonance patterns in English*, Proc. of the IEE Conf.: Speech Signal I/O 1983.
- [28] U. KOSIEL, *Correlations between fundamental frequency and formant frequencies in Polish vowels*, in: Speech Analysis and Synthesis, vol. 3, PWN, Warszawa 1973, pp. 117–120.
- [29] J. KRÁMSKÝ, *The phoneme. Introduction to the history and theories of a concept*, Wilhelm Fink Verlag, Munchen 1974.
- [30] K. KUDELA, *A study of the optimal formant frequency values of Polish vowels using synthetic speech*, in: Speech Analysis and Synthesis vol. 2 PWN, Warszawa 1970, pp. 221–238.
- [31] K. KUDELA-DOBROGOWSKA, *Further studies of the optimal formant frequency values of Polish vowels*, in: Speech Analysis and Synthesis vol. 3, PWN, Warszawa 1973, pp. 265–285.
- [32] P. LADEFOGED, *Representing phonetic structure*, Working papers in Phonetics UCLA, Los Angeles No. 73 1989.
- [33] B. LINDBLOM, *On the notion of „possible speech sound”*, Journal of Phonetics, 19, 2, 135–151 (1990).
- [34] P. ŁOBACZ, *The effect of speech tempo on the courses of vowel formants*, in: Speech Analysis and Synthesis vol. 2 PWN, Warszawa 1970, pp. 71–94.
- [35] P. ŁOBACZ, *Speech rate and vowels formants*, in: Speech Analysis and Synthesis vol. 4, PWN, Warszawa 1976, pp. 187–218.
- [36] P. ŁOBACZ, G. DEMENKO, *The effect of long-term phono-lexical memory on the perception of the segmental features of Polish vowels* (in Polish), IFTR Reports 40 (1983).
- [37] W. MAJEWSKI, H. HOLLIEN, *Formant frequency regions of Polish vowels*, Journ. Acoust. Soc. of Am. 42, 5, 1031–1037 (1967).
- [38] T. NAVARRO-TOMAS, *Manual de pronunciación española*, Ed. Desimoctava, Madrid 1974.
- [39] J.J. CHALA, *Phonological evidence for top-down processing in speech perception*, in: Invariance and Variability in Speech Processes Eds. J.S. Perkell and D. Klatt, Erlbaum Ass. Publ., Hillside, NJ 1986, pp. 386397.
- [40] D. O'SHAUGHNESSY, *Speech communication*, Addison-Wesley Publ. Co., Reading Mass. 1987.
- [41] L. RICHTER, *A preliminary description of accentual isochrony in Polish* (in Polish), IFTR Reports 4 (1983).
- [42] L. RICHTER, *A statistical analysis of the rhythmical structure of Polish utterances* (in Polish), IFTR Reports 8 (1984).
- [43] P. ROACH, *English phonetics and phonology*, Cambridge Univ. Press, 1983.
- [44] P. ROACH, H. ROACH, A. DEW and P. ROWLANDS, *Phonetic analysis and the automatic segmentation and labeling of speech sounds*. Journal of the Intern. Phonetic Ass'n 20, 1 15–21 (1990).
- [45] S. SAITO, K. NAKATA, *Fundamentals of speech signal processing*, Academic Press, Tokyo 1985.

- [46] M.E.H. SCHOUTEN, L.C.W. POLS, *Vowel segments in consonantal contexts: a spectral study of coarticulation*, Part I, *Journal of Phonetics* 7, 1, 123 (1979).
- [47] M. STEFFEN-BATOGOWA, *Automatic transcription of Polish texts*, (in Polish), PWN, Warszawa 1975.
- [48] J.C. WELLS, *Accents of English*, Cambridge Univ. Press, Cambridge 1982.
- [49] D.H. WHALEN, *Coarticulation is largely planned*, *Journal of Phonetics*, 18, 1, 3-35 (1990).
- [50] B. WIERZCHOWSKA, *A phonetic description of Polish*, (in Polish) PWN, Warszawa 1967.
- [51] B. WIERZCHOWSKA, *Polish phonetics and phonology*, (in Polish) Ossolineum, Wrocław 1980.

Received on February 11, 1991

A METHOD FOR CONNECTED WORD RECOGNITION

S. GROCHOLEWSKI

Institute of Computing Science
Technical University of Poznań
(60-965 Poznań, Piotrowo 3a)

In this paper, the description of the method for connected word recognition derived from the algorithm introduced by VINTSYUK is illustrated by means of a hypothetical example. Such a detailed presentation of the method should be useful from the practical point of view. The cited results of the real experiments confirm the ability of the method to perform reliable connected word recognition.

1. Introduction

Automatic speech recognition systems have initially been limited to the recognition of isolated speech consisting of a restricted set of vocabulary items. Among these early methods the so-called "global" approach, which requires that the incoming utterances be compared with template words, has been most popular. However, this approach fails when the utterance is composed of an unknown number of words and does not contain the pauses in between them.

During the early seventies a number of different solutions to this problem were considered in the USSR [10], Japan [7] and, subsequently, in the USA [5]. During the early eighties the approach introduced by VINTSYUK [10] which was unknown in the USA and Japan (his paper was not cited in [5], [7]), was adopted in a modified form by BRIDLE and BROWN [1] and NEY [6].

All the above solutions were discussed and compared in [4]. Their common feature is that they use a dynamic programming technique which serves to match optimally an unknown utterance with the "super" reference pattern [6] obtained by concatenation of single word templates.

A specific method used to find the optimally "super" reference pattern will be presented and illustrated by means of hypothetical data. This method is based on the approach introduced by VINTSYUK which was chosen because of the advantages pointed out in [4].

2. Dynamic programming in connected word recognition

At the beginning the reasons for which the dynamic programming technique is used in isolated word recognition systems [8], [3], with the global approach will be briefly reviewed.

This approach requires that the unknown utterance to be compared with each of the reference words from a lexicon. Two of many more possible time alignments between the utterance X and the reference word $W(n)$ are presented as paths f_1 and f_2 in Fig. 1. In the case of f_1 the unknown word was uttered exactly in the same manner as the corresponding reference word. In the case of f_2 the temporal relations between the parts of the words X and $W(n)$ are different. If we assume that the path f_2 is the set of points representing the optimal relation between the successive vectors in the utterance X and the reference word, and if we assign for each point (i, j) the distance $d(i, j)$ between the vectors, then the sum of distances corresponding to all points of the path gives the total distance $D(X, W(n))$ between the words X and $W(n)$.

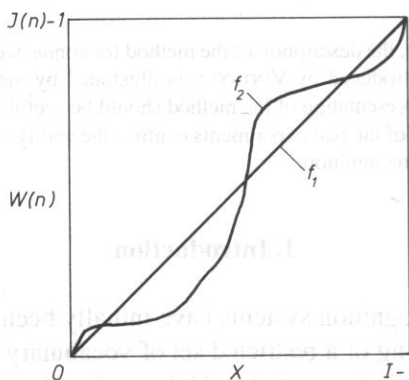


FIG. 1. Two time alignments represented by path f_1 and f_2 between the utterance X and reference word $W(n)$.

Since in practice the optimal warping function never coincides with the diagonal as in the case of f_1 in Fig. 1, it is necessary to determine it. The problem of determining the optimal warping function i.e., the optimal temporal relations between two words can be solved with the aid of the dynamic programming (DP) technique [8], [3], which allows for the assignment of the optimal path from point $(0, 0)$ to point $(I-1, J-1)$ through the use of the following equations:

$$D(0, 0) = d(0, 0),$$

$$D(i, j) = d(i, j) + \min \begin{cases} D(i-1, j) \\ D(i-1, j-1) \\ D(i, j-1) \end{cases} \quad (1)$$

where $D(i, j)$ – the minimal accumulated distance calculated from the point $0, 0$ to the point i, j .

The use of the term "optimal path" signifies that the sum $D(I-1, J-1)$ of the local distances $d(i, j)$ along this path attains its minimum value.

Let us consider a more difficult case, where an utterance consists of several words uttered without the pause in between. The number of words is not specified, it is only known that they all belong to a limited vocabulary set consisting of single word utterances (templates) that were spoken in isolation during the learning phase.

The above problem can be solved by decomposing the matching procedure into two levels: a single template matching level and a word string construction level [5], [7] or by treating the matching procedure as a one-stage procedure [6]. Figure 2 presents a synopsis of this second approach.

Let us consider the plane where an unknown utterance (composed of the words: C, A, D, B, A) is presented along the abscissa, and all the templates along the ordinate. In the second approach the matching procedure is the same as in the case of isolated word recognition, i.e., the goal is to find the best matching patch representing the optimal temporal relations between the parts (words) of the utterance and the templates from the vocabulary set.

The problem presented in Figs. 1 and 2 differ as follows:

the initial point of the path from Fig. 2 is unknown; we only know that it coincides with the beginning of any template,

the terminal point of the path from Fig. 2 is also unknown; we only know that it coincides with the end of any template,

the path in Fig. 2 possesses some (generally unknown number) points of discontinuity corresponding to the transitions between the templates,

the minimal accumulated distance $D^*(I-1, J-1)$ is sufficient to recognize the un-

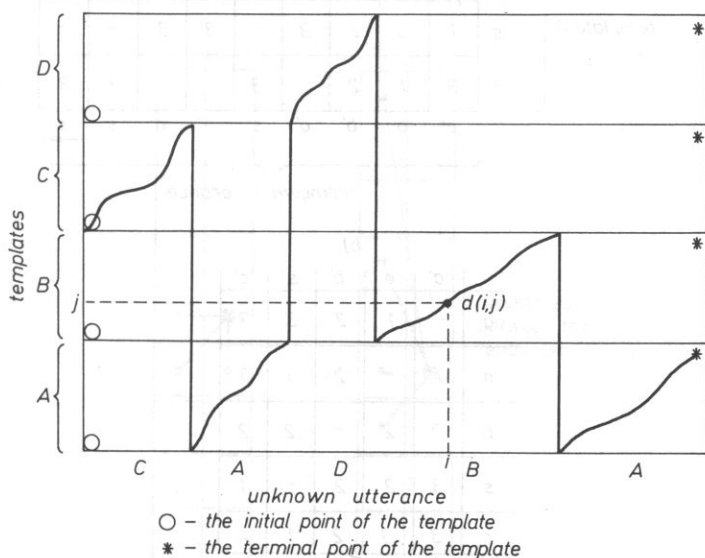
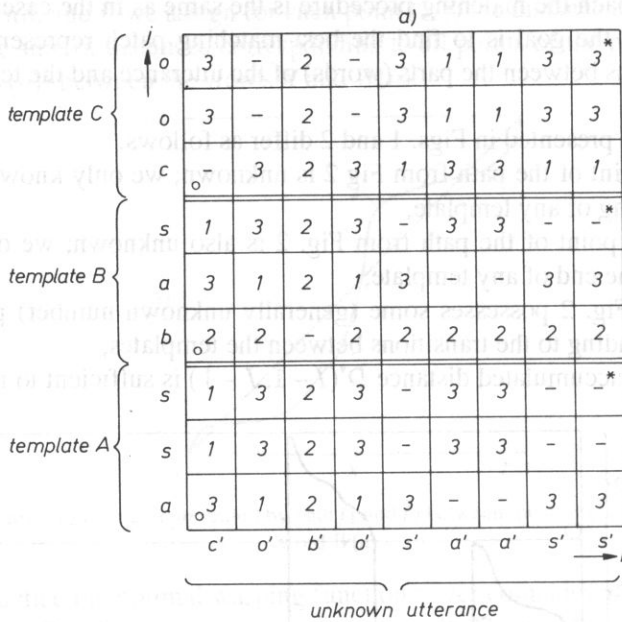


FIG. 2. Synopsis of the one-stage recognition procedure

known word in Fig. 1, whereas $D^*(I-1, J-1)$ for the optimal path in Fig. 2 gives no information about the unknown sequence of words.

The one common element in both problems (from Figs. 1 and 2) is that the global distance (i.e. the sum of the local distances along the path) is the criterion for the matching procedure. From the optimal path the searched sequence of templates can be uniquely recovered (see Fig. 2).

The method to be described will be illustrated by means of a hypothetical example presented in Fig. 3a. Let us consider the vocabulary set composed of three words: $A = (a s s)$, $B = (b a s)$, $C = (c o o)$, where for the sake of simplicity letter notations are used with reference to the sequence of vectors describing the speech. In the example each of the words consists of three vectors (letters), whereas in reality one vector corresponds to the 10–20 ms. of speech making the words more cumbersome. For the same



b)

	a'	o'	b'	s'	c'
a	-	1	2	3	3
o	1	-	2	3	3
b	2	2	-	2	2
s	3	3	2	-	1
c	3	3	2	1	-

FIG. 3. Hypothetical example with an unknown utterance $X = (c'o'b'o's'a'a's's')$ and reference words: A, B, C. Local distances between the vectors are presented in Fig. b.

reason, the unknown utterance X is also presented in the simplified form, i.e. $X = (c' \ o' \ b' \ o' \ s' \ a' \ a' \ s' \ s')$.

Following the calculation of all necessary local distances involved according to the data in Fig. 3b where, for example, the distance between the vowels /a/ and /o/ equals 1, the problem can now be formulated as follows: how to use the dynamic programming technique in order to find such a path connecting one of the initial points (marked by o) with one of the terminal points (marked by $*$), for which the sum of local distances along this path attains its minimal value.

In order to use the DP technique, it is necessary to supplement the DP equations (1) for the parts corresponding to the transition from the end of one template to the beginning of the next one. It is evident that the path may attain the point (i, j) (except the initial ones) from the following points: $(i-1, j)$, $(i-1, j-1)$, $(i, j-1)$ (see Fig. 4a). The initial points (see Fig. 2) can be reached from the point $(i-1, j)$, or, which is the above mentioned supplement, from the terminal point of any template including the same template (Fig. 4b). In these cases Eq. (1) must be supplemented with the following equations which applies to the initial points

$$D(i, j) = d(i, j) + \min \begin{cases} D(i-1, j) \\ D(i-1, j_{k,1}) \\ D(i-1, j_{k,w}) \\ D(i-1, j_{k,w}) \end{cases} \quad (2)$$

where $j_{k,w}$ indicates the terminal point of the w -th template.

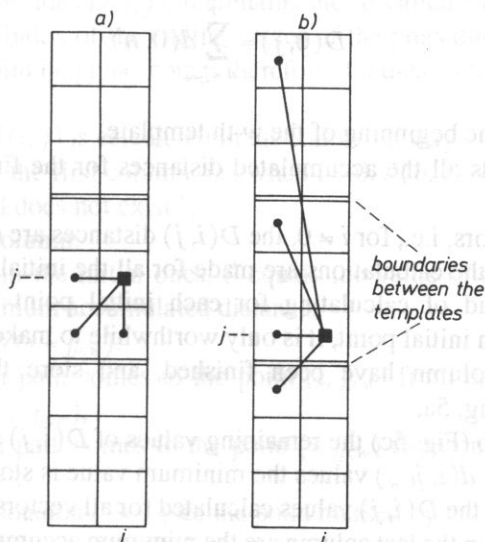


FIG. 4. Illustration of Eq. (1) for noninitial points (Fig. a) and Eq. (2) - for initial ones (Fig. b).

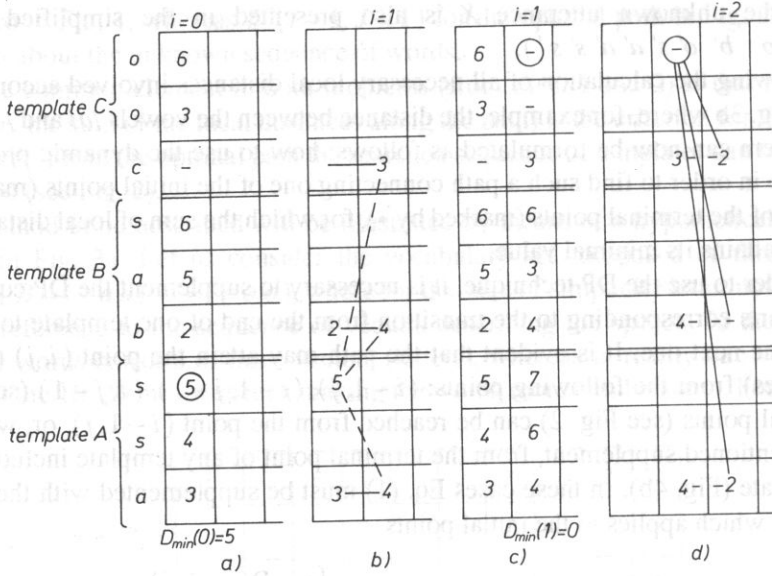


FIG. 5. Some initial steps of the calculations for the example from Fig. 3a.

Figure 5 presents some initial steps of calculations, for the example from Fig. 3a. All the calculations, except the column indexed as $i = 0$, are realized according to Eqs. (1) and (2). For $i = 0$, due to the fact that the optimal path reaches the point $(0, j)$ always from the point $0, j - 1$, except for $j = j_{p,w}$ which is treated as initial for the path, the minimal accumulated distances $D(i, j)$ are calculated as follows:

$$D(0, j) = \sum_{n=j_{p,w}}^j d(0, n) \quad (3)$$

where $j_{p,w}$ indicates the beginning of the w -th template.

Figure 5a presents all the accumulated distances for the first vector ($i = 0$) of the incoming speech.

For all other vectors, i.e., for $i \neq 0$, the $D(i, j)$ distances are calculated in two steps: at first (Fig. 5b), the calculations are made for all the initial points according to Eq. (2). Note that instead of calculating for each initial point the minimum from all $D(i - 1, j_{k,w})$ for each initial point, it is only worthwhile to make it after the calculations for the preceding column have been finished, and store this minimum value as $D_{\min}(i - 1)$ - see Fig. 5a,

in the second step (Fig. 5c) the remaining values of $D(i, j)$ are calculated according to Eq. (1). Among all $d(i, j_{k,w})$ values the minimum value is stored as $D_{\min} i$.

Figure 6 presents the $D(i, j)$ values calculated for all vectors of unknown utterances. The circled numbers in the last column are the minimum accumulated distances from the

template A	o	6	-	2	2	5	5	5	8	(8)
	o	3	-	2	2	5	4	5	8	5
	c	-	3	2	5	3	4	7	6	2
template B	s	6	6	4	4	1	4	6	3	(3)
	a	5	3	2	1	4	3	3	6	6
	b	2	4	-	2	4	3	5	7	3
template A	s	5	7	6	7	3	6	7	1	(1)
	s	4	6	4	5	3	4	4	1	1
	s	3	4	2	3	5	1	1	4	4
		0	1	2	3	4	5	6	7	8
		c'	o'	b'	o'	s'	a'	a'	s'	s'
		unknown utterance								

FIG. 6. All $D(i, j)$ values for all the vectors of an unknown utterance.

beginning to the end of the utterance, assuming that the last words in the utterance are: A, B or C. It should be noted that $D^*(X, A) = 1$, $D^*(X, B) = 3$, $D^*(X, C) = 8$.

Since the minimal accumulated distance applies to the case when the last word is A ($D_{\min} = 1$), it can be recognized as the last word in an unknown sequence. Unfortunately it is impossible to recognize the remaining part of the utterance on the basis of only the data from Fig. 6. To allow for additional data, let us consider the table in Fig. 7a. For each point (i, j) , besides $D(i, j)$, it contains the so-called backpointer $i'(i, j)$ which can be defined as the index of the ending vector of the preceding word from which the optimal path to the point (i, j) has come; therefore it indicates the position of the end of the preceding word.

The backpointer $i'(i, j)$ is calculated in the following way:

for all the points of the first column, i.e. when $i = 0$, $i'(0, j) = \text{"-"}$. The "-" indicates - "the preceding word does not exist",

for the remaining column:

for points other than the initial ones, i' equals the value of i' from the point which Eq. (1) gives the minimum accumulated distance,

for the initial points ($j = j_{p,w}$):

- if the optimal path comes to the point $(i, j_{p,w})$ from the point $(i-1, j_{p,w})$, the $i'(i, j_{p,w})$ equals $i'(i-1, j_{p,w})$,

- if the optimal path comes to the point $(i, j_{p,w})$ from one of the terminal points $(i-1, j_{k,w})$ the $i' = i-1$.

For example, the notation $i' = 1$ (see the point marked by the asterisk in Fig. 7a) indicates that the last precedent terminal point on the optimal path which comes to the

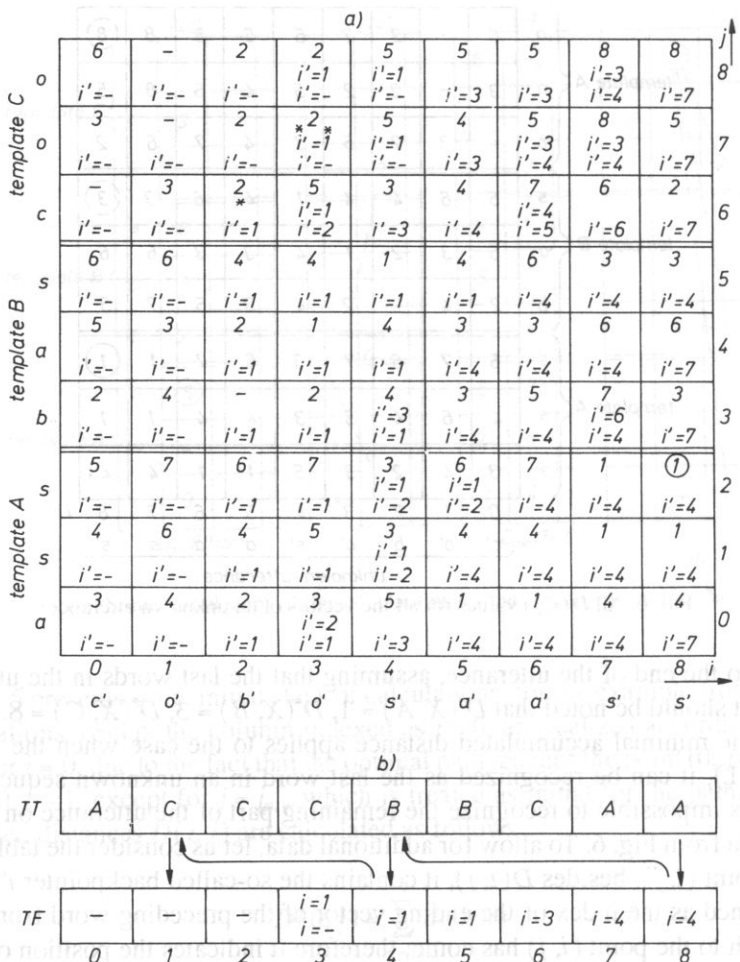


FIG. 7. Table of $D(i, j)$ values supplemented by the backpointers $i'(i, j)$ - Fig. a. Tables TT and TF for the above example - Fig. b.

marked point had appeared in the first ($i = 1$) column. In Fig. 7a the optimal path comes to the point (2, 6) from the terminal point of the template of the word C for which the accumulated distance is minimum.

The point marked by a double asterisk presents the situation when two different backpointers must be stored.

Figure 7b presents two additional tables: TT and TF . Each time after the calculations for the i -th vector have been finished, it may be assumed that this is the last vector of the utterance. In the i -th position of the table TT , i.e., $TT(i)$, the number of this template for which the terminal point attains minimum is stored; $TT(i)$ indicates the last most likely word in the incoming speech which terminates with the current vector.

In the $TF(i)$ the value of the i' from the terminal point which has the minimum $D(i, j_{k,w})$ should be rewritten.

The pair $\{TT(i), TF(i)\}$ indicates which word ends the utterance, assuming that the i -th vector is the last one, and which vector was the last in the precedent word.

After both tables are completed, the recognition process is trivial. In the example from Fig. 7 the position $TF(8)$ indicates the word *A* as the last word in the utterance. The $TF(8)$ indicates the last vector of the precedent word, which was the 4-th vector. It ended the word *B* because $TT(4)$ contains the code of the word *B*. The $TF(4)$ indicates the ending vector ($TF(4) = 1$) for the third word from the end of the utterance. It is evident that it was the word *C*, and that no other word preceded the word *C* ($TF(1) = "-"$).

Hence the sequence of the templates $\{CBA\}$ is most likely to be unknown utterance. The accumulated distance $D_{min} = 1$ results from the incorrect analysis of the word "bas" which has been identified as "bos". Note that in Fig. 3 b the $d(a, o) = 1$.

It should be noted that on the basis of the data in the tables TT and TF more than one decision can be made. Let us suppose that the 4-th vector of the speech agrees with the end of the utterance. From the $TF(3)$ it results that the word *C* is the last word in the sequence and that:

- the precedent word does not exist - it applies to the case when $TF(3) = "-"$, or
- the precedent word exists and ends with the second vector $TF(3) = 1$. From the $TT(1)$ it results that it is also the word *C*.

These decisions can be interpreted as follows: it was the word *C* with the drawled out vowel /o/ ("cooo"), or there were two words: *CC* ("co co"). In both cases illustrated in Fig. 8 $D_{min} = 2$ because of $d(b, o) = 2$ (in the first case) or $d(b, c) = 2$ (in the second one).

	first case ($i' = -$)				second case ($i' = 1$)			
utterance	" c	o	b	o "	" c	o	b	o "
	=	=	≠	=	=	=	≠	=
decision	" c	o	o	o "	" c	o	" c	o "
	$d(b, o) = 1$				$d(b, c) = 1$			

FIG. 8. Illustration of two possible optimal decisions.

3. Some aspects of the method

Let us note that for the vocabulary set composed of 64 templates, when each template is the sequence of 32 vectors, the table in Fig. 7a must have 64 (templates) $\times 32$ (vectors per template) $\times 250$ (number of vectors in the utterance of 5 s. duration) $\times 2$ (parameters: $D(i, j), i'$) = ca 1 MB storage locations.

It is easy to mention that the calculations connected with the i -th vector require only the data from the column $i - 1$. It decreases considerably the storage requirements but only on condition that all the calculations are finished before the vector $i + 1$ comes. Most frequently it is maximum 20 ms. For the data as above (64 templates, 32 vectors per template) the time required for $d(i, j), D(i, j), i'(i, j)$ calculations is about 10 μ s.

The number of 2048 $d(i, j)$ calculations (64×32) can be considerably reduced after the vector quantization (VQ) procedure [2]. The use of rather "economical" 8-bit VQ yielded, for example, in [9] only 0.4% of the recognition quality deterioration. Note that 8-bit VQ implies 8 times fewer $d(i, j)$ calculations - 256 instead of 2048.

The next practical aspect concerns the following theorem: if for the i -th column it occurs that $i' = c$ for all j (see Fig. 7a), then the c -th vector of an utterance is the ending vector of some word in this utterance. The proof is very simple; the identical value of c signifies that independently of the point through which the optimal path crosses the i -th column, the previous word ends with the c -th vector.

The above theorem allows to recognize the word before the end of the whole utterance.

4. Experiments and results

Figure 9 presents a block diagram of the experimental system. This system is based on the IBM PC/AT microcomputer with additional blocks connected to the AT bus: analog/digital converter ADC, spectrum analyzer FFT, specialized block MPD for some DP calculations introduced in order to perform real time recognition for a 10-word vocabulary set.

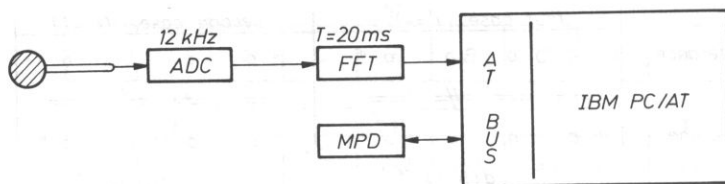


FIG. 9. Block diagram of the experimental system.

The speech signal is sampled at a 12 kHz rate with a 12 bit code, and the FFT is carried out every 20 ms. The output of the FFT is transformed into an 8 channel spectrum in the frequency range $200 \text{ Hz} \div 6 \text{ kHz}$.

In the learning phase (see Fig. 10) the isolated words are stored in memory. After all the words are completed, which implies several hundreds of speech vectors, the 64 cluster search procedure and vector quantization (VQ) procedure are initialized.

In the result, the description of word templates is 8 times reduced; 8 bytes of each spectrum is replaced by a 6-bit number (index) of the nearest cluster obtained by averaging all of the vectors (spectrums) belonging to this cluster.

After the VQ procedure and linear normalization to the length of N numbers ($N = 16 \div 32$), the word templates are stored in MPD block. Another advantage from the

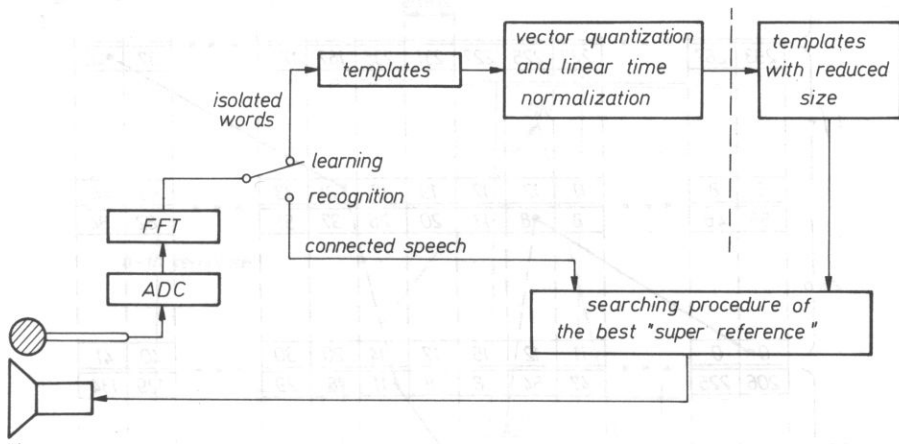


FIG. 10. Functional block-diagram of the experimental system.

VQ procedure is that instead of calculating 160 to 320 local distances between the current vector of incoming speech and all vectors creating word templates (16 to 32 spectrums for each template) only 64 distances should be calculated. These 64 local distances form the table of local distances. The values of $d(i, j)$ in Eq. (1) are taken from the table according to the vector's index in the template.

In our experiment the number of 64 clusters was sufficient from the point of view of the recognition score and was found to be maximum to recognize the connected word in real time.

In the real time systems the recognition procedure starts after the first vector of an utterance is obtained. All the necessary calculations must be finished before the next incoming vector, i.e., in 20 ms. These calculations include:

- calculations of 64 local distances,
- calculations of 10 accumulated distances $D(i, j)$ and 10 backpointers $i'(i, j)$ for the initial points according to (2),
- calculations of 150–310 accumulated distances $D(i, j)$ and 150–310 backpointers for all other points according to (1),
- calculation of $TT(i)$ and $TF(i)$.

The calculations of $D(i, j)$ according to (1) were performed by the hardware, realized by a specialized circuit on the MPD block in one instruction cycle of the microcomputer. This was possible because the memory for accumulated distances and backpointers was also situated on the MPD block.

The first experiments demonstrated the need to introduce the template of pause for two reasons:

- the recognized utterance can include some short pauses between words,
- if a vocabulary set contains words beginning with affricates, the short pause characteristic of such a consonant can appear, which does not exist in other templates. As the example of such a case, Fig. 11 presents the simplified (i.e., containing only the initial and terminal points for each template) table with the $D(i, j)$ values for several vectors of

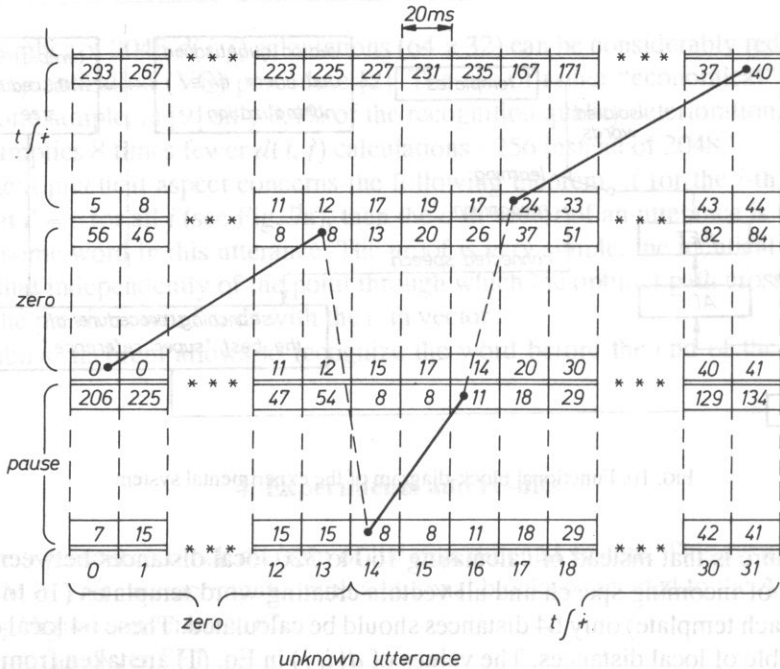


FIG. 11. Part of the table containing $D(i, j)$ values for the utterance /zerotʃi/ and the optimal warping function. The template of the word /tʃi/ uttered in isolation in the learning phase does not contain the pause.

a real utterance “zerotʃi”. The optimal path contains the part (vectors 14+16) corresponding to the 60 ms of the pause made by stopping the air completely at the beginning of the affricate /tʃ/. In Fig. 11 only the templates for the pause, and the words “zero”, “tʃi” are shown. Since the subject of our experiments was the presented method, and not the parametrization level, only three words were chosen to create the 10 word vocabulary set. It contains the template of pause, and three repetition of these three words: “zero”, “tʃi”, “tʃteri”.

The recognized set contained all (81) combinations in four-word utterances repeated twice by the same speaker.

The results of the recognition of 162 sentences are presented in Table 1.

In the first experiment the normalized length of each template was equal to 32 vectors, and the “block city” metric was used to calculate the distance between either two vectors. In this experiment 10 words were deleted.

The detailed analysis has shown that these deletions occur when the word uttered in a phrase is much shorter than its templates. Figure 12 presents an example when a part of the phrase contains two of the same words, but the first one was uttered in a very fast manner. A much smaller number of local distances on the path d_1 towards the path d_N , can result in $D_1 < D_N$, and in effect the optimal path runs along the path marked by the solid line rather than along the path marked by the dashed line. The first word will be deleted because the backpointer in the point $(1, i + 1)$ will be different from i .

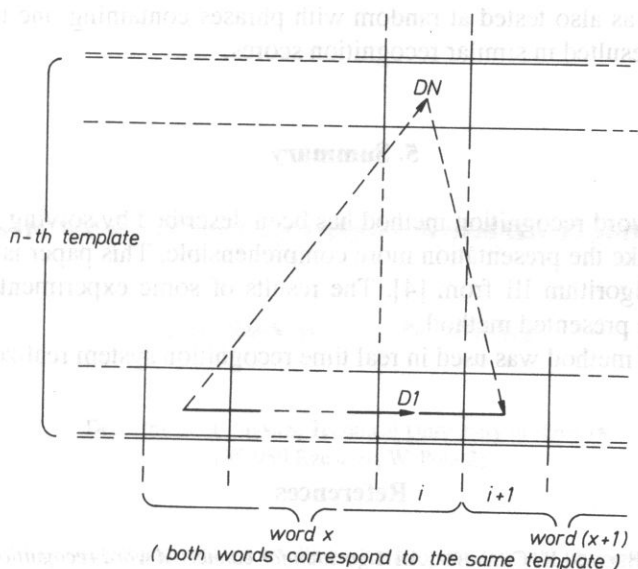


FIG. 12. Simplified figure for a word deletion mechanism.

The above case was caused by the parametrization level (8 digital filters), for which the average distances between the vectors belonging to different phonetic classes were insufficiently greater than the distances between the vectors belonging to the same phonetic class.

In order to confirm this fact in the second experiment the nonlinear "city" metric was used. The distances smaller than a certain threshold was replaced by zero. The threshold was chosen as the average distance between the vectors belonging to the same phonetic class. The above nonlinearity diminished the number of deletions to 4 cases.

Another way to solve the problem connected with quickly uttered words consists in experiments III and IV in shortening the length of the templates to 16 vectors instead of 32. In experiment IV with nonlinear "city" metric any deletion was noted. The recognition score for the phrases was about 99,4% - the word "zero" was misidentified as "tjteri".

Table 1. Results of the recognition of 162 four-word sentences

Experiment	Normalized length	Metric	Deleted	Misidentified
I	32	lin.	10	—
II	32	nonlin.	4	—
III	16	lin.	3	—
IV	16	nonlin.	—	1

The method was also tested at random with phrases containing one to nine words. These tests have resulted in similar recognition scores.

5. Summary

A connected word recognition method has been described by solving the hypothetical problem to make the presentation more comprehensible. This paper is a detailed description of the algorithm III from [4]. The results of some experiments confirm the effectiveness of the presented method.

The described method was used in real time recognition system realized under grant CPBR 7.1.

References

- [1] J. BRIDLE, M. BROWN, R. CHAMBER, *An Algorithm for connected word recognition*, Proc. ICASSP 1982, pp. 899–902.
- [2] R.M. GRAY, *Vector quantization*, IEEE ASSP Mag., 1, 2, pp. 4–29 (1984).
- [3] S. GROCHOLEWSKI, *Dynamic programming in automatic speech recognition* (in Polish), Elektrotechnika (AGH), 4, 1, pp. 106–126 (1985).
- [4] S. GROCHOLEWSKI, *Algorithms for connected word recognition – A global approach*, Archives of Acoustics, 16, 3/4, pp. (1991).
- [5] C.S. MYERS, L.R. RABINER, *A level building dynamic time warping algorithm for connected word recognition*, IEEE Trans. ASSP, 29, 2, pp. 284–297 (1987).
- [6] H. NEY, *The use of a one-stage dynamic programming algorithm for connected word recognition*, IEEE Trans. ASSP, 32, 2, pp. 263–271 (1984).
- [7] H. SAKOE, *Two-Level DP Matching – A dynamic programming based pattern matching algorithm for connected word recognition*, IEEE Trans. ASSP, 27, 6, pp. 588–595 (1979).
- [8] H. SAKOE, S. CHIBA, *Dynamic programming optimization for spoken word recognition*, IEEE Trans. ASSP, 26, 2, pp. 43–49 (1978).
- [9] N. SUGAMURA, S. FURUI, *Speaker-Dependent Large Vocabulary Word Recognition Using SPLIT Method*, Review of the Electrical Communications Laboratories, 34, 3, pp. 327–332 (1986).
- [10] T.K. VINTSYUK, *Element-wise recognition of continuous speech composed of words from a specified dictionary*, Kibernetika, 7, 2, pp. 133–143 (1971).

Received on January 10, 1990

ACOUSTIC WAVE DAMPING ANISOTROPY IN NEMATIC LIQUID CRYSTALS

H. HERBA and A. DRZYMAŁA

Department of Physics, Technical University in Rzeszów
(35-959 Rzeszów, W. Pola 2)

This paper presents the results of damping and velocity measurements of an ultrasonic wave with 5 MHz frequency performed in two nematic liquid crystals: pentylcyanobiphenyl (PCB) and 4-n-methoxybenzoate-4-n-pentylphenyl. Measurements were carried out in materials oriented with an external magnetic field.

An acoustic wave damping anisotropy was observed. It manifested itself with a dependence between the damping coefficient and angle between the direction of wave propagation and the direction of the magnetic field which orientates the material.

The obtained results were confronted with the results of rheological measurements carried out for mentioned materials by other authors.

1. Introduction

Theoretical foundations of the rheology of nematic liquid crystals, treated as incompressible liquids, have been formulated by ERICKSEN and LESLIE [1, 2, 3], as well as PARODI [4]. Flows of the nematic without the assumption of its incompressibility have been considered by FOSTER and collaborators [5], and HUANG [6]. Foster and his collaborators have also introduced a relation describing the behaviour of the ultrasonic wave damping coefficient in terms of the angle θ between the direction of propagation of the sound wave and the orientation direction of the nematic. This relationship can be expressed as follows

$$\alpha(\theta) = \frac{\omega^2}{2\rho c^3} \left\{ \left[(2\nu_1 + \nu_2 - \nu_4 + 2\nu_5 + \left(\frac{1}{c_v} - \frac{1}{c_p}\right) \kappa_{\parallel}) \right] - \left[2(\nu_1 - \nu_4 + \nu_5) + \left(\frac{1}{c_v} - \frac{1}{c_p}\right) (\kappa_{\parallel} - \kappa_{\perp}) \right] \sin^2 \theta + - \frac{1}{2} (\nu_1 + \nu_2 - 2\nu_3) \sin^2 2\theta \right\} \quad (1)$$

Where: ν_i ($i = 1, \dots, 5$) – coefficients expressed in viscosity units, κ_{\perp} – heat conduction in a direction perpendicular to the orientation direction of molecules, κ_{\parallel} – heat conduction in a direction parallel to the orientation direction of molecules, ω – wave frequency, ρ – density of the nematic, c – wave velocity.

Expression (1) changes into a known expression for an isotropic liquid if:

$$\begin{aligned}\nu_1 &= \nu_2 = \nu_3 = \eta_s, \\ \nu_5 &= \nu_4 - \nu_2 = \eta_v - 2/3 \eta_s, \\ \kappa_{\perp} &= \kappa_{\parallel} = \kappa,\end{aligned}\quad (2)$$

where: η_s – shear viscosity, η_v – volumetric viscosity, κ – heat conductivity. Substituting in the expression (1), we have:

$$\begin{aligned}A &= \frac{\omega^2}{2\rho c^3} \left[2\nu_1 + \nu_2 - \nu_4 + 2\nu_s + \left(\frac{1}{c_v} - \frac{1}{c_p} \right) \kappa_{\parallel} \right], \\ B &= \frac{\omega^2}{2\rho c^3} \left[2(\nu_1 - \nu_4 + \nu_5) + \left(\frac{1}{c_v} - \frac{1}{c_p} \right) (\kappa_{\parallel} - \kappa_{\perp}) \right], \\ C &= \frac{\omega^2}{2\rho c^3} \frac{1}{2} (\nu_1 + \nu_2 - 2\nu_3).\end{aligned}\quad (3)$$

It is clear that:

$$\begin{aligned}\alpha(0) &= A, \quad \alpha(\Pi/2) = A - B, \\ \Delta\alpha &= \alpha(0) - \alpha(\Pi/2) = B.\end{aligned}\quad (4)$$

Foster's theory does not include velocity anisotropy. The occurrence of this phenomenon for high frequencies (7) can be caused by the fact that the reaction of the material to compression requires a definite amount of time. If the period during which compression is applied is short in comparison with this time, then compressibility can be anisotropic.

2. Measuring apparatus

An original ultrasonic system was used to perform measurements. It made possible damping and velocity measurements of an ultrasonic wave in liquid crystals. An external magnetic field was applied to orientate the material. The mechanical system including ultrasonic transducers and measuring vessel is considerably miniaturized and the ultrasonic wave propagates horizontally. This makes it easier to apply typical electromagnets. The minimal distance between pole shoes necessary to place the device in the magnetic field is equal to 80 mm. The block diagram of the system is presented in Fig. 1. This system was made in the Institute of Fundamental Technological Research of PAS in Warsaw. Temperature stabilization not worse than 0.1°C was achieved by using an ultrathermostat. Damping and velocity of the ultrasonic wave were measured with the application of a magnetic field with induction of 0.7 T.

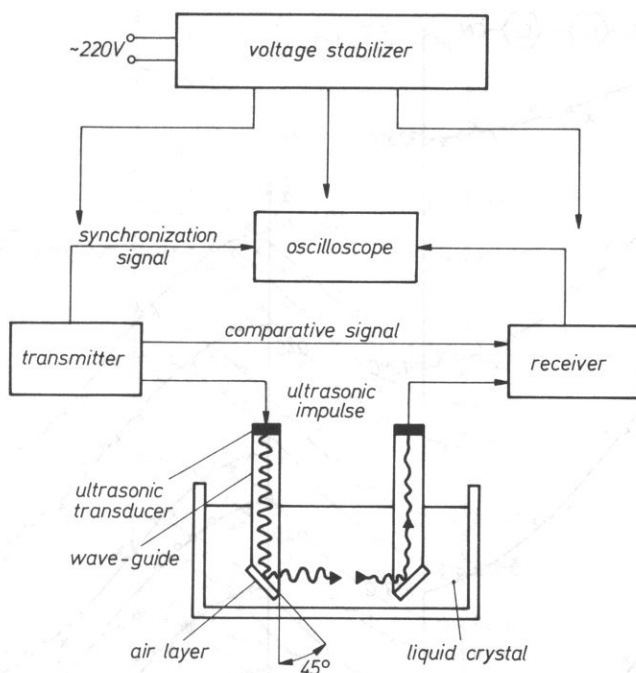


FIG. 1. Block diagram of the system for ultrasonic wave damping and velocity in liquid crystals.

3. Characteristic of tested liquid crystals

Measurements were performed for two nematic liquid crystals: p-pentyl-p'-cyano-biphenyl (PCB) and 4-n-methoxybenzoate 4-n-pentylphenyl (MBPP). Structural formulae and phase transition of tested materials are given in Table 1.

Table 1.

Material	Method	Phase trans. temperature [°C]	
		solid state nematic	nematic isotropic
p-pentyl-p'-cyanobiphenyl $C_5H_{11}-\langle \overline{O} \rangle - \langle \overline{O} \rangle - CN$	Microscopic observation (cooling)	18,9	33,9
	DSC (heating)	—	35,0
4-n-methoxybenzoate-4n-pentylphenyl $C_5H_{11}-\langle \overline{O} \rangle - COO - \langle \overline{O} \rangle - OCH_3$	Microscopic observation (cooling)	25,1	40,4
	DSC (heating)	—	41,3

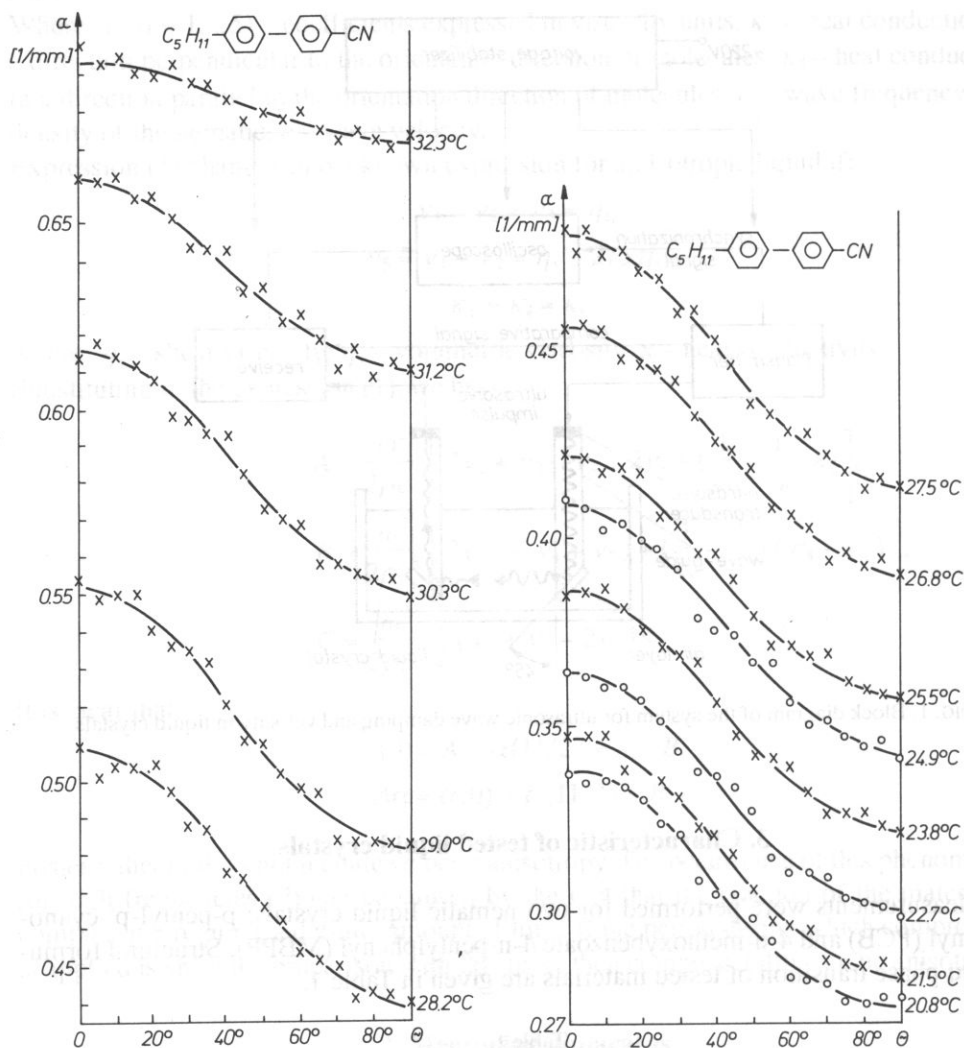


FIG. 2. Results of damping measurements for an ultrasonic wave with 5 MHz frequency in PCB material.

4. Ultrasonic wave damping and velocity measurements

Damping and velocity were measured for an ultrasonic wave with 5 MHz frequency in terms of temperature and angle between the direction of wave propagation and direction of orientating magnetic field. Their relation (1) was matched using the method of least squares with results achieved at a given temperature and quantities A , B and C were determined (Formula (3)). Measurement results for PCB and 4-n-methoxybenzoate 4-n-pentylphenyl are presented in Figs. 2 and 3, respectively. Full curves in Figs. 2 and 3 are

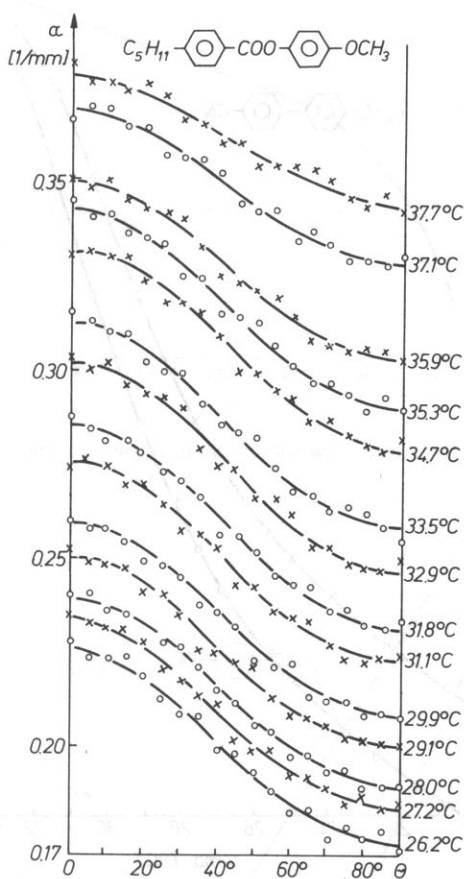


FIG. 3. Results of damping measurements for an ultrasonic wave with 5 MHz frequency in 4-n-methoxybenzoate-4-n-pentylphenyl.

described with Eq. (1). The determined quantities A and B have a simple physical sense. Quantity A corresponds with the value of ultrasonic wave damping for angle $\theta = 0^\circ$, while value $A - B$ with this value for angle $\theta = 90^\circ$. The B/A ratio defines damping anisotropy. The values A , $(A - B)$ and B/A in terms of temperature is shown in Figs. 4 and 5 for PCB and Figs. 6 and 7 for 4-n-methoxybenzoate-4-n-pentylphenyl. Standard deviation of A and $A - B$ quantities, calculated on the basis of matching the expression (1) and experimental data with the method of least squares are marked in Figs. 4 and 6.

Once the quantities A and B are known, the coefficients of volumetric viscosity, ν_4 and ν_5 , can be calculated. However, this requires knowledge of the coefficients for shear viscosity, ν_1 , ν_2 , ν_3 , and the coefficients of heat conductivity, κ_1 and κ_1 . In the case of most liquids the contribution of heat conductivity in ultrasonic wave damping is small in comparison with the contributions of shear viscosity and volumetric viscosity.

The estimation of the influence of heat conductivity was impossible because of the lack of complete data for tested materials. Such an estimation can be carried out for

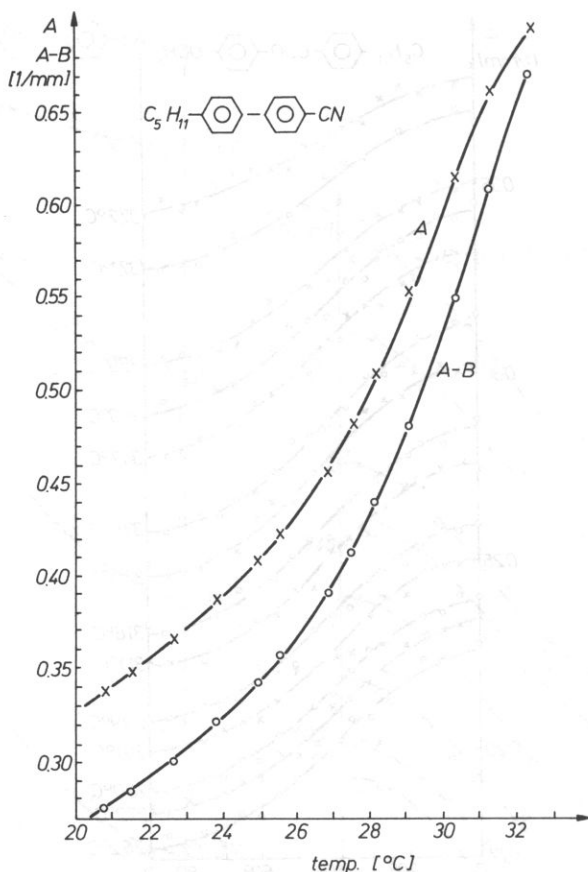


Fig. 4. Temperature dependence of quantities A and $A-B$ for PCB (5 MHz).

nematic MBBA on the basis of data from papers [7, 8]. For this material at 30°C the temperature of heat conductivity is equal to 0.32% in quality B .

As for volumetric viscosities, the presented contributions of heat conductivity are many times smaller. For this reason we can accept that the influence of heat conductivity for tested materials is negligibly small as for MBBA and most liquids. The authors have determined the coefficients of shear viscosity for PCB and 4-*n*-methoxybenzoate-4-pentylphenyl by testing the flow of the material oriented with a magnetic field through a capillary with a rectangular section [9]. Taking the coefficients of shear viscosity given in [9] into consideration, the quantities ν_4 and ν_5 were calculated.

The velocity of an ultrasonic wave necessary to determine ν_4 and ν_5 was measured using the pulse-phase method with the application of the previously described system. The results of velocity measurements are presented in Figs. 8 and 9. The temperature dependence of volumetric viscosity is illustrated in Figs. 10 and 11. Quantity C (Expression (3)) depends only on the coefficients of shear viscosity. Adequate comparisons were made using the quantities given in the paper. The results of these comparisons are shown in Figs. 12 and 13. Also measuring errors are included in these figures.

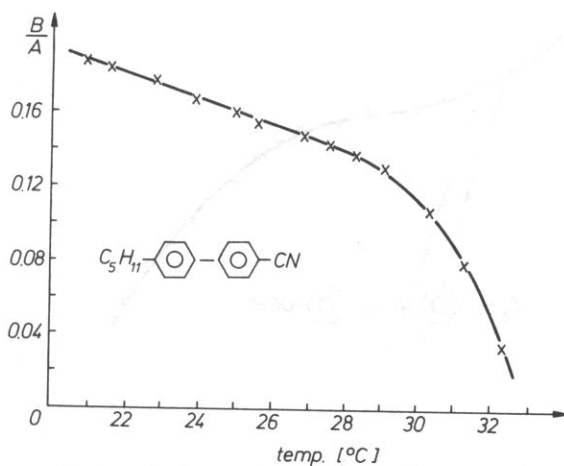


FIG. 5. Damping anisotropy of an acoustic wave with 5 MHz frequency in PCB.

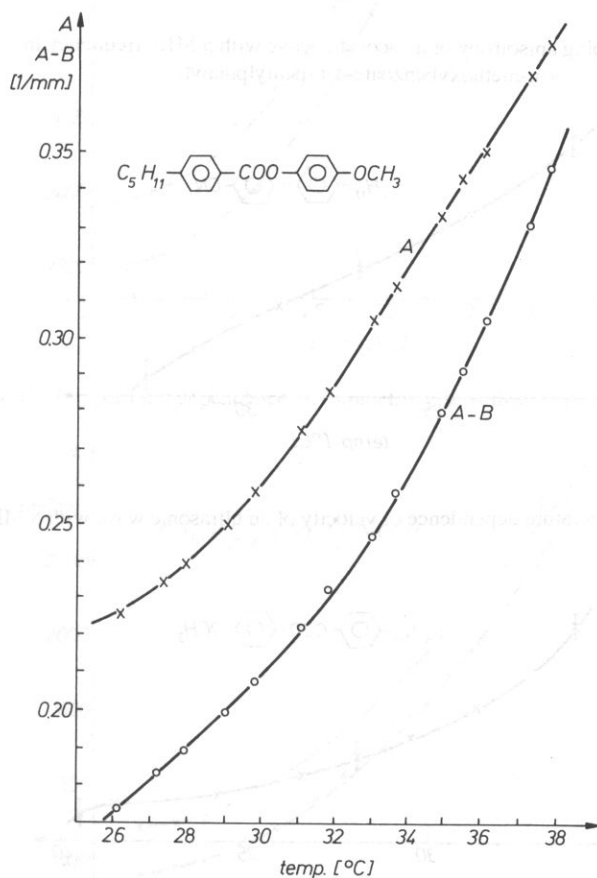


FIG. 6. Temperature dependence of quantities A and $A-B$ for 4-n-methoxybenzoate-4-n-pentylphenyl (5 MHz).

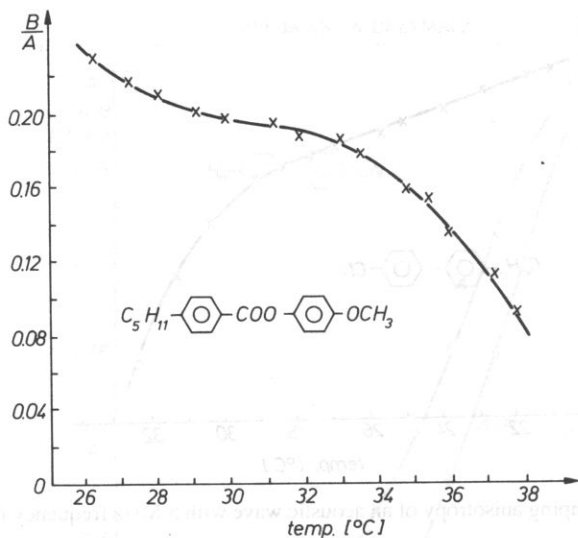


Fig. 7. Damping anisotropy of an acoustic wave with 5 MHz frequency in 4-n-methoxybenzoate-4-n-pentylphenyl.

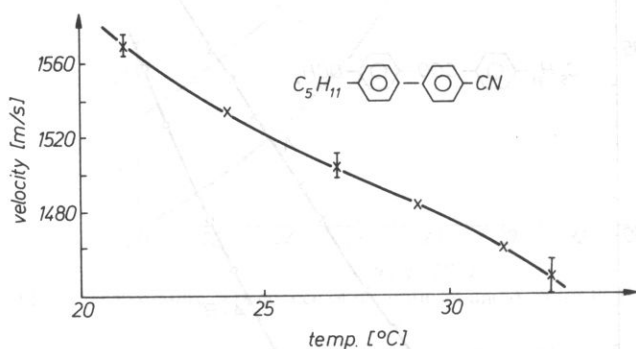


FIG. 8. Temperature dependence of velocity of an ultrasonic wave with 5 MHz for PCB.

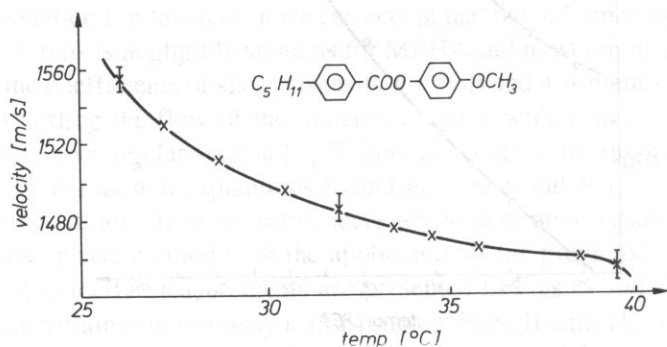


Fig. 9. Temperature dependence of velocity of an ultrasonic wave with 5 MHz frequency for 4-n-methoxybenzoate-4-n-pentylphenyl.

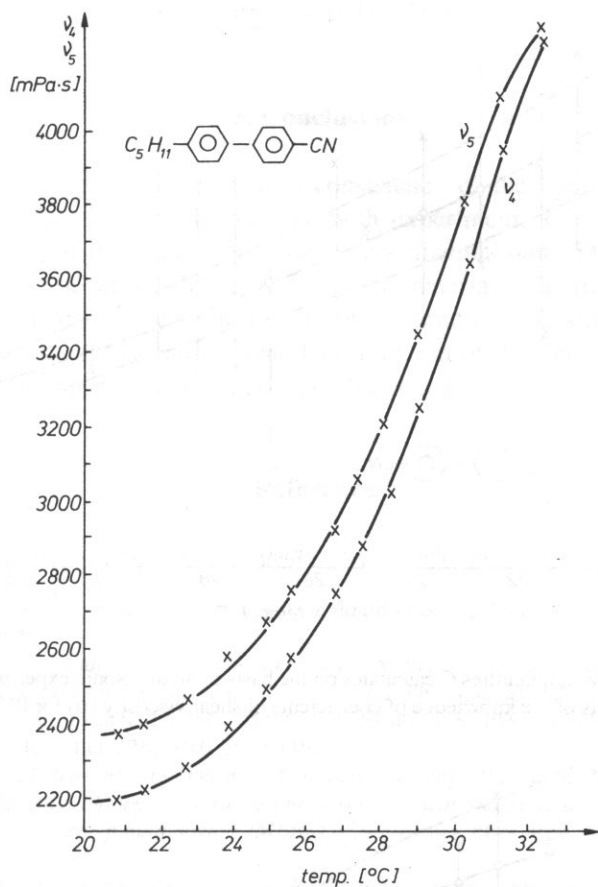


FIG. 10. Temperature dependence of volumetric viscosities for PCB.

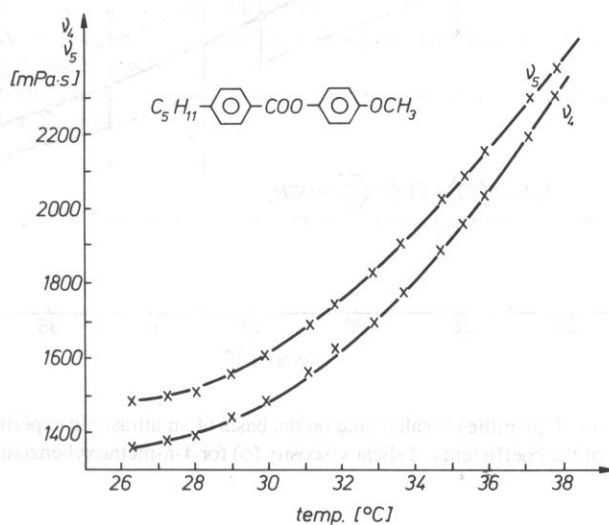


FIG. 11. Temperature dependence of volumetric viscosities for 4-n-methoxybenzoate-4-n-pentylphenyl.

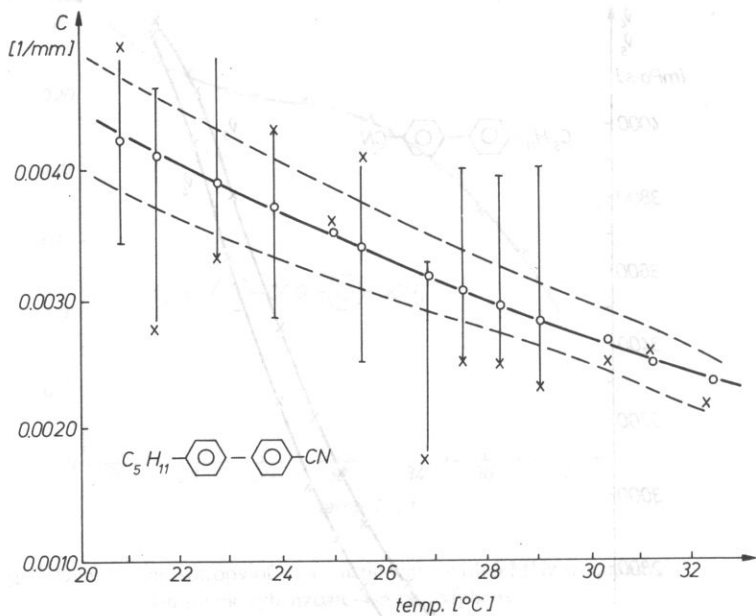


FIG. 12. Comparison of quantities C calculated on the basis of an ultrasonic experiment (x) and on the basis of the knowledge of coefficients of shear viscosity (o) for PCB.

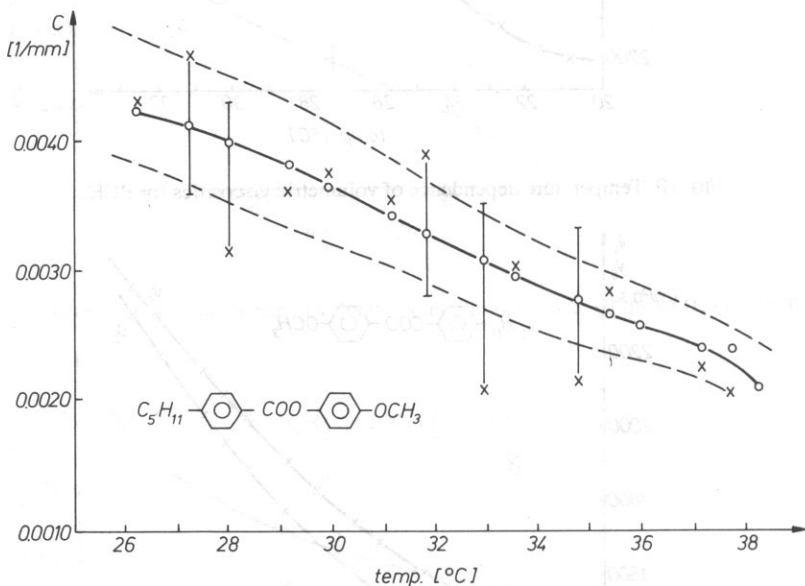


FIG. 13. Comparison of quantities C calculated on the basis of an ultrasonic experiment (x) and on the basis of knowledge of the coefficients of shear viscosity (o) for 4-n-methoxybenzoate-4-n-pentylphenyl.

5. Conclusions

The presented measurements prove a consistency of the hydrodynamic theory of FOSTER and co-author [5]; and HUANG [6] with experiment. This is indicated by the quality of matching of theoretical curves and experimental data. The anisotropy of the damping coefficient of ultrasonic waves for tested materials in experimental conditions 5 MHz is caused mainly by the anisotropy of volumetric viscosities which are many times greater than shear viscosities. The determination of volumetric viscosities is important [10] for further research of acoustic absorption and relaxation processes in the presented materials.

References

- [1] J.L. ERICKSEN, *Hydrostatic theory of liquid crystals*, Arch. Ration. Mech. Analysis, **9**, 371–378, (1962).
- [2] F.M. LESLIE, *Some constitutive equations for liquid crystals*, Arch. Ration. Mech. Analysis, **28**, 265–283, (1968).
- [3] J.L. ERICKSEN, *Continuum theory of liquid crystals*, Applied Mech. Rev., **20**, 1029–1032, (1967).
- [4] O. PARODI, *Stress tensor for a nematic liquid crystal*, J. Physique, **31**, 581–584, (1970).
- [5] D. FORSTER, T.C. LUBENSKY, P.C. MARTIN, J. SWIFT, P.S. PERHAN, *Hydrodynamics of liquid crystals*, Phys. Rev. Lett., **26**, 1016–1019, (1971).
- [6] H.W. HUANG, *Hydrodynamics of nematic liquid crystals*, Phys. Rev. Lett., **26**, 1525–1527, (1971).
- [7] G. KOREN, *Thermal blooming measurement of specific heat and thermal conductivity in isotropic p-methoxy benzolide p-butalaniline (MBBA) near clearing*, Phys. Rev. A., **16**, No 3, 1177–1184, (1976).
- [8] H. KNEPPE, F. SCHNEIDER, N.K. SHARMA, *Rotational viscosity of nematic liquid crystals*, J. Chem. Phys., **77**, 3203–3208, (1982).
- [9] H. HERBA, A. DRZYMAŁA, *Experimental test of hydrodynamic theories for nematic liquid crystals*, Mol. Cryst. Liq. Cryst., **127C**, 153–158, (1985).
- [10] B. LINDE, A. ŚLIWIŃSKI, *Ultrasonic testing of organic liquids* (in Polish), Postępy fizyki molekularnej, **2**, 5–40, (1987).
- [11] H. HERBA, A. DRZYMAŁA, *Anisotropic attenuation of acoustic waves in nematic liquid crystals*, Liq. Cryst., **8**, 819–823, (1990).

Received on November 24, 1987, revised English version October 21, 1991

ACOUSTICAL PROPERTIES OF POROUS LAYER – UNDEFORMABLE HALFSpace SYSTEM AT NORMAL INCIDENCE OF HARMONIC WAVE

M. CIESZKO

Department of Mechanics of Porous Media
Institute of Fundamental Technological Research
Polish Academy of Sciences
(61-725 Poznań, Mielżyńskiego 27/29)

The acoustical properties of a system composed of a porous layer and an undeformable solid halfspace, immersed in a barotropic fluid, are analyzed for the case of normal incidence of a harmonic wave. The explicit forms of expressions of the wave absorption coefficients were obtained for different particular configurations of the system. This allowed us to discuss the dependence of the absorption coefficient on the dissipative properties of a fluid and on the parameters characterizing the pore structure of a porous layer, in a wide range of frequencies of the incident wave. It was shown that the dissipative properties of the fluid do not considerably change the value of resonance frequencies. However, these properties as well as the parameters of the skeleton pore structure strongly influence the coefficient of wave absorption.

1. Introduction

The determination of acoustical properties of systems composed of porous elements is of great importance in many technical problems occurring, for example, in aircraft and machinery noise control or in architectural acoustics. In these systems the porous material in the form of layers, plates or halfspaces (ground), immersed in a fluid, strongly interacts with waves propagating in the fluid in a wide range of frequencies.

The complexity of a theoretical investigation of the properties of such systems is connected with the variety of transfer ways of acoustic energy. In the general case of a deformable skeleton of porous material the acoustic waves are transmitted both by the skeleton and by the fluid filling its pores, and also by vibrational movement of particular elements of the system.

In the majority of papers devoted to the interaction of waves with porous material (e.g. [1], [7], [11], [13], [16]) and to the investigation of its properties (e.g. [2], [14],

[15]), the authors exploit the analogy between the propagation of plane waves in the absorbant media and the propagation of electric disturbances in the loss lines. They characterize the acoustical properties of a porous medium by two quantities: the propagation constant of a wave and the wave impedance. They also formulate the boundary conditions at the surface of a porous medium by means of the surface impedance. Some authors (e.g. [1], [16]) use at the same time the existing equations of the dynamics of porous media to determine the relations between the quantities and the parameters characterizing a porous medium filled with a fluid. Such a characteristic, although sufficient for the media which can be modelled as a modified fluid (the skeleton being undeformable), needs to be extended by other quantities in the case of a deformable skeleton [16].

The other approach, rarely presented in the papers on this subject, consists in solving the boundary problem formulated strictly within mechanical notions.

In spite of a great variety of papers concerning the interaction of acoustic waves with porous materials and with their systems in the literature, there is a lack of theoretical papers devoted to the analysis of the influence of the parameters characterizing the properties of porous media and the geometry of the system on its acoustical properties.

The main purpose of this paper is to analyze the acoustical properties of a system consisting of a rigid immovable porous layer and undeformable solid halfspace, immersed in a fluid, at the normal incidence of a harmonic wave.

The starting point for the description of the dynamics of a fluid in pores of a rigid skeleton are the equations of the two-parameter theory of deformable porous media filled with a fluid ([5], [6], [8–10]), in which the skeleton pore structure is characterized by two parameters: volume porosity and structural permeability parameter. These parameters are explicitly present in the continuity and motion equations of the fluid as well as in the boundary conditions representing the continuity of the fluid mass flux and its effective pressure at both surfaces of a porous layer.

Solving the boundary problem resulted in obtaining the explicit forms of the absorption, reflection and transmission coefficients of waves for different configurations of the system. This enabled us to discuss the dependence of these coefficients on the dissipative properties of the fluid filling the pores of the layer, on the pore structure parameters and the geometry of the system in a wide frequency range of the incident wave.

2. Interaction of a plane acoustic wave with the porous layer-undeformable halfspace system

Formulation of the problem.

We analyze the acoustical properties of the system consisting of a rigid immovable porous layer of thickness b immersed in a fluid at distance d from the undeformable solid halfspace. We consider the case when a plane harmonic wave of frequency f ($\omega = 2\pi f$) and of amplitude A_1 , propagating in a fluid, falls normally at the surface of the porous layer (Fig. 1.). We assume that the fluid is barotropic, i.e., the effective pres-

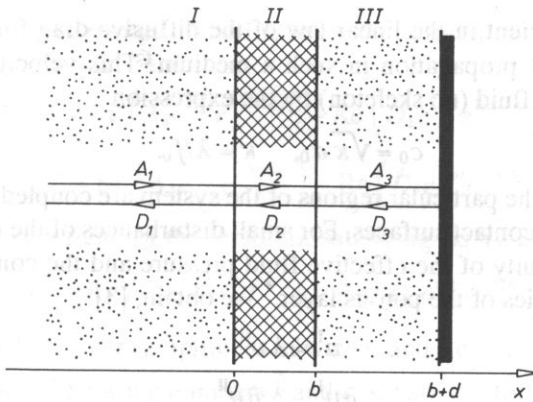


FIG. 1. Scheme of wave interaction with a system composed of a porous layer and undeformable solid halfspace.

sure p^f is in one to one relation with its effective mass density ρ^f ($p^f = p^f(\rho^f)$), and that the viscosity of the fluid does not influence its macroscopic state of stress (the deviators of the stress tensors in the bulk fluid and in the fluid filling porous medium are omitted) but it is taken into account in the interface interaction force with the porous skeleton.

At the above assumptions the propagation of disturbances with small amplitude in halfspace $x < 0$ (region I) and in the layer of the fluid (region III) is described by a linear wave equation for the barotropic fluid

$$\frac{\partial^2 v}{\partial x^2} = \frac{1}{a_0^2} \frac{\partial^2 v}{\partial t^2} \quad (2.1)$$

where v is the velocity of fluid particles and

$$a_0 = \left(\frac{dp^f}{d\rho^f} \right)^{\frac{1}{2}} \Big|_{\rho^f = \rho_0^f}$$

is the velocity of wave propagation in the bulk fluid, whereas ρ_0^f stands for its mass density in the undisturbed state of medium.

The description of fluid motion in the pores of an undeformable porous layer (region II) is based on the two-parameter theory of deformable porous medium filled with a fluid ([5], [6], [8–10]) in which the skeleton pore structure is characterized by two macroparameters: the volume porosity f_v and structural permeability parameter λ ($\lambda \leq f_v$). The problem of fluid motion in pores of an undeformable skeleton is then the particular case of this theory, and the equation describing the propagation of waves with small amplitude takes the form [3]

$$\frac{\partial^2 v}{\partial x^2} = \frac{1}{c_0^2} \left(\frac{\partial^2 v}{\partial t^2} + \bar{k} \frac{\partial v}{\partial t} \right), \quad (2.2)$$

$$\bar{k} = \bar{k}' / (\lambda \rho_0^f)$$

where \bar{k}' is the coefficient in the linear law of the diffusive drag force while c_0 is the velocity of wave front propagation in such a medium. This velocity is related to the velocity a_0 in the bulk fluid (no skeleton) by the expression

$$c_0 = \sqrt{\kappa} a_0, \quad \kappa = \lambda/f_v. \quad (2.3)$$

Acoustic fields in the particular regions of the system are coupled via the compatibility conditions at their contact surfaces. For small disturbances of the medium these conditions are: the continuity of the effective fluid pressure and the continuity of its mass fluxes at both boundaries of the porous layer.* We obtain, [3]

$$v^I = \lambda v^{II}, \quad (2.4)$$

$$\frac{\partial v^I}{\partial x} = \kappa \frac{\partial v^{II}}{\partial x} \quad (2.5)$$

for $x = 0$, and

$$\lambda v^{II} = v^{III}, \quad (2.6)$$

$$\kappa \frac{\partial v^{II}}{\partial x} = \frac{\partial v^{III}}{\partial x} \quad (2.7)$$

for $x = b$, where v^α ($\alpha = I, II, III$) is the resultant velocity field in the region α of the system.

An additional limitation for the velocity field v^{III} in the layer of the bulk fluid is the boundary condition at the surface $x = b + d$. Due to the underformability of halfspace $x > b + d$, we have

$$v^{III} = 0. \quad (2.8)$$

Equation (2.1) and (2.2) together with the conditions (2.4)–(2.8) describe the dynamic behaviour of the fluid in the system shown in Fig. 1. It is evident that apart from the parameters b , d and \bar{k} which characterize the geometry of the system and the dissipative properties of the fluid in its viscous interaction with the pores of the layer, the real influence on the acoustical properties of the system is exerted by the pore structure parameters of the porous layer. These parameters are explicitly present both in the motion equation (2.2) and compatibility conditions (2.4)–(2.7).

Solution of the problem

The resultant acoustic field in each region of the system consists of two waves propagating in opposite directions (Fig. 1). These waves are the superposition of all elementary waves with proper directions resulting from the subsequent reflection and transmission of the incident wave at the boundaries of the particular regions.

* Continuity conditions of this kind are analogical to the conditions imposed at places of a rapid change of the cross-section in the analysis of wave propagation in wave guides of stepwise-changing cross-sections [13].

The acoustic fields in regions I and III, being the solution of equation (2.1), may be represented by the functions

$$v^I = \operatorname{Re} \left(A_1 e^{i\omega t} e^{-2\pi i \hat{k} x} \right) - \operatorname{Re} \left(D_1 e^{i\omega t} e^{2\pi i \hat{k} x} \right). \quad (2.9)$$

$$v^{III} = \operatorname{Re} \left(A_3 e^{i\omega t} e^{-2\pi i \hat{k} x} \right) - \operatorname{Re} \left(D_3 e^{i\omega t} e^{2\pi i \hat{k} x} \right). \quad (2.10)$$

respectively, and such a field for the region II, satisfying Eq. (2.2), takes the form

$$v^{II} = \operatorname{Re} \left(A_2 e^{i\omega t} e^{-2\pi i k' x} \right) - \operatorname{Re} \left(D_2 e^{i\omega t} e^{2\pi i k' x} \right). \quad (2.11)$$

where A_α, D_α ($\alpha = 1, 2, 3$) are amplitudes of waves, and $\operatorname{Re}(\cdot)$ stands for the real part of a complex expression. The wave numbers \hat{k} and k' satisfy the following relations:

$$\hat{k} = f/a_0, \quad k'^2 = k^2(1 - ik_0/k) \quad (2.12)$$

where

$$k = f/c_0, \quad k_0 = \bar{k}/(2\pi c_0). \quad (2.13)$$

The expressions (2.9)–(2.11) involve five unknown amplitudes of waves. To determine them, we have five boundary conditions (2.4)–(2.8). Introducing Eqs. (2.9)–(2.11) into the proper boundary conditions (2.4)–(2.8), we obtain the following algebraic system of equations

$$\begin{aligned} A_1 - D_1 &= \lambda(A_2 - D_2), \\ A_1 + D_1 &= \sqrt{\kappa}K(A_2 + D_2), \\ \lambda(A_2 e^{-2\pi i \eta K} - D_2 e^{2\pi i \eta K}) &= A_3 e^{-2\pi i \sqrt{\kappa} \eta} - D_3 e^{2\pi i \sqrt{\kappa} \eta}, \\ \sqrt{\kappa}K(A_2 e^{-2\pi i \eta K} + D_2 e^{2\pi i \eta K}) &= A_3 e^{-2\pi i \sqrt{\kappa} \eta} + D_3 e^{2\pi i \sqrt{\kappa} \eta}, \\ D_3 &= A_3 e^{-4\pi i \sqrt{\kappa} \eta(1+\varepsilon)} \end{aligned} \quad (2.14)$$

where

$$K = k'/k, \quad \eta = bk, \quad \varepsilon = d/b. \quad (2.15)$$

The above equations allow us to determine the ratios of wave amplitudes propagating in the system to the amplitude of the incident wave as the explicit functions of the quantities characterizing the pore structure of a porous layer, the dissipative properties of the fluid and the macroscopic geometry of the system, for various frequencies of the incident wave. In particular, they allow us to determine the absorption coefficient α defined as the ratio of energy absorbed by the system to the energy of the incident wave. This coefficient takes the form

$$\alpha = 1 - |D_1/A_1|^2 = f_1(\eta, \eta_0, \varepsilon, f, \kappa) \quad (2.16)$$

where $|\cdot|$ stands for the absolute value of a complex number, and

$$\eta_0 = bk_0$$

is the dimensionless parameter characterizing the dissipative properties of the system.

The explicit form of the function f_1 is given in Appendix A.

From the practical point of view, the absorption coefficient α is the most important quantity characterizing the global properties of the system under consideration. Further, we analyze the influence of internal parameters of the system: η_0 , ε , f_v , κ on the absorption coefficient α for various frequencies of the incident wave and different configurations of the system.

3. Influence of internal parameters of the system on wave absorption coefficient. Special configuration of the system

3.1. Absorption properties of halfspace of a porous medium immersed in a fluid

The simplest case of a configuration of the system depicted in Fig. 1 is the halfspace of a porous medium immersed in a fluid (Fig. 2). This case is obtained by increasing the thickness b of a porous layer to infinity.

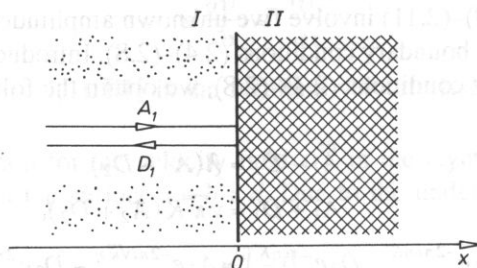


FIG. 2. Scheme of wave interaction with a halfspace of a porous material.

The absorption coefficient α_∞ of a such a system is given by the expression (2.16) for $b \rightarrow \infty$ ($k_0 \neq 0$) and takes the form

$$\alpha_\infty = \frac{4\sqrt{\kappa}f_v P}{(\sqrt{\kappa}f_v + P)^2 + Q^2} \quad (3.1)$$

where

$$P = \text{Re}(K) = \sqrt{\left(1 + \sqrt{1 + (k_0/k)^2}\right)/2}, \quad (3.2)$$

$$Q = \text{Im}(K) = -\sqrt{\left(-1 + \sqrt{1 + (k_0/k)^2}\right)/2}.$$

The dependence of the coefficient α_∞ on the dimensionless wave frequency $2\pi f/\bar{k}$ for two different pore structures of a porous medium is depicted in Fig. 3. This figure shows that the absorption coefficient α_∞ for low frequencies of the wave is small and increases when the frequency increases, approaching asymptotically the value

$$\alpha_\infty^0 = 4\sqrt{\kappa}f_v/(\sqrt{\kappa}f_v + 1)^2, \quad (3.3)$$

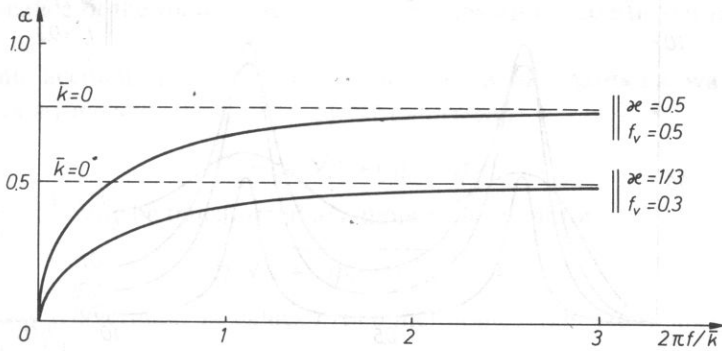


FIG. 3. Dependence of the absorption coefficient α on the dimensionless frequency $2\pi f/\bar{k}$ (for an acoustic plaster filled with air [16]; $2\pi f/\bar{k} = 1$ corresponds to $f = 400$ Hz).

which is entirely defined by the pore structure parameters. The quantity α_∞^0 is at the same time the absorption coefficient of the porous halfspace for the case when the fluid is inviscid ($\bar{k} = 0$). This means that in the range of higher frequencies the pore structure is the main factor determining the value of the coefficient of wave absorption by the porous halfspace, whereas in the range of low frequencies the predominant influence is exerted by the diffusive drag force characterized by the parameter \bar{k} .

3.2. Absorption properties of a porous layer with an impervious back surface

Let us now analyze the absorptive properties of the considered system in the case when the porous layer lies on the surface of an underformable solid material ($\varepsilon = 0$, Fig. 4). For such a configuration of the system, the absorption coefficient α given by the expression (2.16) takes the form

$$\alpha = f_i(\eta, \eta_0, \varepsilon, f_v, \kappa)|_{\varepsilon=0} \quad (3.4)$$

The dependence of the coefficient α on the dimensionless wave frequency η is shown in Fig. 5.

An important element in understanding the character of the course of the curves in Fig. 5 are the notions of (anti) resonance (resonance and/or antiresonance) frequencies of

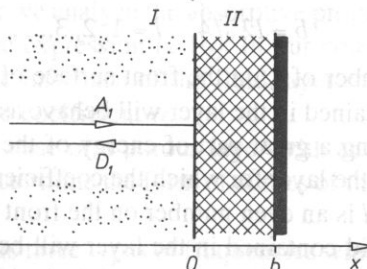


FIG. 4. Scheme of wave interaction with a porous layer with an impervious back surface.

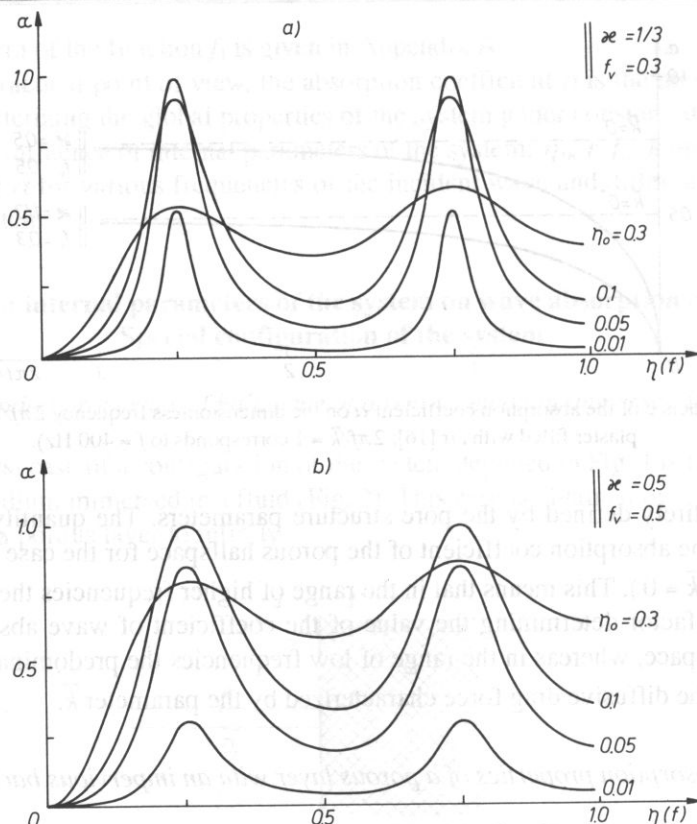


FIG. 5. Dependence of the absorption coefficient α on the dimensionless frequency η for two different pore structures of a porous layer and various values of the coefficient η_0 (for air and $b = .02$ m; a) $\eta = 1$ corresponds to $f \approx 9.8$ kHz; b) $\eta = 1$ corresponds to $f \approx 12$ kHz).

the fluid filling the porous layer. These frequencies determine the position of extremal values of the coefficient α . Taking into account the fact that both waves propagating in the layer form a standing wave, the node of which is placed on the contact surface with the undeformable halfspace, the (anti) resonance of the fluid in the layer occurs when the multiple of one fourth of the wave length λ_0 , propagating in the layer, is equal to the thickness of the layer, i.e., for

$$b = l\lambda_0/4 \quad l = 1, 2, 3, \dots \quad (3.5)$$

Then, for an odd number of l , on the front surface of the layer, the loop of a wave appears and the fluid contained in the layer will behave as a material of great flexibility, intercepting and dissipating a great part of energy of the incident wave. These are the resonance frequencies of the layer for which the coefficient α takes maximal values.

In turn, in the case when l is an even number on the front surface of the layer, a node of wave appears and the fluid contained in the layer will behave as a material with small flexibility, reflecting a great part of the energy of the incident wave. In this case we deal

with antiresonance of the fluid in the layer and the absorption coefficient α takes minimal values.

Taking into account the fact that the phase velocity of a harmonic wave in a fluid filling pores of a rigid skeleton is given by the expression

$$V_\varphi = c_0 / \sqrt{1 + (\eta_0/2\eta)^2}, \quad (3.6)$$

the condition (3.5) may be transformed to a more convenient form:

$$\eta_l \sqrt{1 + (\eta_0/2\eta_l)^2} = l/4 \quad (3.7)$$

which allows us to determine the values η_l of dimensionless (anti) resonance frequencies of the fluid in the layer.

As Fig. 5 shows, the parameter η_0 characterizing the dissipative properties of the fluid in a porous layer does not influence significantly the position of extremal values of the coefficient α . This means that in order to determine the (anti) resonance frequencies and the values of the coefficient α corresponding to them, the approximated form of the condition (3.7) and of the expression (3.4) may be used.

For $\eta_0/\eta \gg 1$, from Eqs. (3.7) and (3.4) we have

$$\eta_l = l/4, \quad (3.8)$$

$$\alpha = \frac{4\sqrt{\kappa} f_v \text{th}(\pi\eta_0)}{(1 + \sqrt{\kappa} f_v \text{th}(\pi\eta_0))^2 - \sin^2(2\pi\eta)(1 - \kappa f_v^2)/\text{ch}^2(\pi\eta_0)}. \quad (3.9)$$

From Fig. 5 and the expression (3.9) it is evident that both parameters η_0 and κ strongly change the form of curves of the coefficient. Moreover, the pore structure parameter κ influences the position of extremal values of the coefficient α . This parameter is explicitly present in the expression defining the dimensionless frequency η and therefore its influence, however not evident in Fig. 5, appears as a change of the scale on the axis of frequency.

The condition (3.8) together with the expression (3.9) are convenient for the calculation of the parameter κ of the pore structure and of the coefficient k' from the experimental data for the absorption coefficient α .

3.3. The absorption properties of the porous layer – solid halfspace system

In this section of the paper we analyze the absorptive properties of the system shown in Fig. 1 and described by the expression (2.16). In our considerations we put special stress on the discussion of the influence of the fluid layer separating both parts of the system on the wave absorption coefficient α .

Similarly as it was in the case of a porous layer with an impervious back surface, (anti)resonance frequencies determine the form of curves of the absorption coefficient of a system of two layers.

The system shown in Fig. 1 has three types of frequencies which determine the positions of extremal values of the coefficient α . The first type of these frequencies is connected

with (anti)resonance of the fluid filling porous layer and it appears when the condition (3.7) or (3.8) is satisfied. The second type of (anti) resonance frequencies results from anti resonance of the fluid contained between the porous layer and the undeformable halfspace. They are given by the condition

$$d = m\lambda_0/4 \quad m = 1, 2, 3, \dots,$$

which, due to constant phase velocity in a bulk fluid, equal to a_0 , may be expressed in the form

$$\eta_m = \frac{m}{4} \frac{1}{\sqrt{\kappa \varepsilon}}. \quad (3.10)$$

The third type of (anti) resonance frequencies of the system results from (anti) resonance of the fluid contained in both layers as a whole. In this case the condition for the (anti) resonance frequencies is obtained by requiring the time of transition of the wave through both layers to be equal to the multiple of one fourth of the wave period.

When the phase velocities of waves in each layer is considered, this condition takes the form

$$\eta_n (\sqrt{1 + (\eta_0/2\eta_n)^2} + \sqrt{\kappa \varepsilon}) = n/4 \quad n = 1, 2, 3, \dots \quad (3.11)$$

or

$$\eta_n = \frac{n}{4} \frac{1}{1 + \sqrt{\kappa \varepsilon}} \quad (3.12)$$

for $\eta/\eta_0 \gg 1$.

The conditions (3.7), (3.9) and (3.11) or their approximated forms allow one to evaluate the influence of particular types of (anti) resonances (parameters of the system) on the form of the curves of the coefficient α . These conditions determine the exact position of extremal values of the coefficient α only in the case when the parameters of the system are so chosen that all three conditions are fulfilled at the same time, i.e., when all three (anti) resonances are present. Then the value of the number n determines the type of extremum. For even n there appears a minimum of the coefficient α , and for odd n , there appears its maximum. In the remaining cases the positions of extrema are determined by neighbouring (anti) resonance frequencies of different types.

The conditions (3.8), (3.10) and (3.12) provide that for small values of the parameter ε , the (anti) resonance frequencies of the fluid in a porous layer and in both layers as a whole are close to one another, and the (anti) resonance of the layer of a bulk fluid occurs at higher frequencies of the wave. This means that for low frequencies and small values of ε , the position of extrema of the coefficient α is determined by the (anti) resonance frequencies of the fluid in a porous layer and both layers as a whole.

Since the (anti) resonance frequencies given by the formula (3.12) decrease when the parameter ε increases, the extrema of the coefficient α displace in the direction of lower frequencies (Fig. 6a). From Fig. 6b it is seen that a further increase of the parameter ε does not change significantly the absorption coefficient α for low frequencies but it causes the appearance of extrema connected with (anti) resonances of the layer of a bulk fluid.

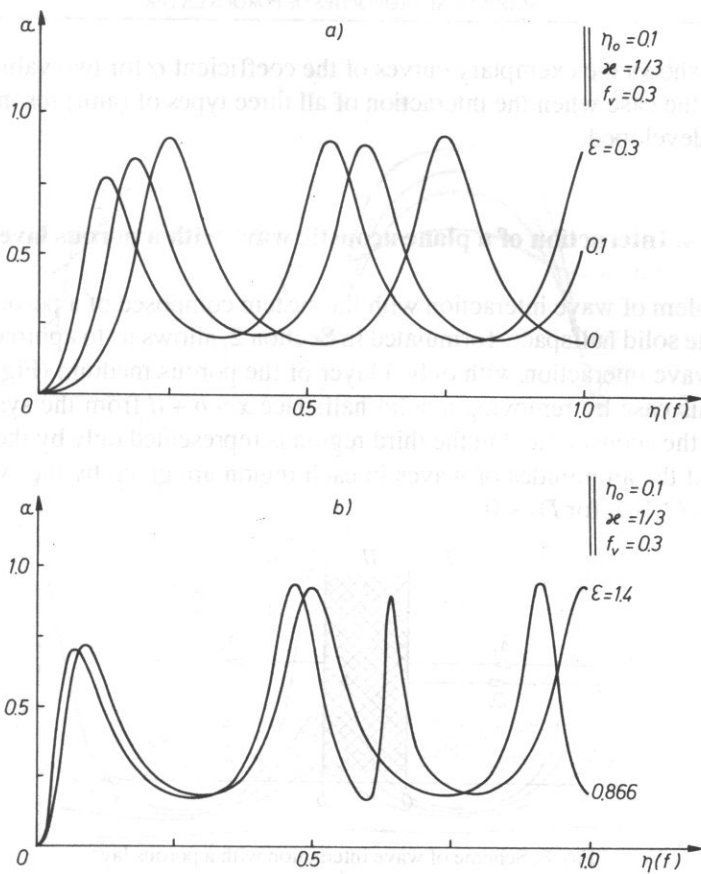


FIG. 6. Dependence of the absorption coefficient α on the dimensionless frequency η for two different pore structures of a porous layer and various values of the coefficient ϵ (for air and $b = .02\text{m}$; a) $\eta = 1$ corresponds to $f \approx 9.8$ kHz; b) $\eta = 1$ corresponds to $f \approx 12$ kHz).

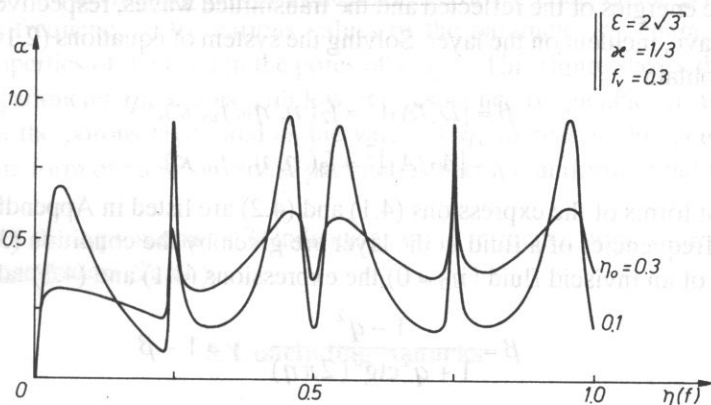


FIG. 7. Dependence of the absorption coefficient α on the dimensionless frequency η (for air and $b = .02$ m $\eta = 1$ corresponds to $f = 9.8$ kHz).

Figure 7 shows the exemplary curves of the coefficient α for two values of the parameter η_0 , in the case when the interaction of all three types of (anti) resonance frequencies is fully developed.

4. Interaction of a plane acoustic wave with a porous layer

The problem of wave interaction with the system composed of a porous layer and an undeformable solid halfspace, formulated in Section 2, allows us to approach directly the problem of wave interaction with only a layer of the porous medium (Fig. 8). Formally, we obtain this case by removing a solid halfspace $x > b + d$ from the system shown in Fig. 1. Then the acoustic field in the third region is represented only by the wave leaving the layer, and the amplitudes of waves in each region are given by the system of equations (2.14)₁–(2.14)₄ for $D_3 = 0$.

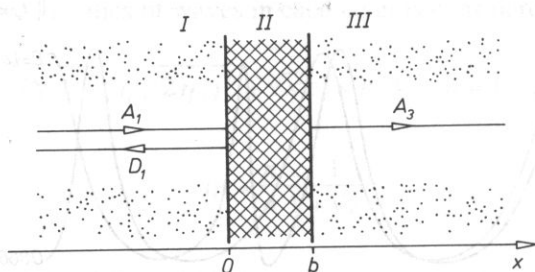


FIG. 8. Scheme of wave interaction with a porous layer.

The acoustical properties of a porous layer are characterized by two quantities: the reflection coefficient β and the transmission coefficient γ . These quantities are defined as ratios of the energies of the reflected and the transmitted waves, respectively, to the energy of the wave, incident on the layer. Solving the system of equations (2.14)₁–(2.14)₄, for $D_3 = 0$ we obtain

$$\beta = |D_1/A_1|^2 = f_2(\eta, \eta_0, f_v, \kappa), \quad (4.1)$$

$$\gamma = |A_3/A_1|^2 = f_3(\eta, \eta_0, f_v, \kappa). \quad (4.2)$$

The explicit forms of the expressions (4.1) and (4.2) are listed in Appendix B. The (anti) resonance frequencies of a fluid in the layer are given by the condition (3.8) or (3.9).

In the case of an inviscid fluid ($\eta_0 = 0$) the expressions (4.1) and (4.2) take the forms

$$\beta = \frac{1 - q^2}{1 + q^2 \operatorname{ctg}^2(2\pi\eta)}, \quad \gamma = 1 - \beta \quad (4.3)$$

where

$$q^2 = \frac{4\kappa f_v^2}{(\kappa f_v^2 + 1)^2}.$$

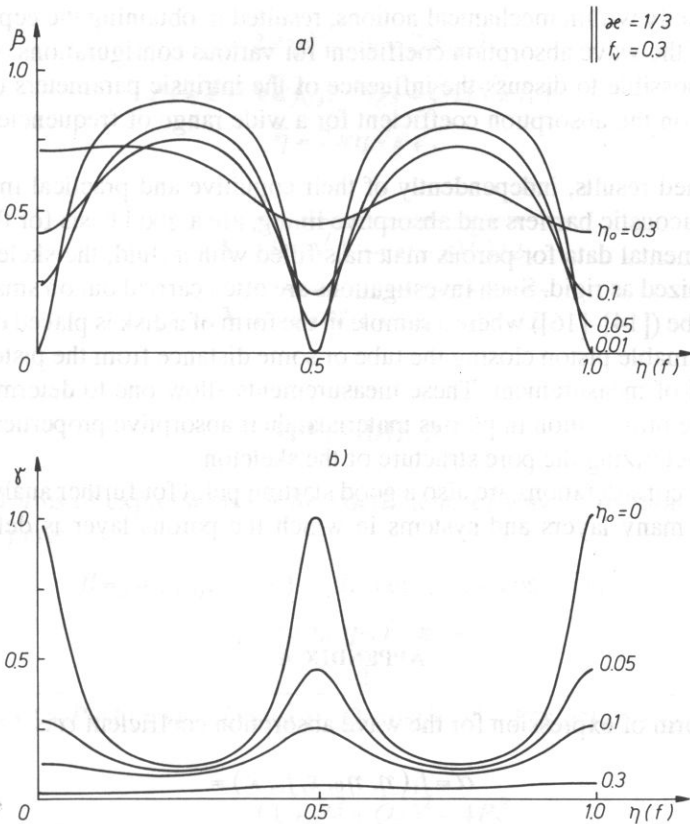


FIG. 9. Dependence of the reflection coefficient β a) and the transmission coefficient γ b) on the dimensionless frequency η (for air and $b = .02$ m $\eta = 1$ correspond to $f \approx 9.8$ kHz).

Figure 9 shows the exemplary curves of dependence of the coefficients β and γ on the dimensionless frequency η for various values of the parameter η_0 characterizing the dissipative properties of the fluid in the pores of a layer. This figure shows that for small values of the parameter η_0 , waves with low and resonance frequencies penetrate intensively through the porous layer, and as the value of η_0 increases, this penetration decreases, and the form of curves for both parameters become uniform in the whole range of frequencies.

The form of the expressions (4.3) indicate a strong influence of pore structure on the values of the parameters β and γ .

5. Concluding remarks

In the paper we have considered the problem of wave interaction with a system composed of a porous layer and an undeformable halfspace immersed in a barotropic fluid, for the case of normal incidence of a harmonic wave. Solving the boundary problem,

formulated strictly within mechanical notions, resulted in obtaining the explicit forms of expressions of the wave absorption coefficient for various configurations of the system. This made it possible to discuss the influence of the intrinsic parameters of the system ($b, d, \kappa, f_v, \bar{k}$) on the absorption coefficient for a wide range of frequencies of the incident wave.

The obtained results, independently of their cognitive and practical importance for designing the acoustic barriers and absorptive lining, are a good basis for the interpretation of experimental data for porous materials filled with a fluid, the skeleton of which may be recognized as rigid. Such investigations are often carried out on small samples in a resonance tube ([14]–[16]) where a sample in the form of a disk is placed either directly on the undeformable piston closing the tube or some distance from the piston depending on the method of measurement. These measurements allow one to determine the parameters of wave propagation in porous materials, their absorptive properties, and the parameters characterizing the pore structure of the skeleton.

The above considerations are also a good starting point for further analysis extended to systems of many layers and systems in which the porous layer is deformable and movable.

APPENDIX A

The explicit form of expression for the wave absorption coefficient α is:

$$\alpha = f_1(\eta, \eta_0, \varepsilon, f_v, \kappa) =$$

$$= 1 - [(\operatorname{ch}(\bar{y}) + P_G \operatorname{sh}(\bar{y}))^2 - (\sin(\bar{x}) - Q_G \cos(\bar{x}))^2 + \\ + P_G^2 \sin^2(\bar{x}) + Q_G^2 \operatorname{ch}^2(\bar{y})] / [P_D^2 \sin^2(\bar{y}) + Q_D^2 \operatorname{ch}^2(\bar{y}) + \\ + (\operatorname{ch}(\bar{y}) + P_D \operatorname{sh}(\bar{y}))^2 - (\sin(\bar{x}) - Q_D \cos(\bar{x}))^2]$$

where

$$P_G = \frac{P_S + \sin(\bar{\eta})[P_S(P_S^2 + Q_S^2 - 1)\sin(\bar{\eta}) + Q_S(P_S^2 + Q_S^2 + 1)\cos(\bar{\eta})]}{P_S^2 + Q_S^2},$$

$$Q_G = \frac{-Q_S + \sin(\bar{\eta})[Q_S(P_S^2 + Q_S^2 + 1)\sin(\bar{\eta}) - P_S(P_S^2 + Q_S^2 - 1)\cos(\bar{\eta})]}{P_S^2 + Q_S^2},$$

$$P_D = -\frac{P_S + \sin(\bar{\eta})[P_S(P_S^2 + Q_S^2 - 1)\sin(\bar{\eta}) - Q_S(P_S^2 + Q_S^2 + 1)\cos(\bar{\eta})]}{P_S^2 + Q_S^2},$$

$$Q_D = \frac{Q_S - \sin(\bar{\eta})[Q_S(P_S^2 + Q_S^2 + 1)\sin(\bar{\eta}) + P_S(P_S^2 + Q_S^2 - 1)\cos(\bar{\eta})]}{P_S^2 + Q_S^2},$$

and

$$\bar{x} = 2\pi\eta P; \quad \bar{y} = 2\pi\eta Q;$$

$$P_S = P/(\sqrt{\kappa}f_v); \quad Q_S = Q/(\sqrt{\kappa}f_v);$$

$$\bar{\eta} = 2\pi\eta\sqrt{\kappa}\varepsilon,$$

whereas

$$P = \sqrt{(1 + \sqrt{1 + (\eta_0/\eta)^2})/2},$$

$$Q = -\sqrt{(-1 + \sqrt{1 + (\eta_0/\eta)^2})/2}.$$

APPENDIX B

The explicit forms of expressions for the coefficients of wave reflection β and of wave transmission γ are:

$$\beta = f_2(\eta, \eta_0, f_v, \kappa) = \gamma K_0 (\text{ch}^2(\bar{y}) - \cos^2(\bar{x}))^2;$$

$$\gamma = f_3(\eta, \eta_0, f_v, \kappa) =$$

$$= \frac{1}{(\text{ch}(\bar{y}) + P_0 \text{sh}(\bar{y}))^2 - (\sin(\bar{x}) - Q_0 \cos(\bar{x}))^2 + P_0^2 \sin^2(\bar{x}) + Q_0^2 \text{ch}^2(\bar{y})}$$

where

$$K_0 = \frac{(1 + P_S^2 + Q_S^2)^2 - 4P_S^2}{4(P_S^2 + Q_S^2)},$$

$$P_0 = -\frac{P_S}{2} \frac{P_S^2 + Q_S^2 + 1}{P_S^2 + Q_S^2}; \quad Q_0 = -\frac{P_S}{2} \frac{P_S^2 + Q_S^2 - 1}{P_S^2 + Q_S^2},$$

and $\bar{x}, \bar{y}, P_S, Q_S$ are the quantities defined in Appendix A.

References

- [1] K. ATTENBOROUGH, *Acoustical characteristics of rigid fibrous absorbents and granular materials*, JASA, **73**, 3, 785-799 (1983).
- [2] J.Y. CHUNG, D.A. BLASER, *Transfer function method of measuring in-duct acoustic properties*. I. Theory, JASA, **68**, 3, 907-913 (1980).
- [3] M. CIESZKO, *Reflection and refraction of a plane acoustic wave in a fluid at the interface between two porous media* (in Polish), Eng. Trans., **37**, 4, 76-88 (1989).
- [4] H. DERESIEWICZ, J.T. RICE, *The effect of boundaries on wave plane waves in a liquid-filled porous solid. Reflection of plane waves at a free plane boundary (General case)*, Bull. Seismol. Soc. Am., **52**, 3, 595-625 (1962).
- [5] W. DERSKI, *Equation of motion for a fluid-saturated porous solid*, Bull. Acad. Polon. Sci., Serie Sci. Tech., **26**, 1, 11-16 (1978).
- [6] W. DERSKI, S.J. KOWALSKI, *On the motion and mass continuity equations in a fluid-saturated*

- porous medium*, *Studia Geotech. et Mech.*, **2**, 3–12 (1980).
- [7] M.A. FERRERO, G.G. SACERDOTE, *The acoustic impedance of thin layers of porous material*, *Acoustica*, **10**, 336–339 (1960).
- [8] J. KUBIK, *Mechanics of deformable media with anisotropic permeability* (in Polish), *Prace IPPT*, **29** (1981).
- [9] J. KUBIK, *A macroscopic description of geometrical pore structure of porous solids*, *Int. J. Engng. Sci.*, **24**, 6, 971–980 (1986).
- [10] J. KUBIK, M. CIESZKO, *On internal forces in porous liquid-saturated medium* (in Polish), *Engng. Trans.*, **35**, 1, 55–70 (1987).
- [11] P.M. MORSE, K.U. INGARD, *Linear acoustic theory*, in „*Handbuch der Physik*“, Band 11/1, Springer, Berlin 1961.
- [12] J.M. SABATIER, H.E. BASS, L.N. BOLEN, K. ATTENBOROUGH, V.S. SASTRY, *The interaction of airborne sound with porous ground. The theoretical formulation*, *JASA*, **79**, 5, 1345–1352 (1986).
- [13] E. SKUDRZYK, *The foundations of acoustics*, Springer, Vienna 1971.
- [14] H. UTSUNO, T. TANAKA, T. FUJIKAWA, *Transfer function method for measuring characteristic impedance and propagation constant of porous materials*, *JASA*, **86**, 2, 637–643 (1989).
- [15] S.L. YANIV, *Impedance tube measurement of propagation constant and characteristic impedance of porous acoustical material*, *JASA*, **54**, 5, 1138–1142 (1973).
- [16] C. ZWICKER, C.W. KOSTEN, *Sound absorbing materials*, Elsevier, Amsterdam 1949.

Received on December 11, 1990

FAR FIELD OF A CONCENTRIC RING VIBRATING WITH CONSTANT VELOCITY ON A RIGID SPHERE

A. BRAŃSKI and L. LENIOWSKA

Department of Technics, Pedagogical University
(35-310 Rzeszów, Rejtana 16a)

PART I - THEORY

1. Introduction

The monograph [2] presents the theory of sound radiation from such sources as: a point on sphere, a spherical cup on a sphere and a pulsating sphere. Every mentioned source has a separate theory.

In this paper the theory of sound radiation of sources with the geometry mentioned above and described with spherical coordinates is generalized. A vibrating ring on a sphere was chosen as the source. The sources under consideration in the monograph [2] can be obtained from such a source.

Part I of this paper presents the theory of sound radiation from a ring placed on a sphere. The theory is verified in several numerical examples in Part II. The directivity function was calculated in terms of the width of the ring its position on the sphere with constant width and its vibration frequency with fixed position and fixed width.

2. Geometry of the problem

A vibrating ring placed on a rigid sphere (acoustic baffle) symmetrically with respect to the z -axis (Fig. 1) was chosen as the source (vibrating surface + acoustic baffle). This ring is cut out from a sphere with radius R by two rotational cones with a common vertex and with apex angles equal to $2\theta_1$ and $2\theta_2$. Two cones also cut out a second ring for $z < 0$. Only the ring in the top part of the sphere is taken into account.

If we assume that the acoustic parameters on the ring surface are axially symmetrical, then the distribution of the field around the sphere is also axially symmetrical. Only

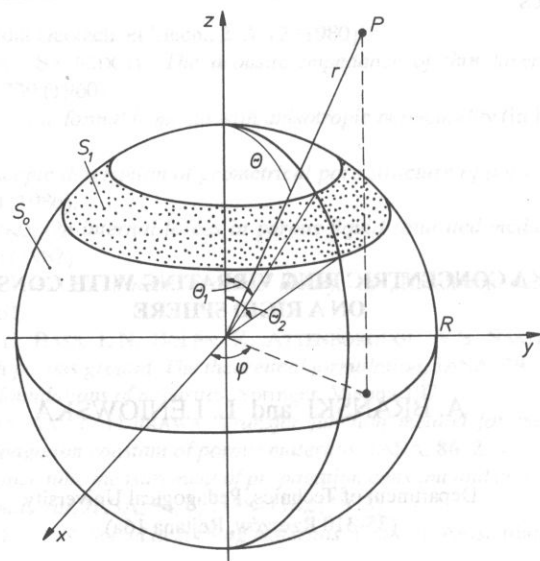


FIG. 1. Geometry of the problem.

two parameters in the spherical coordinate system r, θ, ϕ are sufficient to describe it. These are radius r and angle θ . In Fig. 1 we have S_1 – area of the ring, S_0 – area of the spherical baffle, $S_1 + S_0 = 4\pi R^2$.

3. Formulation of the boundary problem

For a steady, time-harmonic state the distribution of the field around the source is the solution to the boundary problem for a Helmholtz equation $(\Delta + k^2)\Psi = 0$, noted in the spherical coordinates [2], with the following boundary condition on a sphere with radius R

$$\frac{\partial \Psi}{\partial n} = -v_0, \quad \theta \in \langle \theta_1, \theta_2 \rangle,$$

$$\frac{\partial \Psi}{\partial n} = 0, \quad \theta \notin \langle \theta_1, \theta_2 \rangle. \quad (1)$$

where Ψ – velocity potential of acoustic field, n – unit vector of normal to the surface of the sphere, v_0 – vibration velocity of the ring. The potential Ψ must satisfy the Sommerfeld radiation conditions

$$\lim_{r \rightarrow \infty} |r \Psi| < A, \quad A - \text{constant},$$

$$\lim_{r \rightarrow \infty} \left(\frac{\partial \Psi}{\partial n} + ik \Psi \right) r = 0. \quad (2)$$

For the condition (1) the ring is a time-harmonic pulsating surface radial vibrations. The following sources can be obtained from a ring: in the form of a spherical cup ($\theta_1 = 0, \theta_2 \in (0, \pi/2)$), of a pulsating sphere ($\theta_1 = 0, \theta_2 = \pi$ and of a point source ($\theta_1 = 0, \theta_2 \rightarrow 0$).

4. Solution of the Helmholtz equation in spherical coordinates

Elementary solutions of the Helmholtz equation obtained with the Fourier method have the following form:

$$\Psi_{mn} = h_m^{(2)}(kr) P_m^n(\cos \theta) e^{in\phi}, \quad (3)$$

where $h_m^{(2)}(kr)$ spherical Hankel function of the second kind and order m , $P_m^n(\cos \theta)$ – associated Legendre function of the first kind of order m and degree n , $k = 2\pi/\lambda$.

Product

$$Y_{mn} = P_m^n(\cos \theta) e^{in\phi} \quad (4)$$

is called the surface spherical harmonics. Including Eq. (4) in Eq. (3), we achieve

$$\Psi_{mn} = h_m^{(2)}(kr) Y_{mn}, \quad (5)$$

For the axisymmetric problem $n = 0$ and the function (5) assumes a specific form:

$$\Psi_{m0} = h_m^{(2)}(kr) P_m^0(\cos \theta) = h_m P_m(\cos \theta), \quad (6)$$

where $h_m = h_m^{(2)}(kr)$, $P_m(\cos \theta) = P_m^0(\cos \theta)$.

5. Solution of the boundary problem

The solution to the problem given in paragraph 3 is picked out in the form of a series

$$\Psi = \sum_{m=0}^{\infty} A_m \Psi_m, \quad (7)$$

where $\Psi_m = \Psi_{m0}$ – formula (6).

Substituting (6) in (7) we have

$$\Psi = \sum_{m=0}^{\infty} A_m h_m(kr) P_m(\cos \theta). \quad (8)$$

Expansion coefficients A_m are calculated on the basis of the fact that the surface harmonics are orthogonal. To this end Eq. (8) is substitutes in the boundary condition (1). Thus

$$-v_0 = \sum_{m=0}^{\infty} A_m h'_m(kr) P_m(\cos \theta), \quad (9)$$

where

$$h'_m(kR) = \frac{\partial}{\partial n} h_m(kr) \Big|_{r=R} = \frac{\partial}{\partial r} h_m(kr) \Big|_{r=R}. \quad (10)$$

Then the formula (9) is multiplied by $P_m(\cos \theta)$ and integrated along the surface of the sphere. For an arbitrary m we obtain

$$-v_0 \int_S P'_m(\cos \theta) d\sigma = A_m h'_m(kR) \int_S P_m(\cos \theta) P'_m(\cos \theta) d\sigma, \quad (11)$$

The integral on the right hand side is

$$\begin{aligned} & \int_S P_m(\cos \theta) P'_m(\cos \theta) d\sigma = \\ & = R^2 \int_0^{2\pi} \int_0^\pi P_m(\cos \theta) P'_m(\cos \theta) \sin \theta d\theta d\phi = 2\pi R^2 \frac{2}{2m+1}. \end{aligned} \quad (12)$$

The orthogonality relation of the Legendre polynomials [1] was applied to calculate Eq. (12)

$$\int_{-1}^1 P_m(z) P_{m'}(z) dz = \begin{cases} \frac{2}{2m+1}, & m' = m, \\ 0, & m' \neq m. \end{cases} \quad (13)$$

Since v_0 differs from zero for $\theta \in < \theta_1, \theta_2 >$ only, then the integral on the left hand side in Eq. (11) can be calculated over the surface S_1 instead of S .

$$\int_{S_1} P_m(\cos \theta) d\sigma = 2\pi R^2 \int_{\theta_1}^{\theta_2} P_m(\cos \theta) \sin \theta d\theta = \frac{2\pi R^2}{2m+1} P_m(\theta_1, \theta_2), \quad (14)$$

where

$$P_m(\theta_1, \theta_2) = P_{m+1}(\cos \theta_2) - P_{m-1}(\cos \theta_2) - P_{m+1}(\cos \theta_1) + P_{m-1}(\cos \theta_1). \quad (15)$$

The relationship [1]

$$\int_{z_1}^{z_2} P_m(z) dz = \frac{1}{2m+1} [P_{m+1}(z) - P_{m-1}(z)] \Big|_{z_1}^{z_2} \quad (16)$$

was used to calculate the integral (14).

Substituting Eq. (12) and (14) in Eq. (11), we have

$$A_m = \frac{v_0 P_m(\theta_1, \theta_2)}{2h'_m(kR)}, \quad (17)$$

Therefore the solution of the boundary problem is given by the formula (8) with the constant A_m defined by Eq. (17).

6. Specific solutions

To check the validity of the solution for a ring, its specific form can be compared with the solutions given in the monograph [2] for a spherical cup, a point on a sphere and a vibrating sphere. For example, for a spherical cup $\theta_1 = 0$, $\theta_2 \in (0, \pi/2)$. From the expression (17): we have ($P_m(1) = 1$ for every m)

$$A_m = \frac{v_0}{2h'_m(kR)} [P_{m+1}(\cos \theta_2) - P_{m-1}(\cos \theta_2)]. \quad (18)$$

Substituting Eq. (18) in Eq. (8), we obtain the solution to the problem of sound radiation of a spherical cup. The same solution is given in the monograph [2]. Chapter XX, formulae (22) and (39). The solution (8) described the acoustic field for an arbitrary distance $r > R$. The specific form of this solution describes the far field: for $r \rightarrow \infty$ in accordance with [2]

$$h_m(kr) = \exp \frac{-i[kr - (m+1)\frac{\pi}{2}]}{kr}, \quad (19)$$

Equations (8) and (17) lead to

$$\Psi = \sum_{m=0}^{\infty} \frac{v_0}{2h'_m(kR)} \exp \frac{-i[kr - (m+1)\frac{\pi}{2}]}{kr} P_m(\theta_1, \theta_2) P_m(\cos \theta) \quad (20)$$

The formula (20) was used to calculate of numerical examples.

PART II – NUMERICAL CALCULATIONS

7. Frame of numerical calculations

First, verifying calculations were carried out:

- since the series in the formula (8) is infinite, the number of terms ensuring adequate accuracy of results was numerically determined,
- the distance from the sphere which can be assumed as the approximate boundary of the far field was estimated also numerically. Furthermore the directivity function was calculated in terms of:

- the width of the ring,
- the position of the ring with constant width,
- the dimensionless wave number ka for a fixed position of the ring on the sphere and for a fixed width.

Up to now there are no papers concerning the directivity function of a ring placed on a sphere. Therefore the validity of the computer programme was checked by comparing

the directional function calculated for a spherical cup with the characteristic for such a source given in the monograph [2].

8. Directivity function of a source

This means the far field defined by

$$D = \frac{|p|}{|p_0|} \quad (21)$$

where: $|p|$ – pressure amplitude measured in an arbitrary direction, $|p_0|$ – amplitude of maximal pressure.

The formula (21) express the pressure drop in an arbitrary direction in dimensionless units. It is convenient to express this drop in dB. Then

$$D_{dB} = 20 \lg_{10} \frac{|p|}{|p_0|} \quad (22)$$

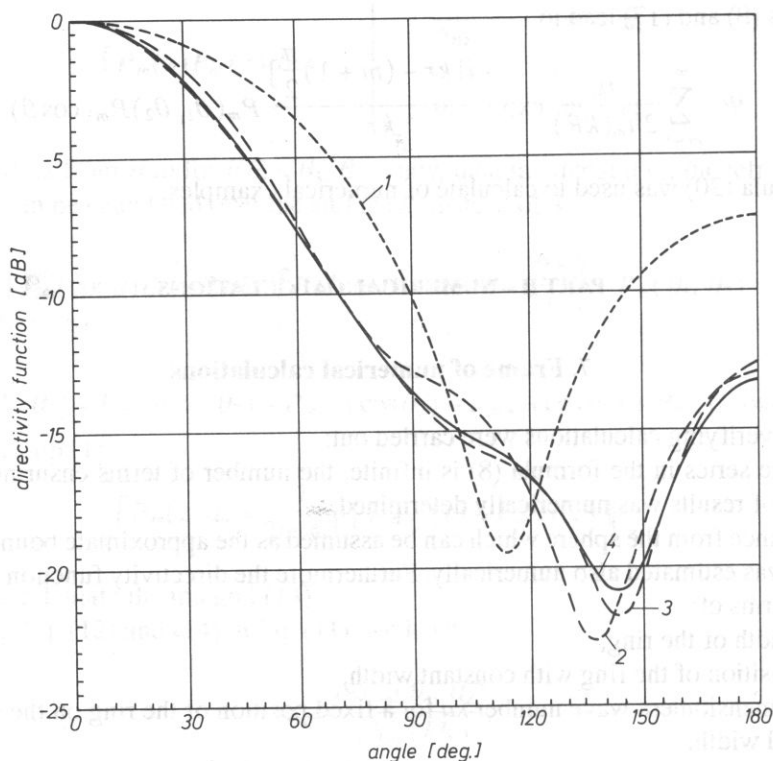


FIG. 2. Directivity of the source as a function of the terms' number of the series (8).

Since $p(t) = \rho_0 \frac{\partial \Psi}{\partial t}$, then time harmonic radiation the spatial distribution of acoustical pressure is $p = i\omega\rho_0\Psi$, where Ψ is defined by the formula (8).

9. Examples

9.1. The shape of the far field was investigated as a function of the number of terms in the sum (8).

A spherical cup defined by angles $\theta_1 = 0$, $\theta_2 = 60$ and $kR = 3$, $R = 0.1$, $k = 30$, $f = 1600$ [Hz] was assumed. The results of calculations are presented in Fig. 2. Line "1" was plotted for $m = 2$, line "2" for $m = 3$ line "3" for $m = 5$ and line "4" for $m = 10$. Examination of Fig. 2 indicates that the difference between the directivity function calculated for $m = 5$ and $m = 10$ are small. Calculations were carried out on an IBM PC/AT computer, so even when much greater values of m were taken into consideration, e.g. $m = 50$, the calculating time was not very much longer, $m = 10$ was accepted for further calculations.

9.2. The distance from the surface of the sphere which can be assumed as the boundary of the Fraunhofer zone. The following values were assumed: $kR = 3$, $R = 0.1$,

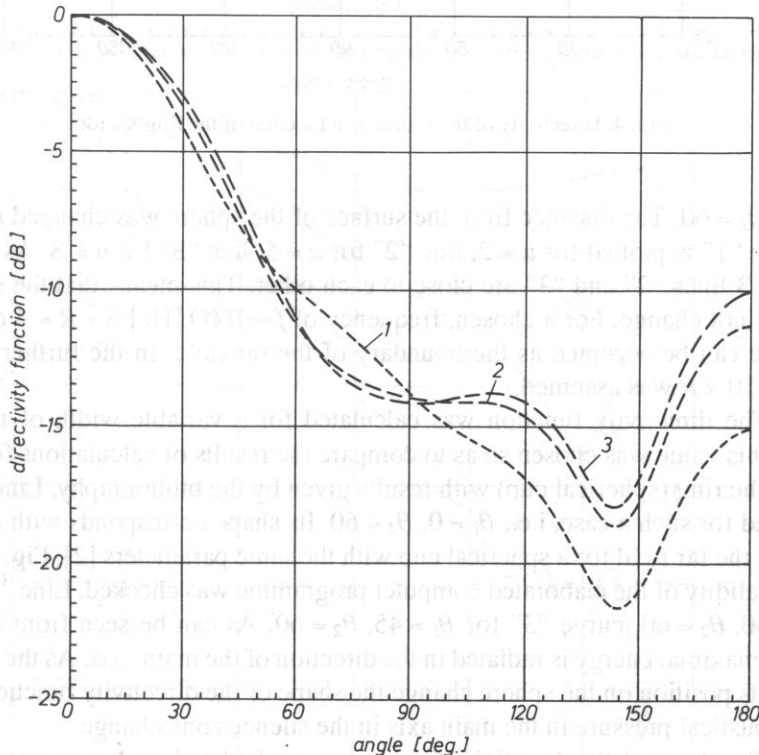


FIG. 3. Directivity of the source as a function of the distance r .

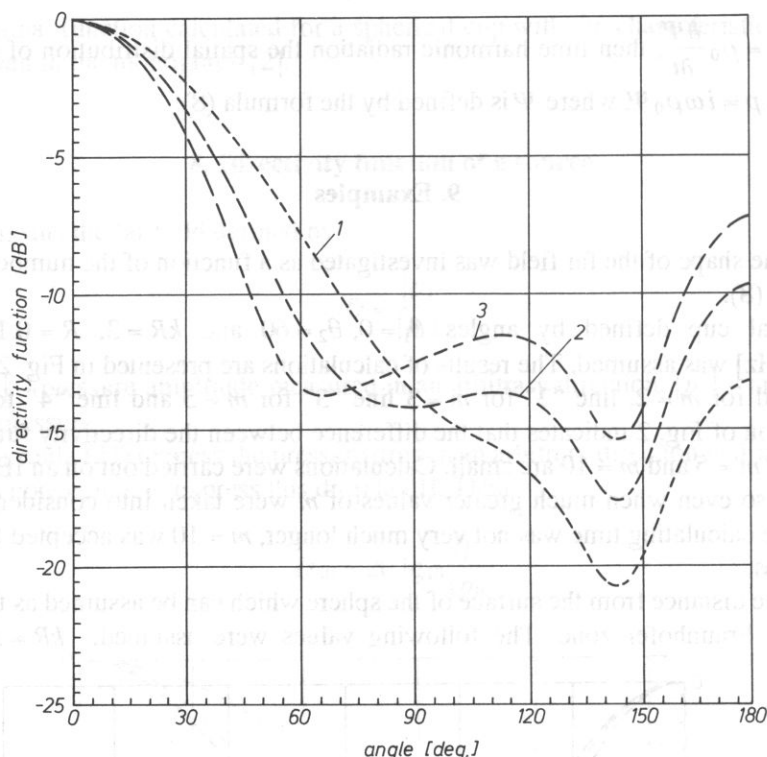


FIG. 4. Directivity of the source as a function of the ring's width.

$\theta_1 = 30$, $\theta_2 = 60$. The distance from the surface of the sphere was changed $r = u \times R$. In Fig. 3 line "1" is plotted for $u = 2$, line "2" for $u = 5$, line "3" for $u = 8$. As can be seen from Fig. 3 lines "2" and "3" are close to each other. This means that the shape of the field does not change. For a chosen, frequency of $f = 1600$ [Hz] $8 \times R = 4$ diameters of the source can be accepted as the boundary of the far field. In the further part of this paper $r = 10 \times R$ was assumed.

9.3. The directivity function was calculated for a variable width of the ring, for $kR = 3$. This value was chosen so as to compare the results of calculations for a specific shape of the ring (spherical cup) with results given by the bibliography. Line "1" in Fig. 4 is plotted for such a case, i.e., $\theta_1 = 0$, $\theta_2 = 60$. Its shape corresponds with a line which illustrates the far field for a spherical cup with the same parameters [2], Fig. 20.7. In this way the validity of the elaborated computer programme was checked. Line "2" is plotted for $\theta_1 = 30$, $\theta_2 = 60$, curve "3" for $\theta_1 = 45$, $\theta_2 = 60$. As can be seen from Fig. 4 in all cases the maximal energy is radiated in the direction of the main axis. As the width of the ring and its position on the sphere change the shape of the directivity function and value of the acoustical pressure in the main axis in the silence zone change.

9.4. The shape of the directivity function was calculated for a constant width of the ring and various positions of the ring on the sphere ($kR = 3$). In Fig. 5 line "1" is for a

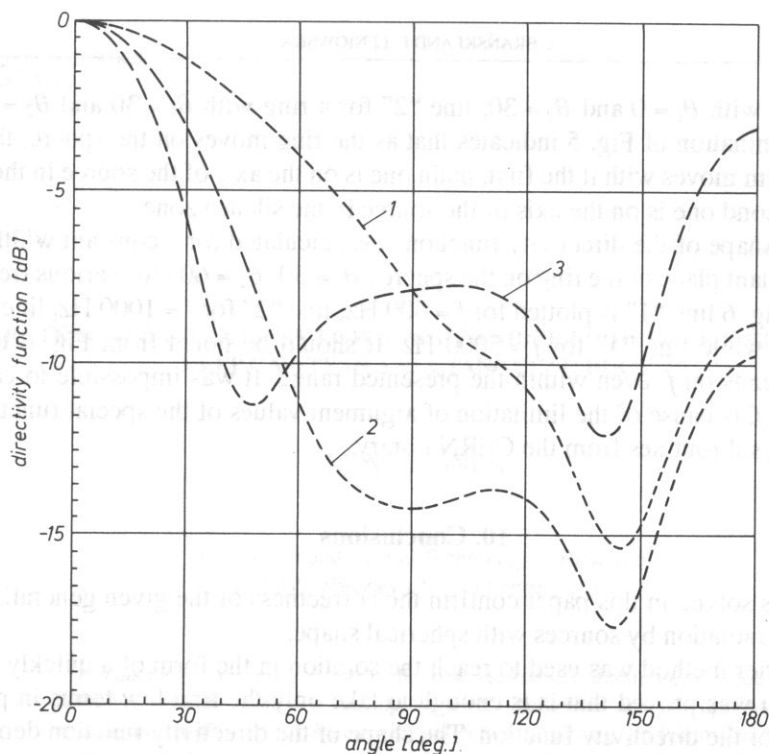


FIG. 5. Directivity of the source as a function of the ring's place on the sphere with constant ring width.

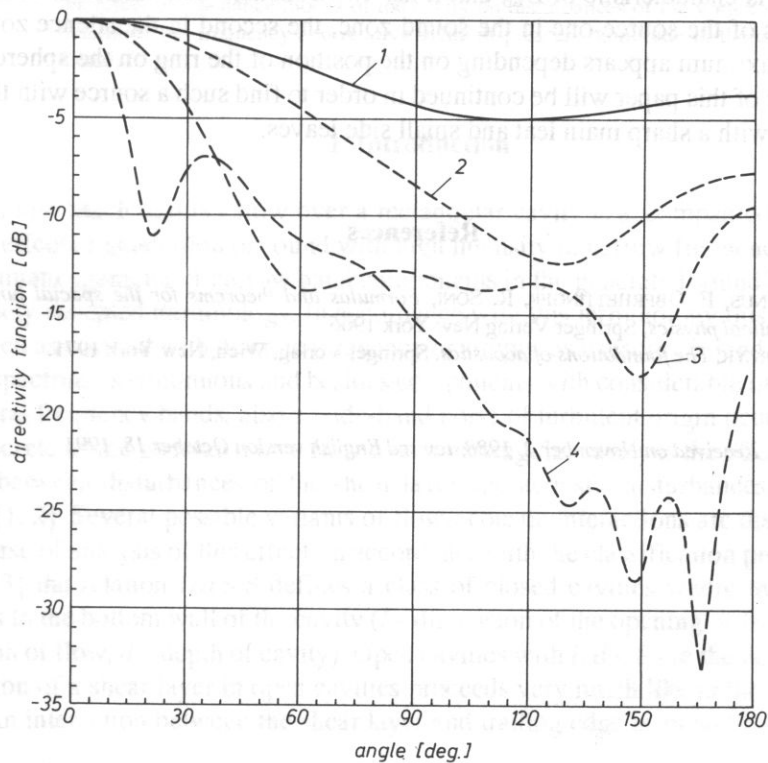


FIG. 6. Directivity of the source as a function of the ring's vibration frequencies.

spherical cup with $\theta_1 = 0$ and $\theta_2 = 30$, line "2" for a ring with $\theta_1 = 30$ and $\theta_2 = 60$ and $\theta_2 = 90$. Examination of Fig. 5 indicates that as the ring moves on the sphere, the third local maximum moves with it the first, main one is on the axis of the source in the sound zone. The second one is on the axis of the source in the silence zone.

9.5. The shape of the directivity function was calculated for a constant width of the ring and constant place of the ring on the sphere ($\theta_1 = 30$, $\theta_2 = 60$) for various frequency f values. In Fig. 6 line "1" is plotted for $f = 500$ Hz, line "2" for $f = 1000$ Hz, line "3" for $f = 2000$ Hz, while line "4" for $f = 5000$ Hz. It should be noted from Fig. 6 that D_{dB} strongly depends on f , even within the presented range. It was impossible to calculate D_{dB} for other f , because of the limitation of argument values of the special function calculated using subroutines from the CERN library.

10. Conclusions

Examples solved in this paper confirm the correctness of the given generalized theory of sound radiation by sources with spherical shape.

The Fourier method was used to reach the solution in the form of a quickly convergent series. It was proved that it is enough to take only the first few terms in practical calculations of the directivity function. The shape of the directivity function depends on the width of the ring, its place on the sphere and also very strongly on the vibration frequency. It is characteristic of D_{dB} that it has two constant local maxima; both are on the main axis of the source—one in the sound zone, the second in the silence zone. The third local maximum appears depending on the position of the ring on the sphere.

The topic of this paper will be continued in order to find such a source with the most directive i.e. with a sharp main lobe and small side lobes.

References

- [1] W. MAGNUS, F. OBERHETTINGER, R. SONI, *Formulas and theorems for the special functions of mathematical physics*, Springer Verlag New York 1966.
- [2] R. SKUDRZYK, *The foundations of acoustics*, Springer Verlag, Wien, New York 1971.

Received on November 2, 1988, revised English version October 18, 1991

DISCRETE SOUND INDUCED BY LOW MACH NUMBER FLOW OVER SIDE BRANCH DEEP CAVITY IN A RECTANGULAR DUCT

M. MEISSNER

Institute of Fundamental Technological Research
(00-049 Warszawa, Świątokrzyska 21)

This paper presents a model of the discrete sound induction effect due to a flow over a deep cavity in the wall of a rectangular duct. Theoretical analysis applies shear layer approximation with a vortex sheet, with deflection satisfying the Kutta-Žukowski condition, and an equivalent impedance system of a deep cavity with cavity impedance change in the presence of the flow included. The applied theoretical method makes it possible to determine the effect of resonance modes of the cavity on disturbances of the vortex sheet and also to determine the frequency and relative value of pressure amplitude in the case of a discrete sound.

1. Introduction

The low Mach number flow over a rectangular cavity is accompanied by a characteristic effect of generation of sound with high intensity in narrow frequency bands. The predominant character of narrow band components in the generated sound is reflected in the widely accepted terminology. In accordance with this terminology this type of noise is defined as a sound with discrete frequency or simply, as a discrete sound. In reality the sound spectrum is continuous and besides components with considerable intensity in one or several frequency bands, also a wide-band noise of turbulent origin occurs.

Discrete sound generated by a flow over a rectangular cavity is the effect of an interaction between disturbances of the shear layer and acoustic disturbances induced in a cavity [1, 2]. Several possible variants of flow-acoustic interactions are distinguished in the course of analysis of this effect. In accordance with the classification presented in the paper [3] the relation $l/d > 8$ defines a class of closed cavities where the shear layer adheres to the bottom wall of the cavity (l – dimension of the opening of the cavity in the direction of flow, d – depth of cavity). Open cavities with $l/d < 8$ are the next group. The formation of a shear layer in open cavities proceeds very much like in the case of a free flow. An interaction between the shear layer and trailing edge is an additional source of

flow disturbance [4, 5]. Open cavities are divided into two categories shallow and deep, and the condition $l/d = 1$ sets the boundary between them.

In the case of a deep cavity, for which $l/d < 1$ the effect of discrete sound induction is related with the shear layer instability due to two factors. The influence of resonance modes of the cavity on disturbances of the shear layer is the first factor, while the second one is the flow-acoustic interaction at the leading and trailing edges. If only the first factor occurs in the process of sound generation then the instability of the shear layer can take place solely for frequencies f close to definite values f_m which are determined by the resonance condition for a quarter-wave resonator [6]

$$k\Delta d - \text{ctan}(kd) = 0 \quad (1)$$

and thus

$$f_m \approx \frac{c(2m-1)}{4(d+\Delta d)}, \quad m = 1, 2, 3, \dots \quad (2)$$

where m defines the acoustic mode; k and c are the wave number and sound velocity, respectively; and Δd is the resonator end correction. In the case in which only the second factor would occur in the process of sound generation, the following relation between the dimension l of the cavity and wave length λ for disturbances of the shear layer [7] is the necessary condition for pulsation induction

$$l/\lambda = n - \gamma, \quad n = 1, 2, 3, \dots \quad (3)$$

where n defines the hydrodynamic mode, while $2\pi\gamma = \text{const}$ is the phase shift due to the edge effect. Therefore the instability of the shear layer can only occur for strictly defined λ values.

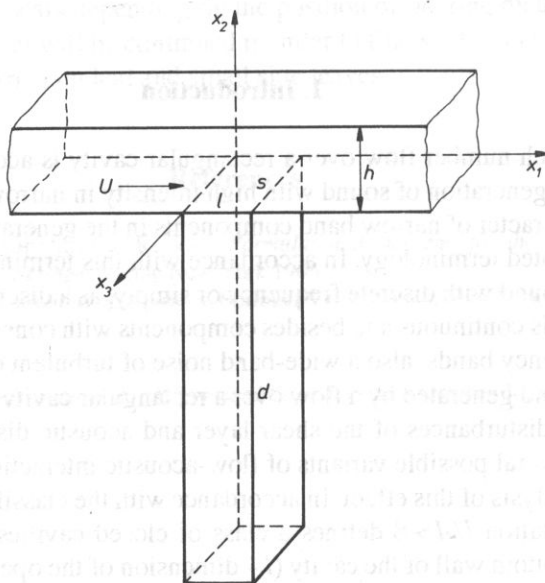


FIG. 1. Deep cavity as a side branch in a rectangular duct l, s – dimensions of cavity, d – depth of cavity, h – height of duct, U – main flow velocity.

In industrial installations for compressed air transport air discharge channels from the main channel may be a potential source of sound with discrete frequency [8]. Such a situation occurs when the discharge channel is closed while air flows in the main channel. In this paper we analyse the most unfavourable case when the discharge channel joins the main channel under a right angle and forms a deep rectangular cavity during cut-off (Fig. 1). An equivalent impedance system of a deep cavity with a gas stream flowing past it (Subsection 2.1) was used in the presented model and the interaction between resonance modes of the cavity and flow disturbances near the entry to the cavity (Subsection 2.2) was also taken into consideration. Calculation results of dimensionless frequency and values of relative pressure amplitude for discrete sound are compared with the results of measurements presented in paper [8] (Section 3).

2. Theoretical analysis

The case of a flow past a deep cavity with an opening with the following dimensions $-l$ and s (s – perpendicular to the direction of flow) – located in the wall of a rectangular channel is analysed here (Fig. 1). Low Mach number flow in the channel characterized the main velocity U . Hence, $M^2 \ll 1$, where $M = U/c$. We assume that the dimension of the opening of the cavity $-l$ and s – and the height of the channel $-h$ – are much smaller than the depth of the cavity $-d$

$$l/d \ll 1, \quad s/d \ll 1, \quad (4)$$

$$h/d \ll 1 \quad (5)$$

and so for frequencies close to the fundamental frequency f_1 ($m = 1$ in formula (2)) we obtain:

$$kl \ll 1, \quad ks \ll 1, \quad (6)$$

$$kh \ll 1, \quad (7)$$

where $k = 2\pi f/c$. On the basis of the condition (7) we can substitute the shear layer which forms near the opening of the cavity with a vortex sheet. If the displacement of the vortex sheet is defined by the function ξ , which is a harmonic function of t

$$\xi = \xi_a(x_1, x_3) e^{-j\omega t}, \quad (8)$$

where $\omega = 2\pi f$ then the velocity components in the direction normal to the plane of the opening just above and just below the vortex sheet are as follows:

$$v(\bar{x}, t) \Big|_{x_2 = +0} = \left(-j\omega + U \frac{\partial}{\partial x_1} \right) \xi = v_+, \quad (9)$$

$$v(\bar{x}, t) \Big|_{x_2 = -0} = -j\omega \xi = v_-, \quad (10)$$

where $\bar{x} = (x_1, x_2, x_3)$. The velocity v is discontinuous for $x_2 = 0$ only when $0 < x_1 < l$, because the velocities v_+ and v_- at the leading edge and the trailing edge must be equal to zero

$$v_{\pm}(x_1 = 0) = v_{\pm}(x_1 = l) = 0. \quad (11)$$

The condition (11) leads to the so-called Kutta-Žukowski boundary condition

$$\xi(x_1 = 0) = \partial \xi / \partial x_1(x_1 = 0) = 0, \quad (12)$$

which says that the vortex sheet can only leave the leading edge tangentially. The condition (12) has another important consequence – the condition of pressure equality on both sides of the vortex sheet is transferred to the leading edge. It would be very difficult to determine the boundary conditions at the trailing edge on the basis of the expression (11). In real conditions the influence of the trailing edge on the disturbances of the shear layer is strongly nonlinear. In order to take this nonlinearity into consideration in the presented linear model, we accepted that the displacement of the vortex sheet undergoes a jump at the trailing edge

$$\begin{aligned} \xi &\neq 0 \quad \text{for } x_1 = l, \\ \xi &= 0 \quad \text{for } x_1 > l. \end{aligned} \quad (13)$$

what means that only the right-hand limit of the function ξ satisfies the boundary condition (11) at the trailing edge. The introduction of nonlinearity of the function ξ at the trailing edge is a necessary condition for flow energy transfer to the cavity and for the induction of self-excited oscillations, as HOWE [9] and KELLER and ESCUDIER [10] papers have proved. This conclusion also finds confirmation in the analysis of an impedance model of a cavity presented in the following part of this paper.

2.1. Impedance model of a deep cavity

It results from the condition (6) that the dimensions of the cavity – l and s – are much smaller than the length of an acoustic wave. Thus the system formed by the deep cavity can be considered as a system with lumped elements. The properties of such a system are characterized by specific acoustic impedance defined as the ratio of acoustic pressure in the plane of the opening of the cavity to the acoustic velocity component in the direction perpendicular to this plane. In the case under analysis, pressure as well as the normal component of velocity depend on the displacement of the vortex sheet and thus are functions of the coordinates x_1 and x_3 . Therefore, in an impedance model of a cavity the pressure corresponds with the mean value of pressure on the surface of the opening of the cavity, while the normal component of velocity corresponds with the mean value of the normal component on this surface. In further parts of this paper these quantities will be called mean pressure and mean normal velocity.

As it results from Eqs. (9) and (10), there is a discontinuity of the normal component of velocity in the plane of the opening of the cavity. This leads to a discontinuity of the mean normal velocity. This means, from the acoustic point of view, that the cavity treated as a system with lumped elements, can be divided into two systems: outer in which the input signal is determined by the mean normal velocity for $x_2 = +0$, and inner in which the input signal is determined by the mean normal velocity for $x_2 = -0$.

If these quantities are noted as V_1 and V_2 , then on the basis of Eqs. (9) and (10) we have

$$V_1 = \frac{1}{ls} \int_0^s \int_0^l \left(-j\omega + U \frac{\partial}{\partial x_1} \right) \xi dx_1 dx_3 = V_2 + \frac{U}{ls} \int_0^s \xi(x_1 = l) dx_3 \quad (14)$$

$$V_2 = -\frac{j\omega}{ls} \int_0^s \int_0^l \xi dx_1 dx_3. \quad (15)$$

It results from the conditions of pressure equality on both sides of the vortex sheet that the mean pressure p_s is continuous in the plane of the opening of the cavity. Thus

$$V_1 = -p_s/z_1, \quad (16)$$

$$V_2 = p_s/z_2, \quad (17)$$

where z_1 and z_2 are specific acoustic impedances of the outer and inner system respectively. The minus sign in the expression (16) includes the fact that the phase shift between mean pressure and mean normal velocity is equal to π in the outer system [6]. The formulae (16) and (17) do not characterize the acoustic properties of the whole cavity because they concern the outer and inner system separately. In order to connect these two systems into one and thus obtain an impedance model of the whole cavity, Eqs. (16) and (17) should be substituted in Eq. (14). After conversions we obtain

$$p_s = \frac{z_1 z_2}{z_1 + z_2} V_0, \quad (18)$$

where

$$V_0 = -\frac{U}{ls} \int_0^s \xi(x_1 = l) dx_3. \quad (19)$$

Therefore an equivalent impedance system with a parallel connection of impedances of the outer and inner system is the model of the whole cavity. In this model the mean normal velocity V_0 represents the exciting signal and mean pressure p_s is the response to the excitation. As it results from Eq. (18) p_s differs from zero only when $V_0 \neq 0$. Acoustic oscillations can only be induced in the cavity when $\xi(x_1 = l) \neq 0$ (formula (19)) what is equivalent to the assumption that the function ξ which defines the displacement of the vortex sheet is discontinuous on the trailing edge.

2.1.1. Specific acoustic impedance of the outer system

Impedance z_1 of the outer system characterizes the process of acoustic energy exchange between the oscillating medium in the opening of the cavity and the outer medium. When there is no flow the real component of this impedance corresponds with the energy lost in the system (i.e. radiated energy) and the imaginary component corresponds with the energy of the medium oscillating with the system (i.e. energy initially transferred to the medium, but later transferred back to the system due to inertia). In the presence of a flow the energy transfer between the oscillating medium in the opening of

the cavity and the outer medium is much more complex. In real conditions this process determines mutual interactions between acoustic disturbances and the mobile medium. This causes some acoustic energy transfer to the out side [11]. This effect can be included in the analysed flow model which is an idealization of an actual flow, by introducing a modification of impedance z_1 . To this end we can take advantage of results of impedance z_1 measurements presented in WALKER'S and CHARWAT's paper [12] and the theoretical model suggested by these authors. This model makes it possible to determine changes of impedance z_1 in terms of flow velocity. In accordance with [12], impedance z_1 is the sum of two impedances

$$z_1 = z'_1 + z''_1, \quad (20)$$

where z'_1 characterizes the process of energy transfer between the oscillating medium in the opening of the cavity and the outer medium with no flow, while z''_1 defines the influence of flow on this process

$$z''_1 \approx \frac{\rho c K (M - jkl/2)}{1 + S^2/4}, \quad (21)$$

where K is an empirical constant, $S = \omega l/U$, and ρ is the density of the medium. Impedance z_1 corresponds with the radiation impedance of a rectangular piston with dimensions l and s . Hence, on the basis of [13]

$$z'_1 = r_p + j\rho c k \Delta d, \quad (22)$$

$$r_p = \frac{\rho c k^2}{16} (l^2 + s^2) \quad (23)$$

is the specific acoustic radiation resistance, and

$$\Delta d \approx \frac{8(l^2 + ls + s^2)}{9\pi(l + s)} \quad (24)$$

is the end correction.

2.1.2. Specific acoustic impedance of the inner system

The impedance of the inner system corresponds with the impedance of a rectangular cavity with depth d and other dimensions – l and s , with absorption phenomena included. The effect of acoustic wave damping is related with the occurrence of a tangent force on the walls of the cavity and with losses due to heat exchange between condensations and thinning in the medium. If the depth of the cavity greatly exceeds its other dimensions then the acoustic wave propagating inside the cavity can be considered to be a damped plane wave with a wave-front perpendicular to the axis of the cavity. Thus the velocity potential ϕ in the cavity is as follows

$$\phi_- = \left(A e^{\gamma x_2} + B e^{-\gamma x_2} \right) e^{-j\omega t}, \quad (25)$$

where A and B are constant their ratio depends on the boundary condition on the bottom wall of the cavity ($x_2 = -d$), and $\gamma = \eta + jk$ where η is the attenuation constant [14]

$$\eta = 1.95 \cdot 10^{-5} \left(\frac{\omega}{l_s} \right)^{1/2}. \quad (26)$$

The acoustic pressure p and acoustic velocity v in the cavity can be determined on the basis of the expression (25)

$$p = -\rho \frac{\partial \phi_-}{\partial t} = j\rho c k (A e^{\gamma x_2} + B e^{-\gamma x_2}) e^{-j\omega t}, \quad (27)$$

$$v = \frac{\partial \phi_-}{\partial x_2} = \gamma (A e^{\gamma x_2} - B e^{-\gamma x_2}) e^{-j\omega t}. \quad (28)$$

Since $p_s = p(x_2 = 0)$ and $V_2 = v(x_2 = 0)$, then

$$z_2 = p_s / V_2 = \frac{\rho c}{1 - j\eta/k} \frac{A/B + 1}{A/B - 1}. \quad (29)$$

If we accept that all walls of the cavity are perfectly rigid then the A/B ratio can be determined by applying the condition $v(x_2 = -d) = 0$ in Eq. (28). We obtain

$$A/B = e^{2\gamma d} \quad (30)$$

and finally

$$z_2 = \frac{\rho c}{1 - j\eta/k} \operatorname{cth}(\gamma d). \quad (31)$$

2.1.3. Average acoustic pressure on the surface of the opening of the cavity

The relationship between the exciting signal represented by the mean normal velocity V_0 and mean pressure p_s – the response of the cavity to the excitation – is determined by the expression (18) in the impedance model of the cavity. In this formula pressure p_s remains unknown. It is equivalent to the mean acoustic pressure p on the surface of the opening of the cavity

$$p_s = \frac{1}{l_s} \int_0^s \int_0^l p(x_2 = 0) dx_1 dx_3. \quad (32)$$

Pressure p is continuous for $x_2 = 0$ because p_s can be determined by defining p on the boundary of the outer area, i.e. for $x_2 = +0$. If the function $\phi_+(x, t)$ defines the velocity potential for $x_2 > 0$, then the derivative $\partial \phi_+ / \partial x_2$ for $x_2 = +0$ corresponds with the normal component of velocity v_+ (formula (9))

$$v_+(x_1, x_3, t) = \left. \frac{\partial \phi_+}{\partial x_2} \right|_{x_2 = +0}. \quad (33)$$

Applying in Eq. (33) the following identity

$$v_+(x_1, x_3, t) = \int_{-\infty}^{\infty} \int_{-\infty}^{\infty} v_+(y_1, y_3, t) \delta(x_1 - y_1) \delta(x_3 - y_3) dy_1 dy_3 \quad (34)$$

and the formula (9) which defines the dependence of the normal component v_+ on the displacement of the vortex sheet ξ , we obtain

$$\phi_+ = \int_{-\infty}^{\infty} \int_{-\infty}^{\infty} \left[-j\omega + U \frac{\partial}{\partial y_1} \right] \xi_a(y_1, y_3) \Big] G(y_2 = 0) dy_1 dy_3, \quad (35)$$

where

$$G(\bar{x}, \bar{y}, t), \quad \bar{x} = (x_1, x_2, x_3), \quad \bar{y} = (y_1, y_2, y_3),$$

a Green function which satisfies the following boundary conditions:

$$\frac{\partial G}{\partial x_2}(x_2 = h) = \frac{\partial G}{\partial x_3}(x_3 = 0) = \frac{\partial G}{\partial x_3}(x_3 = s) = 0, \quad (36)$$

$$\frac{\partial G}{\partial x_2}(x_2 = 0) = \delta(x_1 - y_1) \delta(x_3 - y_3) e^{-j\omega t}, \quad x_1 \in \langle 0, l \rangle, \quad (37)$$

$$\frac{\partial G}{\partial x_2}(x_2 = 0) = 0, \quad x_1 \notin \langle 0, l \rangle. \quad (38)$$

The range of variables y_1 and y_3 in the expression (35) can be limited to intervals: $0 \leq y_1 \leq l$, $0 \leq y_3 \leq s$ by extending the conditions $\xi_a(y_1, y_3) = 0$ onto the entire rigid surface limiting the entry to the cavity. This is equivalent to the assumption that the separation of flow only occurs in the entry to the cavity. Since on the boundary of the outer area

$$p(x_2 = 0) = -\rho \left(-j\omega + U \frac{\partial}{\partial x_1} \right) \phi_+(x_2 = 0), \quad (39)$$

then, after substituting Eq. (39) in Eq. (32) and including Eq. (35), we obtain

$$p_s = -\frac{\rho}{ls} \int_0^s \int_0^l \left(-j\omega + U \frac{\partial}{\partial x_1} \right) \int_0^s \int_0^l \left[\left(-j\omega + U \frac{\partial}{\partial y_1} \right) \xi_a(y_1, y_3) \right] \times \\ \times G(x_2 = 0, y_2 = 0) dy_1 dy_3 dx_1 dx_3. \quad (40)$$

Considering Eq. (36) for $x_1 \in \langle 0, l \rangle$, we can present the function G in the following form:

$$G(\bar{x}, \bar{y}, t) = \sum_{n=0}^{\infty} \cos\left(\frac{n\pi x_3}{s}\right) [G_n(\bar{x}_0, \bar{y}, t) + G_n(\bar{x}_0, y_1, y_2 = 2h, y_3, t)], \quad (41)$$

where $\bar{x}_0 = (x_1, x_2)$. The second expression in square brackets in this formula is an additional component of the Green function. It results from the reflection of the acoustic wave from the top wall of the channel $x_2 = h$. In cases of low Mach number flow and $x_1 \in \langle 0, l \rangle$ the function G_n has the same form as in a case without flow (see the Appendix)

$$G_n = -j \frac{\varepsilon_n \cos(\frac{n\pi y_3}{s})}{2s} H_0^{(1)} [k_n \sqrt{(x_1 - y_1)^2 + (x_2 - y_2)^2}] e^{-j\omega t}, \quad (42)$$

where ε_n is the Neumann constant and $k_n = (k^2 - n^2\pi^2/s^2)^{1/2}$.

2.2. Disturbances of the vortex sheet

It results from Eqs. (19) and (40), that two fundamental parameters in the impedance model of a cavity: mean normal velocity V_0 and mean pressure p_s , depend on the unknown function ξ which defines the displacement of the vortex sheet. In the case under analysis we can accept that sheet disturbances are two-dimensional [15, 16]

$$\xi(x_1, t) = \xi_a(x_1) e^{-j\omega t}, \quad (43)$$

therefore the expression (9) can be noted in the following form:

$$v_+ = (-j\omega + U \frac{\partial}{\partial x_1}) \xi(x_1, t) \quad (44)$$

As we can see from Eq. (13) the function ξ is discontinuous at the trailing edge ($x_1 = l$). Thus, if $\xi_c(x_1, t)$ denotes the displacement function-continuous on this edge – then on the basis of Eq. (13) we have

$$\xi(x_1, t) = \xi_c(x_1, t) [1 - H(x_1 - l)], \quad (45)$$

where $H(x_1 - l)$ is the unit step function

$$H(x_1 - l) = \begin{cases} 1, & x_1 > l, \\ 0, & x_1 \leq l. \end{cases} \quad (46)$$

Substituting Eq. (45) in Eq. (44) we hence achieve

$$v_+ = (-j\omega \xi_c + U \frac{\partial \xi_c}{\partial x_1}) [1 - H(x_1 - l)] - U \xi_a(l) \delta(x_1 - l) e^{-j\omega t}. \quad (47)$$

The introduction of a discontinuity in the function ξ leads to an additional component on the right hand side in Eq. (47). It represents the pulse velocity source. This source is a kind of an external force because, as it was assumed in the theoretical model, the discontinuity function ξ described the nonlinear effects accompanying the interaction between the shear layer and the trailing edge. A vortex sheet influenced by such a source exhibits instability which manifests itself in an amplitude increase of the sheet displacement when the distance from the source grows. If the motion of a vortex sheet located on the boundary of a low Mach number flow with velocity U in an unbounded two-dimensional space (no rigid surfaces) is influenced by a velocity source $-U \xi_a(l) \delta(x_1 - l) e^{-j\omega t}$, then the displacement of an unstable vortex sheet is described with the function ξ_c which is a superposition of Kelvin-Helmholtz waves:

$$\xi_c = M \xi_a(l) [a e^{j\varepsilon(x_1 - l)} + b e^{j\varepsilon^*(x_1 - l)}] e^{-j\omega t}, \quad (48)$$

where $\varepsilon = \omega(1 - j)/U$, while ε^* is a quantity conjugate with ε .

In the case if a vortex sheet lies within the area of the opening of the cavity, its unstable motion is a result of the presence of the pulse velocity source at the trailing edge and the influence of an acoustic signal induced in the cavity. Since, in accordance with the condition $kl < 1$, this signal is approximately a plane wave in the plane of the opening of the cavity, we accepted in our approximation method of the function ξ that ξ is a sum of the functions (48) in which an unknown quantity α was introduced in the place of the parameter ε and the component $Qe^{-j\omega t}$, where Q denotes the amplitude of a plane wave acoustic displacement was included. The parameter ε was changed into the parameter α – an unknown function of ω , U , l , s , d , h – in order to include in ξ mutual interactions between disturbances of the vortex sheet and acoustic modes of the cavity. Therefore the following assumption was accepted in the ξ approximation: the acoustic signal induced in the cavity does not change the form of the displacement function in the case of an unstable vortex sheet, it only modifies this function parameters. Hence the form of the function ξ accepted in the theoretical model is as follows:

$$\xi = M \xi_a(l) \left[a e^{j\alpha(x_1-l)} + b e^{j\alpha^*(x_1-l)} \right] e^{-j\omega t} + Q e^{-j\omega t}, \quad (49)$$

where $\alpha = \alpha_r + j\alpha_i$ and $\alpha_r > 0$, $\alpha_i < 0$. The displacement of the vortex sheet ξ must satisfy the Kutta–Zukowski condition at the leading edge, thus

$$\xi(x_1, t) = \xi_a(x_1) e^{-j\omega t} = Q \left(1 - \frac{\beta^*}{\beta + \beta^*} e^{\beta x_1/l} - \frac{\beta}{\beta + \beta^*} e^{-\beta^* x_1/l} \right) e^{-j\omega t}, \quad (50)$$

where $\beta = j\alpha l = \beta_r + j\beta_i$ and

$$\beta_r = -\alpha_i l > 0, \quad \beta_i = \alpha_r l > 0. \quad (51)$$

The amplitude Q and parameter β in the formula (50) are unknown quantities. Equation (18) should be used to determine β . This equation defines the relationship between the mean normal velocity V_0 and mean pressure p_s in the impedance model of a cavity. Once we know the form of the function $\xi(x_1, t)$, V_0 can be determined on the basis of Eq. (19)

$$V_0 = \frac{QU}{l} \left(\frac{\beta}{\beta + \beta^*} e^{\beta} + \frac{\beta^*}{\beta + \beta^*} e^{-\beta^*} - 1 \right) e^{-j\omega t}, \quad (52)$$

while Eqs. (41) and (42) are included in the expression (40) and is integrated in terms of x_3 and y_3 , it can be written in the following form:

$$p_s = \frac{j\rho QU}{2l^2} \int_0^l (-j\omega + U \frac{\partial}{\partial x_1}) \int_0^l (\gamma_1 e^{\beta y_1/l} + \gamma_2 e^{-\beta^* y_1/l} - jS) \times \\ \times \left\{ H_0^{(1)}(k|x_1 - y_1|) + H_0^{(1)} \left[k \sqrt{(x_1 - y_1)^2 + 4h^2} \right] \right\} e^{-j\omega t} dy_1 dx_1, \quad (53)$$

where $\gamma_1 = \beta^*(jS - \beta)/(\beta + \beta^*)$ and $\gamma_2 = \beta(jS + \beta^*)/(\beta + \beta^*)$. Since $kl \ll 1$, then the following approximation of the Hankel function [17] can be applied in the formula (53)

$$H_0^{(1)}(k|x_1 - y_1|) \approx \frac{2j}{\pi} \ln(k|x_1 - y_1|/2), \quad (54)$$

$$H_0^{(1)} \left[k \sqrt{(x_1 - y_1)^2 + 4h^2} \right] \approx \sum_{n=0}^{\infty} \varepsilon_n (-1)^n H_{2n}^{(1)}(2kh) \frac{(k|x_1 - y_1|/2)^{2n}}{(2n)!} \quad (55)$$

When we substitute Eqs. (52) and (53) in the expression (18) and integrate it in terms of x_1 and y_1 we obtain the following equation

$$\beta = jS + \frac{F_1(\beta)}{F_2(\beta)}. \quad (56)$$

The functions F_1 and F_2 which occur in this expression are:

$$F_1(\beta) = \frac{\pi z_1 z_2}{\rho c M(z_1 + z_2)} \left[e^\beta - 1 + \frac{\beta}{\beta^*} (e^{-\beta^*} - 1) \right] \beta + \left(\frac{\beta}{\beta^*} \right)^2 (\beta^* + jS) \times \\ \times \left\{ S \left[j \ln(kl/2) - \frac{\pi}{2} \right] (e^{-\beta^*} - 1) + \frac{1}{2} \pi S \Sigma_1 + (\beta^* + jS) \left[\Sigma_3(-\beta^*) + \frac{1}{2} j \pi \Sigma_4(-\beta^*) \right] \right\} + \\ + S^2 \left[\frac{3}{2} - \ln(kl/2) + j \pi \sigma_2 \right] \left(1 + \frac{\beta}{\beta^*} \right) \beta, \quad (57)$$

$$F_2(\beta) = S \left[j \ln(kl/2) - \frac{\pi}{2} \right] (1 - e^\beta) - \frac{1}{2} \pi S \Sigma_1 + (\beta - jS) \left[\Sigma_3(\beta) + \frac{1}{2} j \pi \Sigma_4(\beta) \right] \quad (58)$$

where Σ_1 , Σ_2 , Σ_3 and Σ_4 are series as follows:

$$\Sigma_1 = \sum_{n=0}^{\infty} \frac{\varepsilon_n (-1)^n (kl/2)^{2n} H_{2n}^{(1)}(2kh)}{(2n+1)!}, \quad (59)$$

$$\Sigma_2 = \sum_{n=0}^{\infty} \frac{\varepsilon_n (-1)^n (kl/2)^{2n} H_{2n}^{(1)}(2kh)}{(2n+2)!}, \quad (60)$$

$$\Sigma_3(z) = \sum_{n=1}^{\infty} \frac{1 + (-1)^n e^z}{n \cdot n!} z^{n-1}, \quad (61)$$

$$\Sigma_4(z) = 2 \sum_{n=1}^{\infty} (-1)^n (kl/2)^{2n} H_{2n}^{(1)}(2kh) \sum_{m=0}^{2n-1} \frac{1 + (-1)^m e^z}{(2n-m)!} z^{-m-1}. \quad (62)$$

In the case of the accepted particular geometry of the system (h , l , s and d are given) Eq. (56) can be presented in the following form

$$\beta_r + j\beta_i = F(f, U, \beta_r, \beta_i), \quad (63)$$

where F is the function found on the right hand side in Eq. (56). Thus we have

$$\beta_r = \text{Re} [F(f, U, \beta_r, \beta_i)], \quad (64)$$

$$\beta_i = \text{Im} [F(f, U, \beta_r, \beta_i)]. \quad (65)$$

Since the frequency f and velocity U are independent variables then for $f = \text{const}$ and $U = \text{const}$ Eqs. (64) and (65) represent a set of equations with two unknown quantities –

β_r and β_i . A numerical procedure is necessary to solve these equations. Roots sought for are such values of β_r and β_i which satisfy the conditions (51).

2.3. Discrete sound frequency

The cavity in experimental studies presented in the paper [8] had the same square section as the main channel, $h = l = s = 6$ cm and depth $d = 53$ cm. The frequency f_d of the discrete sound was determined on the basis of changes of pressure amplitude p_0 measured at the bottom wall of the cavity in terms of f .

If we accept $x_2 = -d$, the pressure p_0 can be determined from the expression (27). Hence we have

$$p_0 = j\rho ck(Ae^{-\gamma d} + Be^{\gamma d})e^{-j\omega t}, \quad (66)$$

where $A = Be^{2\gamma d}$ on the basis of Eq. (30). The relationship between p_0 and p_s can be determined on the basis of the fact that p_s – the pressure in the plane of the opening of the cavity – corresponds with the p value from the expression

$$p_0 = Pe^{j\varphi} = \frac{P_s}{\operatorname{ch}(\gamma d)}, \quad (67)$$

where $P = |p_0|$ and φ is the amplitude and phase of pressure p_0 , respectively. Substituting Eq. (18) and including Eq. (52) in Eq. (67), we obtain

$$P = Q \left[\frac{U}{l} \left| \frac{z_1 z_2}{(z_1 + z_1) \operatorname{ch}(\gamma d)} \left(\frac{\beta}{\beta + \beta^*} e^{\beta} + \frac{\beta^*}{\beta + \beta^*} e^{-\beta^*} - 1 \right) \right| \right]. \quad (68)$$

Since the parameter $\beta = \beta_r + j\beta_i$ is a function of f and U then for fixed values h, l, s and d Eq. (68) can be presented in the following form:

$$P(f, U) = Q \cdot g[f, U, \beta_r(f, U), \beta_i(f, U)], \quad (69)$$

where g is the function to be found in square brackets on the right hand side in Eq. (68). For frequency $f = f_d$ amplitude P achieves a maximum in terms of f , so

$$P_d(U) = P(f_d, U) = \{Q \cdot g[f, U, \beta_r(f, U), \beta_i(f, U)]\}_{\max}. \quad (70)$$

The results of calculations of the parameters β_r and β_i (roots of the set of Eqs. (64) and (65)), presented in Fig. 2, illustrate a typical dependence of these quantities on the frequency f for $U = \text{const}$ in the case of a cavity with the following dimensions: $h = l = s = 6$ cm and $d = 53$ cm. We can see that the function $\beta_r(f)$ achieves a distinct maximum for a certain frequency f (Fig. 2a). Also the greatest changes in the parameter β_i are observed around this frequency (Fig. 2b). Relative changes of the function g for quantities β_r and β_i determined from Figs. 2a, b are of similar character as changes of β_r in terms of f (Fig. 2c). This indicates that the values of the function g depend on the real part of β mainly.

As we can see from Fig. 2c, the function g reaches a maximum in a very narrow frequency f range. This makes this function similar to spectral characteristics typical for

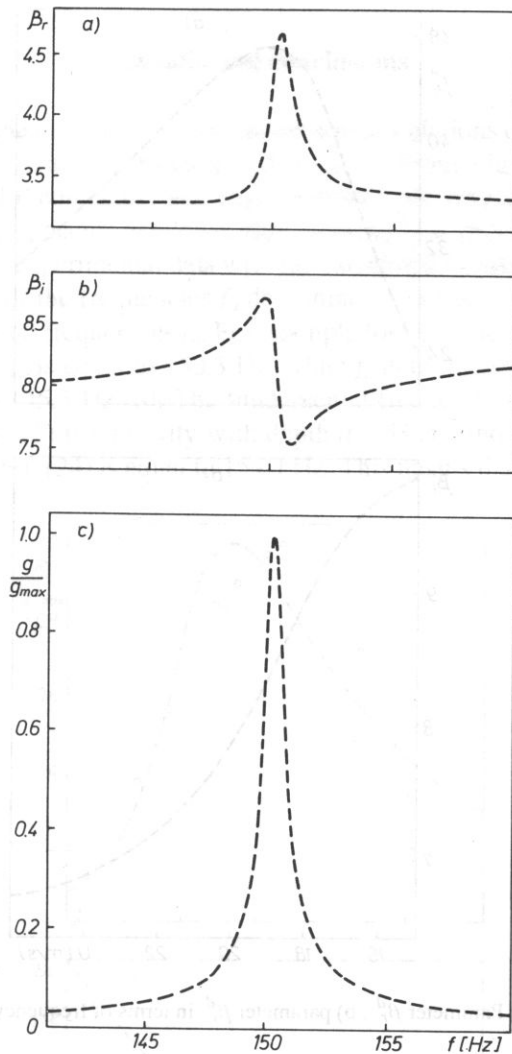


FIG. 2. a) Parameter β_r , b) parameter β_i , c) relative value of function g from the expression (69) in terms of frequency f . Flow velocity $U = 19.5$ m/s.

discrete sound. Therefore basing on the assumption that the parameter Q influences the function P in terms of f only slightly, and here

$$P_d(U) = Q \cdot g[f_d, U, \beta_r^d(U), \beta_i^d(U)], \quad (71)$$

where $\beta_r^d(U) = \beta_r(f_d, U)$, $\beta_i^d(U) = \beta_i(f_d, U)$. Figure 3 presents calculation results of the parameters β_r^d and β_i^d for a range of flow velocity from 15 to 26 m/s. We can observe that changes of β_r^d and β_i^d which accompany an increase of U are clearly of a

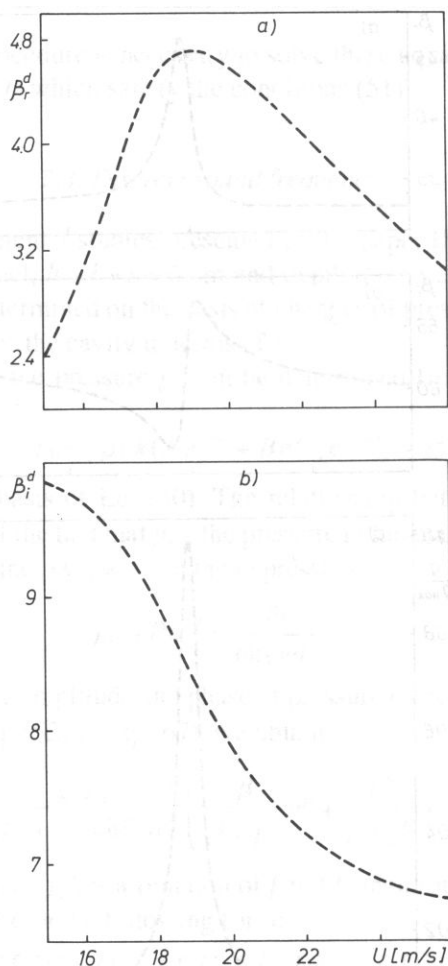


FIG. 3. a) Parameter β_r^d , b) parameter β_i^d in terms of frequency velocity U .

different character. The function which describes β_r^d in terms of U has a maximum (Fig. 3a) while the value of β_i^d always decreases when U grows (Fig. 3b). Since the value of the function g depends mainly on the parameter β_r^d , the function $g[f_d, U, \beta_r^d(U), \beta_i^d(U)]$ reaches a maximum within the flow range 15–26 m/s, as it results from Fig. 3. If we make a hypothesis that the parameter Q also only insignificantly influences the function P_d in terms of U , then relative changes of P_d will correspond with relative changes of the function g . Hence

$$\frac{P_d(U)}{[P_d(U)]_{\max}} = \frac{g[f_d, U, \beta_r^d(U), \beta_i^d(U)]}{\{g[f_d, U, \beta_r^d(U), \beta_i^d(U)]\}_{\max}}. \quad (72)$$

3. Results and conclusions

Figure 4 presents the results of measurements and calculations of the $P_d/(P_d)_{\max}$ ratio as well as of the dimensionless frequency $St = f_d l/U$. From Fig. 4a we can see that $P_d/(P_d)_{\max}$ determined theoretically and experimentally are very similar, but the maximum value of $P_d/(P_d)_{\max}$ occurs at a lower flow velocity $U = 19.5$ m/s.

When we compare experimental data with the calculated results shown in Fig. 4b we notice that the values of the frequencies f_d determined theoretically are always slightly higher than the measured frequencies f_d . For example for $P_d/(P_d)_{\max} = 1$ the theoretically determined frequency f_d is equal to 150.3 Hz, while f_d determined from experiment for $P_d/(P_d)_{\max}$ is equal to 145.5 Hz [8]. The fundamental frequently frequency f_1 is calculated from the formula (2) for a cavity with depth $d = 53$ cm and end correction determined on the basis of Eq. (24) is equal to 154.4 Hz. This means that the maximum gene-

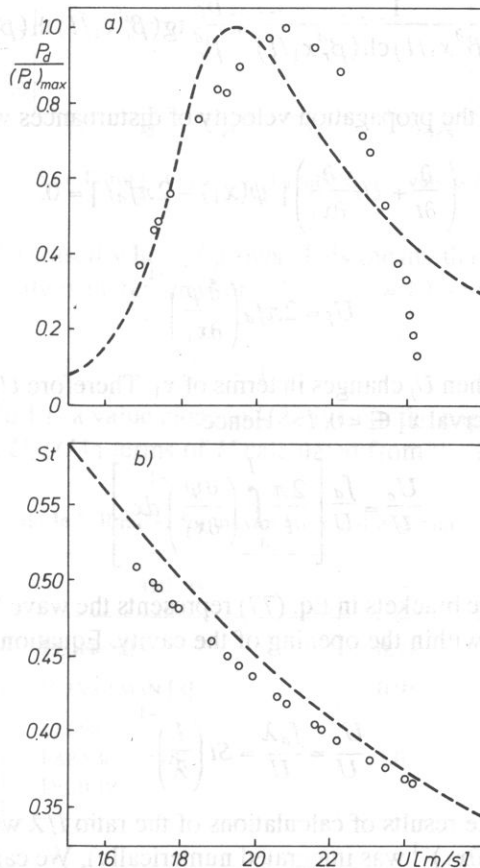


FIG. 4. a) Ratio $P_d/(P_d)_{\max}$, b) dimensions frequency St in terms of velocity(---) – calculated values, (...) – measurement results in accordance with [8].

ration of discrete sound occurs at a frequency f_d slightly lower than the fundamental frequency f_1 of the cavity.

The ratio of propagation velocity U_c of flow disturbances within the opening of the cavity and main flow velocity U is a quantity frequently determined theoretically and experimentally. The velocity U_c presented in the theoretically model in Section 2 is equivalent to the mean phase velocity U_f for disturbances of the vortex sheet described with the function (50) for $f = f_d$. In order to determine U_f , Eq. (50) must be converted into the following form

$$\xi(x_1, t) = |\xi_a(x_1)| e^{j[\psi(x_1) - 2\pi f_d t]}, \quad (73)$$

where

$$\begin{aligned} \psi(x_1) = \arctg \left\{ \left[\operatorname{tg}(\beta_i^d x_1/l) - \frac{\beta_i^d}{\beta_r^d} \operatorname{th}(\beta_r^d x_1/l) \right] \times \right. \\ \left. \times \left[1 - \frac{1}{\cos(\beta_i^d x_1/l) \operatorname{ch}(\beta_r^d x_1/l)} + \frac{\beta_i^d}{\beta_r^d} \operatorname{tg}(\beta_i^d x_1/l) \operatorname{th}(\beta_r^d x_1/l) \right]^{-1} \right\}. \end{aligned} \quad (74)$$

The velocity U_f defines the propagation velocity of disturbances with constant phase

$$\left(\frac{\partial}{\partial t} + U_f \frac{\partial}{\partial x_1} \right) [\psi(x_1) - 2\pi f_d t] = 0, \quad (75)$$

and thus

$$U_f = 2\pi f_d \left(\frac{\partial \psi}{\partial x_1} \right)^{-1}. \quad (76)$$

Since $\partial \psi / \partial x_1 \neq \text{const}$, then U_f changes in terms of x_1 . Therefore U_c corresponds with the mean value U_f in an interval $x_1 \in <0, l>$. Hence

$$\frac{U_c}{U} = \frac{f_d}{U} \left[\frac{2\pi}{l} \int_0^l \left(\frac{\partial \psi}{\partial x_1} \right)^{-1} dx_1 \right]. \quad (77)$$

The expression in square brackets in Eq. (77) represents the wave length λ for disturbances of the vortex sheet within the opening of the cavity. Equation (77) can be noted as follows:

$$\frac{U_c}{U} = \frac{f_d \lambda}{U} = St \left(\frac{l}{\lambda} \right)^{-1}. \quad (78)$$

Figure 5 presents the results of calculations of the ratio l/λ within the flow velocity range 15–26 m/s ($(\partial \psi / \partial x_1)^{-1}$ was integrated numerically). We can see from Fig. 5a that the ratio l/λ changes within the limits

$$0.86 \leq l/\lambda \leq 1.33, \quad (79)$$

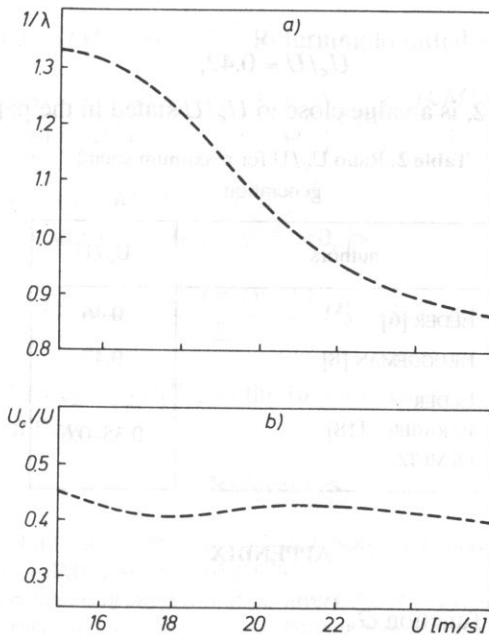


FIG. 5. a) Ratio $1/\lambda$ versus U , b) ratio U_c/U versus U .

and its value always decreased when U grows. This means that the wave length λ increases when flow velocity is increased. For velocity $U = 19.5$ m/s, when $P_d/(P_d)_{\max}$

$$1/\lambda = 1.1, \quad (80)$$

what according to Table 1 is a value close to $1/\lambda$ given in the papers [8], [18].

Figure 5b presents U_c/U in terms of U calculated from the formula (78) for values

Table 1. Ratio $1/\lambda$ for maximum sound generation

authors	$1/\lambda$
ELDER [6]	0.77
BRUGGEMAN [8]	0.91
ELDER FARABEE [18] DEMETZ	1.05

St and $1/\lambda$ from Figs. 4b and 5a. We can see that U_c/U changes are insignificant within the flow velocity range 15–26 m/s because

$$0.4 \leq U_c/U \leq 0.45. \quad (81)$$

when $P_d/P_{d\max} = 1$

$$U_c/U = 0.42, \tag{82}$$

what, according to Table 2, is a value close to U_c/U stated in the papers [6], [8].

Table 2. Ratio U_c/U for maximum sound generation

authors	U_c/U
ELDER [6]	0.46
BRUGGEMAN [8]	0.47
ELDER FARABEE [18] DEMETZ	0.35–0.6

APPENDIX

Calculation of Green function G_n .

The function G_n is a solution of the equation

$$\sum_0^\infty \cos(n\pi x_3/s) \left(\nabla^2 G_n - 2jkM \frac{\partial G_n}{\partial x_1} - M^2 \frac{\partial^2 G_n}{\partial x_1^2} + k_n^2 G_n \right) = \delta(\bar{x} - \bar{y}) e^{-j\omega t}, \tag{A1}$$

where $k_n = (k^2 - n^2 \pi^2/s^2)^{1/2}$. After multiplying A1 by $\cos(n\pi x_3/s)$ and integrating it with respect to x_3 within the interval $x_3 \in <0, s>$, we obtain

$$\begin{aligned} \nabla^2 G_n - 2jkM \frac{\partial G_n}{\partial x_1} - M^2 \frac{\partial^2 G_n}{\partial x_1^2} + k_n^2 G_n = \\ = \frac{\varepsilon_n \cos(n\pi y_3/s)}{s} \delta(x_1 - y_1) \delta(x_2 - y_2) e^{-j\omega t}. \end{aligned} \tag{A2}$$

When we apply the following conversion of variables in Eq. (A2)

$$x'_1 = \mu^2 x_1, y'_1 = \mu^2 y_1, x'_2 = \mu x_2, y'_2 = \mu y_2, t' = t + \mu^2 M(x_1 - y_1)/c, \tag{A3}$$

where $\mu = (1 - M^2)^{-1/2}$, we have

$$\nabla^2 G_n + k_n^2 G_n = f(y_3) \delta(x'_1 - y'_1) \delta(x'_2 - y'_2) e^{-j\omega t'}, \tag{A4}$$

where $f(y_3) = \mu^2 \frac{\varepsilon_n \cos(n\pi y_3/s)}{s}$. Equation (A4) is a inhomogeneous wave equation in two-dimensional space, therefore, when we include the condition (38) we have

$$G_n = -\frac{1}{2} j f(y_3) H_0^{(1)}(k_n r') e^{-j\omega t'}, \tag{A5}$$

where $r' = [(x'_1 - y'_1)^2 + (x'_2 - y'_2)^2]^{1/2}$. Returning to initial variables we obtain

$$G_n = -j \frac{\varepsilon_n \cos(n\pi y_3/s)}{2s(1-M^2)} H_0^{(1)} \left(\frac{k_n r}{1-M^2} \right) \exp \left(\frac{-jkM(x_1 - y_1)}{1-M^2} - j\omega t \right), \quad (A6)$$

where $r' = [(x_1 - y_1)^2 + (1-M^2)(x_2 - y_2)^2]^{1/2}$.

When $M^2 \ll 1$, $kl \ll 1$ and $x_1 \in <0, l>$, $y_1 \in <0, l>$

$$G_n \approx -j \frac{\varepsilon_n \cos(n\pi y_3/s)}{2s} H_0^{(1)}(k_n r) e^{-j\omega t}, \quad (A7)$$

where $r = [(x_1 - y_1)^2 + (x_2 - y_2)^2]^{1/2}$, so the function G_n has the same form as it would have in a case without flow.

References

- [1] D. ROCKWELL, E. NAUDASCHER, *Review – self-sustaining oscillations of flow past cavities*, J. Fluids Engineering, Trans. ASME **100**, 152–165 (1978).
- [2] D. ROCKWELL, *Oscillations of impinging shear layers*, AIAA J. **21**, 5, 645–664 (1983).
- [3] V. SAROHIA, *Experimental investigation of oscillations in flow over shallow cavities*, AIAA J. **15**, 7, 984–991 (1977).
- [4] A.J. BILANIN, E.E. COVERT, *Estimation of possible excitation frequencies for shallow rectangular cavities*, AIAA J. **11**, 3, 347–351 (1973).
- [5] C.K. TAM, P.J. BLOCK, *On the tones and pressure oscillations induced by flow over rectangular cavities*, J. Fluid Mech. **89**, 373–399 (1978).
- [6] S.A. ELDER, *Self-excited depth-mode resonance for wall-mounted cavity in turbulent flow*, J. Acoust. Soc. Am. **64**, 3, 877–890 (1978).
- [7] J.E. ROSSITER, *Wind tunnel experiments on the flow over rectangular cavities at subsonic and transonic speeds*, RAE Report No. 64037, (1964).
- [8] J.C. BRUGGEMAN, *Flow induced pulsations in pipe systems*, Ph.D. thesis, Eindhoven, 1987.
- [9] M.S. HOWE, *The influence of mean shear on unsteady aperture flow, with application to acoustical diffraction and self-sustained oscillations*, J. Fluid Mech. **109**, 125–146 (1981).
- [10] J.J. KELLER, M.P. ESCUDIER, *Flow-excited resonances in covered cavities*, J. Sound Vib. **86**, 2, 199–226 (1983).
- [11] P.A. NELSON, N.A. HALLIWELL, P.E. DOAK, *Fluid dynamics of a flow excited resonance, part II: flow acoustic interaction*, J. Sound Vib. **91**, 3, 375–402 (1983).
- [12] B.E. WALKER, A.F. CHARWAT, *Correlation of the effects of grazing flow on impedance of Helmholtz resonators*, J. Acoust. Soc. Am. **72**, 2, 550–555 (1982).
- [13] P.M. MORSE, K.U. INGARD, *Theoretical acoustics*, McGraw-Hill, New York 1968, p. 394.
- [14] L.E. KINSLER, A.R. FREY, *Fundamentals of acoustics*, John Wiley, New York 1962, p. 241.
- [15] L.F. EAST, *Aerodynamically induced resonance in rectangular cavities*, J. Sound Vib. **3**, 3, 277–287 (1966).
- [16] E.E. COVERT, *An approximate calculation of the onset velocity of cavity oscillations*, AIAA J., **8**, 12, 2189–2194 (1970).
- [17] N.N. LEBEDIEW, *Special functions and their applications* (in Polish), PWN, Warszawa 1957, pp. 135, 146.
- [18] S.A. ELDER, T.M. FARABEE, F.C. DEMETZ, *Mechanisms of flow-excited tones at low Mach number*, J. Acoust. Soc. Am., **72**, 2, 532–549 (1982).

SOUND SOURCES OF HIGH DIRECTIVITY

R. WYRZYKOWSKI

Institute of Physics, Pedagogical College
(35-310 Rzeszów, Rejtana 16a)

The reversibility of Hankel transform suggests the possibility of constructing such a sound source which radiates only within a certain cone. Both the approximate and accurate theories of that source are given. It is proved in the paper that the accurate source is better than the approximate one. The source is called the source of high directivity.

Introduction

In paper [7] was suggested the theoretical possibility of constructing a sound source radiating only within a certain cone. Such a property is exhibited by a baffled piston with a special distribution of the velocity amplitude, given by the Bessel function $J_1(n\frac{r}{a})$ (n will be explained later, " a " – radius of the piston, r – cylindrical coordinate) divided by the argument. The distribution must be extended theoretically to infinity. Such a source was called the source of high directivity. In the present paper we consider the case of the real distribution (only on the piston itself) and we prove that its directivity is better than the theoretical one.

The author is indebted to prof. dr hab. Marek RYTEL for his interesting and stimulating discussions and suggestions.

1. Theoretical basis

The possibility of realizing the directivity pattern mentioned above is the conclusion of reversibility of the Hankel transform [1]. That transform of the velocity distribution $u(r)$ is the main part of the R -directivity index [7]

$$R = \frac{2\pi}{Q} \int_0^a u(r) J_0(krs \sin \gamma) r dr, \quad (1)$$

where Q is the output of the source, γ – the angle between the z – axis perpendicular to the plane of the piston and the given direction, k – the wave number. The Hankel transform of zero order is defined by the formula [1]

$$H_0(\rho) = \int_0^{\infty} u(r) J_0(\rho r) r dr, \quad (2)$$

where $J_0(\rho r)$ denotes the Bessel function of zero order. If the amplitude of velocity on the piston is 0 for $r \geq a$ and $u(r)$ for $r < a$, then

$$H_0(\rho) = \int_0^a u(r) J_0(\rho r) r dr \quad (3)$$

and the directivity index is

$$R = \frac{2\pi}{Q} H_0(k \sin \gamma). \quad (4)$$

It is well known that for the constant amplitude u_0 we have

$$u(r) = \begin{cases} u_0 & r < a, \\ 0 & r \geq a, \end{cases} \quad (5)$$

and the directivity index has the form

$$R = 2 \frac{J_1(k a \sin \gamma)}{k a \sin \gamma}, \quad (6)$$

where $J_1(k a \sin \gamma)$ denotes the Bessel function of the order one. One may expect the velocity amplitude distribution of the form

$$u(r) = 2u_0 \frac{J_1(n \frac{r}{a})}{n \frac{r}{a}}, \quad (7)$$

to have the directivity index

$$R = \begin{cases} \text{const} & \gamma \leq \gamma_{\text{lim}}, \\ 0 & \gamma > \gamma_{\text{lim}}, \end{cases} \quad (8)$$

where γ_{lim} denotes the so-called limiting angle – the half of the cone angle, in which the sound is radiated. Of course, the constant in the formula (8) will be normalized to unity. The directivity (8) can be realized only if the distribution (7) is extended on the entire plane of the baffle. We choose the gauge factor n to diminish the influence of the area $r > a$ under the integral. Such a method is called the approximate one. In the accurate method we choose the velocity distribution as follows:

$$u(r) = \begin{cases} 2u_0 \frac{J_1(n \frac{r}{a})}{n \frac{r}{a}} & r < a \\ 0 & r \geq a. \end{cases} \quad (9)$$

In the present paper both methods were applied and the results compared. One may expect that the distribution (9) will not give the sharp break-off of the directivity pattern for $\gamma = \gamma_{\text{lim}}$.

2. Approximate method

We choose the distribution of the velocity as in the formula (7). It is evident that the best option is to accept for $r = a$ $u(a) = 0$; therefore we must have

$$J_1(n) = 0. \quad (10)$$

The gauge factor n must be equal to the zeros of the function $J_1(n)$ denoted as α_{1m}

$$n = \alpha_{1m}, \quad m = 1, 2, \dots \quad (11)$$

where $\alpha_{10} = 0$, $\alpha_{11} = 3.8317$

The formula (7) now takes the form

$$u(r) = 2u_0 \frac{J_1(\alpha_{1m} \frac{r}{a})}{\alpha_{1m} \frac{r}{a}} \quad (12)$$

For $r \rightarrow 0$ we have [7]:

$$\lim_{r \rightarrow 0} u_0 \frac{J_1(\alpha_{1m} \frac{r}{a})}{\alpha_{1m} \frac{r}{a}} = \frac{1}{2} \quad (13)$$

and

$$u(0) = u_0. \quad (14)$$

That explains the presence of the factor 2 in the formula (12). Owing to the extension of the distribution (12) to infinity, the Hankel transform of $u(r)$ is

$$H_0(k \sin \gamma) = 2u_0 \frac{a}{\alpha_{1m}} \int_0^\infty J_1(\alpha_{1m} \frac{r}{a}) J_0(kr \sin \gamma) dr. \quad (15)$$

The integral in the formula (15) is given in the tables of integrals [1; p. 681]. It has the value

$$\int_0^{\infty} J_1\left(\alpha_{1m} \frac{r}{a}\right) J_0(kr \sin \gamma) dr = \begin{cases} \frac{a}{\alpha_{1m}} & \text{for } k \sin \gamma < \frac{\alpha_{1m}}{a} \\ \frac{2a}{2\alpha_{1m}} & \text{for } k \sin \gamma = \frac{\alpha_{1m}}{a} \\ 0 & \text{for } k \sin \gamma > \frac{\alpha_{1m}}{a} \end{cases} \quad (16)$$

From the formula (15) we calculate the directivity index (4) in the form

$$R = \begin{cases} \frac{4\pi u_0}{Q \left(\frac{\alpha_{1m}}{a}\right)^2} & \text{for } k \sin \gamma < \frac{\alpha_{1m}}{a} \\ \frac{4\pi u_0}{Q \left(\frac{\alpha_{1m}}{a}\right)^2} & \text{for } k \sin \gamma = \frac{\alpha_{1m}}{a} \\ 0 & \text{for } k \sin \gamma > \frac{\alpha_{1m}}{a} \end{cases} \quad (17)$$

The output of the source for the velocity distribution, determined by (7), is

$$Q = 4\pi u_0 \frac{a}{\alpha_{1m}} \int_0^{\infty} J_1\left(\alpha_{1m} \frac{r}{a}\right) dr, \quad (18)$$

and solving the elementary integral we get

$$Q = 4\pi u_0 \left(\frac{a}{\alpha_{1m}}\right)^2. \quad (19)$$

Substituting (19) into (17) we get

$$R = \begin{cases} 1 & \text{for } k \sin \gamma < \frac{\alpha_{1m}}{a} \\ \frac{1}{2} & \text{for } k \sin \gamma = \frac{\alpha_{1m}}{a} \\ 0 & \text{for } k \sin \gamma > \frac{\alpha_{1m}}{a} \end{cases} \quad (20)$$

We see that in our problem does exist a limiting angle

$$\gamma_{\lim} = \sin^{-1} \frac{\alpha_{1m}}{ka}, \quad (21)$$

above which we have no sound field i.e. no radiation of the sound energy. In the physical sense only $\gamma_{\lim} < \pi/2$ or $\sin \gamma_{\lim} < 1$ is acceptable. For that reason only for the case $ka > \alpha_{1m}$ we have the required source.

The condition $ka > \alpha_{1m}$ can be expressed by the corresponding wavelength λ

$$\lambda < \frac{2\pi a}{\alpha_{1m}}. \quad (22)$$

If we take

$$ka = \alpha_{1m}, \quad (23)$$

then:

$$\lambda_{\text{lim}} = \frac{2\pi a}{\alpha_{1m}}. \quad (24)$$

In the physical sense γ_{lim} takes its maximum value

$$\gamma_{\text{lim}}^{\text{max}} = \frac{\pi}{2}. \quad (25)$$

Figure 1 represents the values γ_{lim} versus ka for α_{11} , α_{12} and α_{13} .

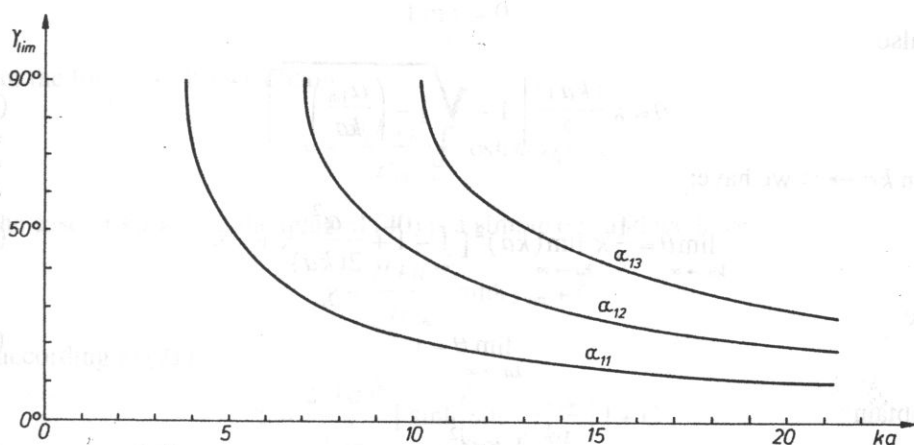


FIG. 1. Values of γ_{lim} versus ka for α_{11} , α_{12} and α_{13} .

Further reduction of ka leads us to a unidirectional source. Coming now to the calculation of the specific impedance of our idealised source, we denote by θ its real part and by χ its imaginary part. To find θ we will modify the method applied in [6] for the constant velocity amplitude. For that purpose we introduce in the formula given in [6] a normalizing coefficient κ and we get

$$\theta = \kappa \frac{(ka)^2}{2} \int_0^{\pi/2} R^2(ka \sin \gamma) \sin \gamma d\gamma. \quad (26)$$

It should be remembered that formula (26) for $\kappa = 1$ was obtained for the constant amplitude by equating the acoustic power emitted by the source (expressed by θ) to the power obtained in the farfield by integrating the square of the directivity index. When the

amplitude is not constant we must remember that the first quantity is proportional to the mean value of squared velocity amplitude, but the second one is based on the output and is proportional to the square of the mean value. When we calculate the accurate values we will demonstrate the method of calculating κ . In the present case we can find it simply by equating the $\lim_{ka \rightarrow \infty} \theta$ to unity. From (20) and (26) we have

$$\theta = \kappa \frac{(ka)^2}{2} \int_0^{\gamma_{\lim}} \sin \gamma d\gamma, \quad (27)$$

from which we directly obtain

$$\theta = \kappa \frac{(ka)^2}{2} (1 - \cos \gamma_{\lim}) \quad (28)$$

Substituting (21) for the value of $\sin \gamma_{\lim}$, we may write

$$\cos \gamma_{\lim} = \sqrt{1 - \sin^2 \gamma_{\lim}} = \sqrt{1 - \left(\frac{\alpha_{1m}}{ka}\right)^2} \quad (29)$$

and also

$$\theta = \kappa \frac{(ka)^2}{2} \left[1 - \sqrt{1 - \left(\frac{\alpha_{1m}}{ka}\right)^2} \right]. \quad (30)$$

When $ka \rightarrow \infty$ we have:

$$\lim_{ka \rightarrow \infty} \theta = \frac{1}{2} \kappa \lim_{ka \rightarrow \infty} (ka)^2 \left[1 - 1 + \frac{\alpha_{1m}^2}{2(ka)^2} + \dots \right]. \quad (31)$$

Since

$$\lim_{ka \rightarrow \infty} \theta = 1 \quad (32)$$

we obtain

$$\frac{1}{2} \kappa \frac{\alpha_{1m}^2}{2} = 1 \quad (33)$$

and the normalizing coefficient:

$$\kappa = \frac{4}{\alpha_{1m}^2}. \quad (34)$$

Substituting (34) into (30) we get:

$$\theta = \frac{2(ka)^2}{\alpha_{1m}^2} \left[1 - \sqrt{1 - \left(\frac{\alpha_{1m}}{ka}\right)^2} \right]. \quad (35)$$

The formula (35) is valid only when $ka \geq \alpha_{1m}$.

When $ka \rightarrow \alpha_{1m}$, we have:

$$\lim_{ka \rightarrow \alpha_{1m}} \theta = 2. \quad (36)$$

As it was explained before, the case $ka < \alpha_{1m}$ does not present any interest. But, to keep continuity of our reasoning, we can admit that for $ka < \alpha_{1m}$, γ_{lim} remains constant and equal to $\pi/2$ in the formula (28), and

$$\theta = \frac{2(ka)^2}{\alpha_{1m}^2}. \quad (37)$$

Of course, when $ka \rightarrow 0$, the value of θ tends to zero. To obtain the imaginary part of the specific impedance we use the method given by W. RDZANEK in [4], and substitute in the formula (26), representing the real part, $\cosh \psi$ for $\sin \gamma$ and integrating with respect to ψ from 0 to ∞ . We have therefore, due to (34):

$$\chi = \frac{2(ka)^2}{\alpha_{1m}^2} \int_0^{\infty} R^2(ka \cosh \psi) \cosh \psi d\psi. \quad (38)$$

In the considered case $R(\cosh \psi)$ is equal to 1 for γ ranging from 0 to γ_{lim} , and 0 for $\gamma > \gamma_{lim}$. It is well known [4] that the application of integral transform (38) gives us the result to within the accuracy of a constant. That value must be found from the condition

$$\lim_{ka \rightarrow \infty} \chi = 0. \quad (39)$$

From the formula (38) we obtain

$$\chi = \frac{2(ka)^2}{\alpha_{1m}^2} \int_0^{\gamma_{lim}} \cosh \psi d\psi + C. \quad (40)$$

In the case of $ka > \alpha_{1m}$, the integral (40) is a simple one and we have

$$\chi = \frac{2(ka)^2}{\alpha_{1m}^2} \sinh \gamma_{lim} + C. \quad (41)$$

or, according to (21)

$$\chi = \frac{2(ka)^2}{\alpha_{1m}^2} \left[\sinh \left(\sin^{-1} \frac{\alpha_{1m}}{ka} \right) \right] + C. \quad (42)$$

Since integration in (40) is performed with respect to ψ , C may be a function of ka , and should be calculated from the condition (39)

When $ka \rightarrow \infty$ we have

$$\sinh \left(\sin^{-1} \frac{\alpha_{1m}}{ka} \right) \approx \sinh \frac{\alpha_{1m}}{ka} \approx \frac{\alpha_{1m}}{ka} + \dots \quad (43)$$

and

$$\lim_{ka \rightarrow \infty} \chi = 2 \lim_{ka \rightarrow \infty} \frac{(ka)^2}{\alpha_{1m}^2} \frac{\alpha_{1m}}{ka} + C = 0. \quad (44)$$

The only possibility of fulfilling the above condition is to take

$$C = -\frac{2ka}{\alpha_{1m}}, \quad (45)$$

and finally we obtain

$$\chi = \frac{2(ka)^2}{\alpha_{1m}^2} \sinh \left(\sin^{-1} \frac{\alpha_{1m}}{ka} \right) - \frac{2ka}{\alpha_{1m}}. \quad (46)$$

When $ka = \alpha_{1m}$ we must replace $\frac{ka}{\alpha_{1m}}$ by 1 and we obtain

$$\chi = 2 \sinh \frac{\pi}{2} - 2 = 2.5986. \quad (47)$$

When $ka < \alpha_{1m}$, the value of γ_{\lim} in the formula (41) remains equal to $\pi/2$. In that case we must choose another value of the constant (from the condition of continuity for $\alpha_{1m} = ka$ and the positive value of χ_2 i.e.

$$\kappa = \frac{2(ka)^2}{\alpha_{1m}^2} (\sinh \frac{\pi}{2} - 1) \quad (48)$$

or, substituting the value of $\sinh \pi/2$,

$$\sinh \pi/2 = 2.2993,$$

we get

$$\chi = 2.5986 \frac{(ka)^2}{\alpha_{1m}^2} \quad (49)$$

We see that for $ka \rightarrow 0$ we have

$$\lim_{ka \rightarrow 0} \chi = 0$$

Of course, the case of $ka < \alpha_{1m}$ is of theoretical interest only, since it has no application in practice.

3. The accurate method

We assume the distribution function of the velocity amplitude as

$$u(r) = \begin{cases} 2u_0 \frac{J_1(\alpha_{1m} \frac{r}{a})}{\alpha_{1m} \frac{r}{a}} & \text{for } 0 < r < a \\ 0 & \text{for } r \geq a \end{cases} \quad (50)$$

The directivity index (1) takes then the form:

$$R = u_0 \frac{4\pi a}{Q \alpha_{1m}} \int_0^a J_1(\alpha_{1m} \frac{r}{a}) J_0(kr \sin \gamma) dr. \quad (51)$$

In order to calculate the output of the source we must replace in (18) the upper limit ∞ by a .

$$Q = 4\pi u_0 \frac{a}{\alpha_{1m_0}} \int_0^{\alpha} J_1\left(\alpha_{1m} \frac{r}{a}\right) dr. \quad (52)$$

The integral is an elementary one and we get

$$Q = 4\pi u_0 \left(\frac{a}{\alpha_{1m}}\right)^2 [1 - J_0(\alpha_{1m})]. \quad (53)$$

Substituting (53) into (51) we obtain the directivity index in the form

$$R = \frac{\alpha_{1m}}{a[1 - J_0(\alpha_{1m})]} \int_0^{\alpha} J_1\left(\alpha_{1m} \frac{r}{a}\right) J_0(kr \sin \gamma) dr. \quad (54)$$

Evidently, for $\gamma = 0$ we get $R = 1$. In the formula (54) we introduce a new variable:

$$x = \frac{r}{a} \quad (55)$$

and we get:

$$R = \frac{\alpha_{1m}}{1 - J_0(\alpha_{1m})} \int_0^1 J_1(\alpha_{1m} x) J_0(kax \sin \gamma) dx, \quad (56)$$

Figures 2, 3, 4 represent the directivity index versus the angle γ for α_{11} , α_{12} and α_{13} . The continuous lines represent the approximate case the dashed line the accurate solutions (56). Of course, the value γ_{lim} has not the same meaning as before. Nevertheless, it is easy to calculate the directivity pattern for $\gamma = \gamma_{lim}$ (21) because the above integral takes then a form given in the tables of integrals. In that case we obtain ($kas \sin \gamma = \alpha_{1m}$)

$$R_{lim} = \frac{\alpha_{1m}}{1 - J_0(\alpha_{1m})} \int_0^1 J_1(\alpha_{1m} x) J_0(\alpha_{1m} x) dx. \quad (57)$$

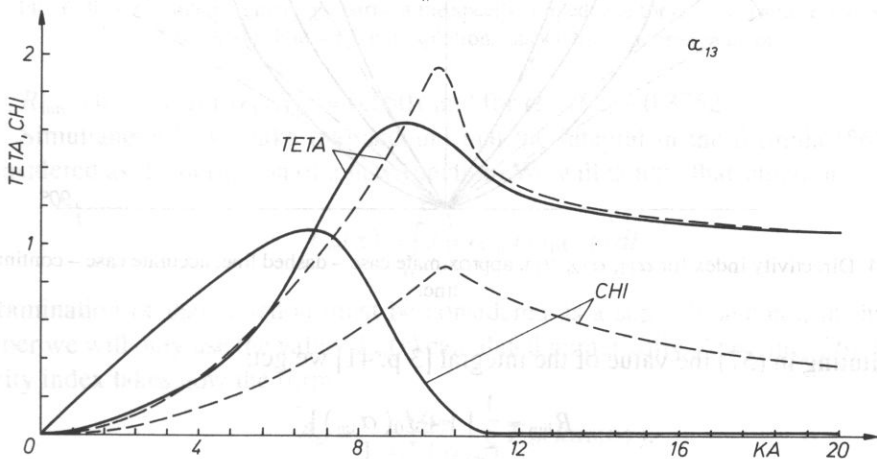


FIG. 2. Directivity index for α_{11} , α_{12} , α_{13} : approximate case – dashed line, accurate case – continuous line.

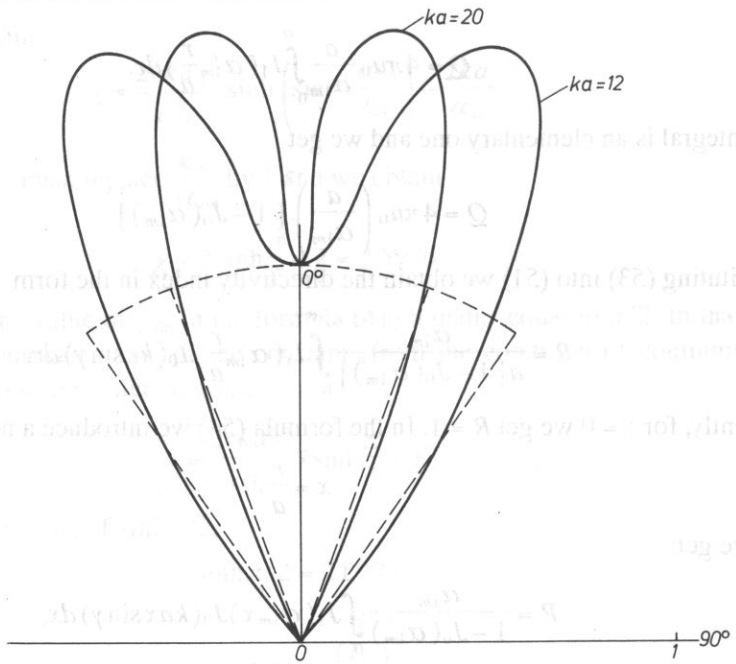


FIG. 3. Directivity index for α_{11} , α_{12} , α_{13} : approximate case – dashed line, accurate case – continuous line.

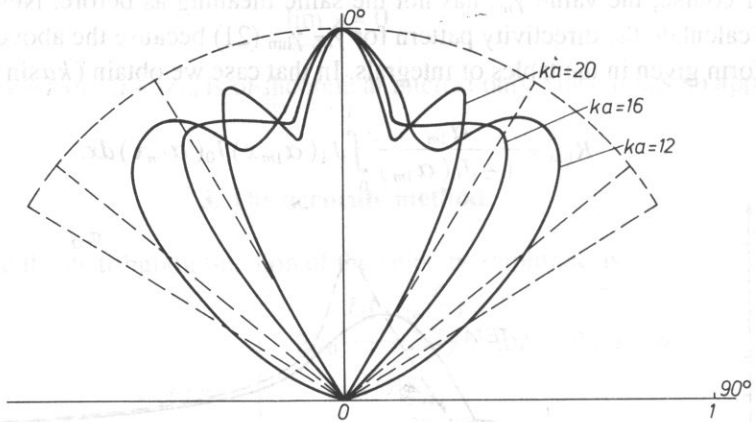


FIG. 4. Directivity index for α_{11} , α_{12} , α_{13} : approximate case – dashed line, accurate case – continuous line.

Substituting in (57) the value of the integral [3 p. 41] we get:

$$R_{\lim} = \frac{1}{2} [1 + J_0(\alpha_{1m})]. \quad (58)$$

We see that the value of the directivity index for γ_{\lim} is independent of ka but, of course, it is obtained for a fixed γ_{\lim} which depends on ka . For example, we have for

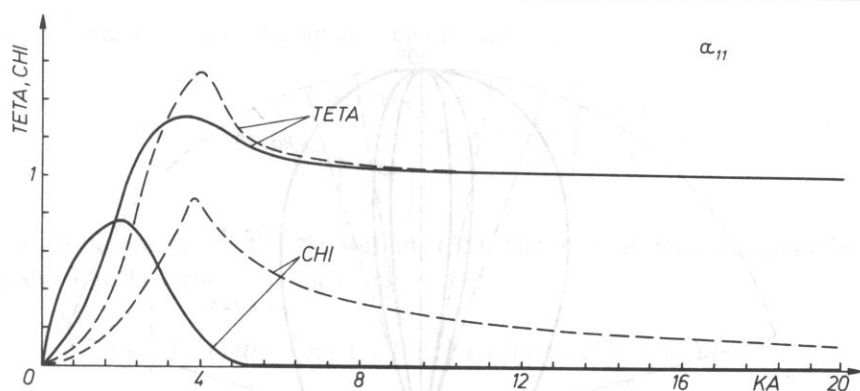


FIG. 5. Real θ_m and imaginary χ_m parts of the specific impedance for α_{11} , α_{12} and α_{13} versus ka . Continuous line – accurate solution, dashed line – approximate one.

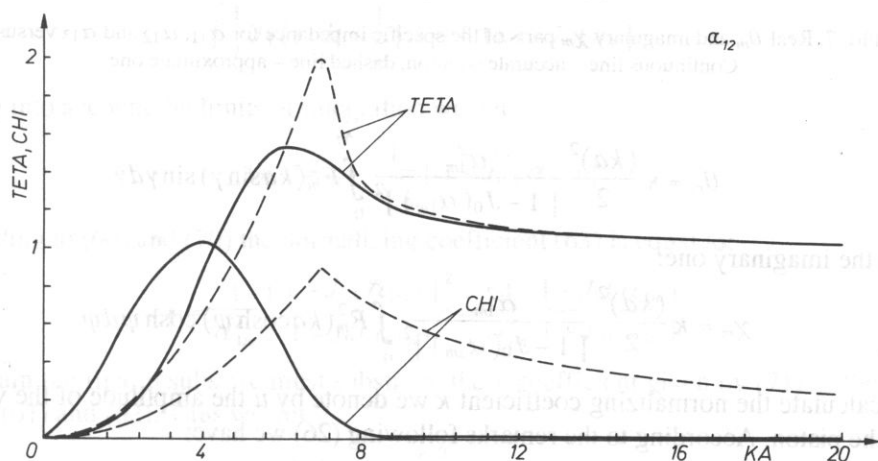


FIG. 6. Real θ_m and imaginary χ_m parts of the specific impedance for α_{11} , α_{12} and α_{13} versus ka . Continuous line – accurate solution, dashed line – approximate one.

$\alpha_{11} R_{\text{lim}} = 0.2981$, for $\alpha_{12} R_{\text{lim}} = 0.6501$ and for $\alpha_{13} R_{\text{lim}} = 0.3752$.

Simultaneously we take into account that the integral in the formula (56) may be considered as the definition of a new function. We will denote that function by $F_m(x)$

$$F_m(x) = \int_0^1 J_1(\alpha_{1m} t) J_0(xt) dt. \quad (59)$$

Examination of that function must be considered as a separate subject; in the present paper we will only use the values $F_m(x)$ calculated numerically. Applying (56), the directivity index takes now the form:

$$R_m = \frac{\alpha_{1m}}{1 - J_0(\alpha_{1m})} F_m(ka \sin \gamma). \quad (60)$$

According to (26) we can write the real part of the specific impedance in the following form:

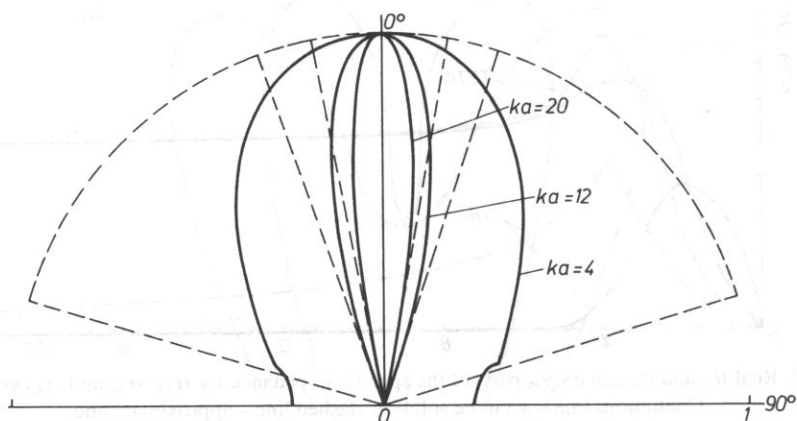


FIG. 7. Real θ_m and imaginary χ_m parts of the specific impedance for α_{11} , α_{12} and α_{13} versus ka . Continuous line – accurate solution, dashed line – approximate one.

$$\theta_m = \kappa \frac{(ka)^2}{2} \frac{\alpha_{1m}^2}{[1 - J_0(\alpha_{1m})]^2} \int_0^{\pi/2} F_m^2(ka \sin \gamma) \sin \gamma d\gamma \quad (61)$$

and the imaginary one:

$$\chi_m = \kappa \frac{(ka)^2}{2} \frac{\alpha_{1m}^2}{[1 - J_0(\alpha_{1m})]^2} \int_0^{\infty} F_m^2(ka \cosh \psi) \cosh \psi d\psi \quad (62)$$

To calculate the normalizing coefficient κ we denote by u the amplitude of the velocity on the piston. According to the remarks following (26) we have:

$$\kappa = \frac{u_{\text{mean}}^2}{(u^2)_{\text{mean}}} \quad (63)$$

Substituting (50) for the value of u in (63) we have $4u_0^2$ both in numerator and denominator. For that reason we may omit that factor and write the mean values:

$$u_{\text{mean}} = \frac{2}{a^2} \int_0^a u(r) r dr = \frac{2}{a^2} \int_0^{\alpha_{1m}} \frac{J_1(\alpha_{1m} \frac{r}{a})}{\frac{\alpha_{1m}}{a}} dr = \frac{2}{\alpha_{1m}^2} \int_0^{\alpha_{1m}} J_1(x) dx. \quad (64)$$

where:

$$x = \alpha_{1m} \frac{r}{a}. \quad (65)$$

The integral in the formula (64) is a simple one and we get:

$$u_{\text{mean}} = \frac{2}{a^2} [1 - J_0(\alpha_{1m})] \quad (66)$$

We obtain the mean value of the square velocity as:

$$(u^2)_{\text{mean}} = \frac{2}{a^2} \int_0^{\alpha} \frac{J_1^2(\alpha_{1m} \frac{r}{a})}{\left(\frac{\alpha_{1m}}{a}\right)^2 r} dr = \frac{2}{\alpha_{1m}^2} \int_0^{\alpha_{1m}} \frac{J_1^2(x)}{x} dx, \quad (67)$$

where x is, as before, defined by the formula (65). The integral in (67) is given in tables of integrals [3, p. 41 form 17] in the form:

$$\int_0^x \frac{1}{t} J_n^2(t) dt = \frac{1}{2} n \left[1 + J_0^2(x) + J_n^2(x) - 2 \sum_{k=0}^n J_k^2(x) \right] \quad (68)$$

In our case we have $n = 1$ and

$$\int_0^x \frac{1}{t} J_1^2(t) dt = \frac{1}{2} \left[1 - J_0^2(x) - J_1^2(x) \right]. \quad (69)$$

Taking into account the limits of integration we get

$$(u^2)_{\text{mean}} = \frac{1}{\alpha_{1m}^2} \left[1 - J_0^2(\alpha_{1m}) \right]. \quad (70)$$

According to (66) and (70) the normalizing coefficient (63) is equal to:

$$\kappa = \frac{4}{\alpha_{1m}^2} \frac{\left[1 - J_0(\alpha_{1m}) \right]^2}{1 - J_0^2(\alpha_{1m})} = \frac{4}{\alpha_{1m}^2} \frac{1 - J_0(\alpha_{1m})}{1 + J_0(\alpha_{1m})}. \quad (71)$$

To obtain the final results we must substitute the κ coefficient given by (71) to the formulae (61) and (62). Thus we get

$$\theta_m = \frac{2(ka)^2}{1 - J_0^2(\alpha_{1m})} \int_0^{\pi/2} F_m^2(ka \sin \gamma) \sin \gamma d\gamma \quad (72)$$

and:

$$\chi_m = \frac{2(ka)^2}{1 - J_0^2(\alpha_{1m})} \int_0^{\infty} F_m^2(k \cosh \psi) \cosh \psi d\psi. \quad (73)$$

The enclosed figures present the values of θ_m and χ_m (72), (73) continuous line and the approximate values dashed line for $m = 1, 2, 3$ versus ka . The results were obtained numerically.

Conclusions

The approximate method of the considered velocity distribution gives us the directivity coefficient equal to 1 in a certain angle, when $ka > \alpha_{1m}$. The results of the accurate

method have a better directivity. Of course, the cut-off of the directivity coefficient does not occur, but practically the pattern is sharper and the lateral lobes are so small, that they can be neglected – they are invisible in the figure. The real part of the specific impedance is practically equal to 1 for $ka > 1.5\alpha_{1m}$, and the imaginary part is then equal to 0. So we may say that the source adjusts well to the medium. If we compare the results for different values of α_{1m} we see that the source for α_{11} has the best properties. Since this is the case the easiest to be realised we have no nodal lines, this value should be chosen.

References

- [1] J.S. GRADSZTEIN, J.M. RYŻIK, *Tablice integralów, sum, rzędów i pochodnych*. Izd. Nauka, Moskwa 1971.
- [2] M.A. ŁAWRIENTIEW, B.W. SZABAT: *Metody teorii funkcji kompleksyjno pieremiennoj*, Gos. Izdat. Fiziko-Mat. Literatury, Moskwa 1959.
- [3] A.P. PRUDNIKOW, J.A. BRYCZKOW, O.J. MARICZEW: *Integraty i riady*. Izd. Nauka, Moskwa 1983.
- [4] W. RDZANEK: *Akustyczna impedancja wzajemna i całkowita układu źródeł o zmiennym powierzchniowym rozkładzie prędkości drgań*, WSP Zielona Góra 1979.
- [5] R. WYRZYKOWSKI: *Liniowa teoria pola akustycznego ośrodków gazowych*, WSP, RTPN, Rzeszów 1972.
- [6] R. WYRZYKOWSKI, CZ. SOŁTYS: *Obliczanie impedancji źródeł dźwięku o znanej kierunkowości*. Arch. Akustyki 7, 3–4, 327–336 (1972).
- [7] R. WYRZYKOWSKI, CZ. SOŁTYS: *Źródła dźwięku o dużej kierunkowości*, Arch. Akustyki 9, 3; 313–319 (1974).

Received August 10, 1990

ACOUSTIC POWER OF RADIATION OF A CIRCULAR PLATE FIXED ON THE RIM AND VIBRATING UNDER EXTERNAL PRESSURE

W. RDZANEK

Institute of Physics, Pedagogical University

(34-310 Rzeszów, Rejtana 16a)

The main scientific aim of our work was the realization of theoretical research on the problem of energy radiation of axially-symmetric forced vibrations of a circular plate. This research focussed on the determination of frequency characteristics of relative acoustic power. A thin plate, fixed on the rim in a rigid and flat acoustic baffle, radiating into a lossless and homogeneous fluid medium was considered. Dynamic interactions between the acoustic wave radiated by the plate and the form of the radiations as well as losses in the plate were neglected.

The active acoustic power of radiation was expressed with a single integral within finite limits and with elementary form in special cases, i.e., for high-frequency wave radiation and when the plate's thickness is sufficiently small in relation to its diameter. The results of calculations are also presented in graphical form.

1. Introduction

The practical application of a circular plate as a vibrating system in acoustic devices – sound emitting and sound receiving – has led to a comprehensive and more detailed description of acoustic properties and of the problem of radiation energy of axially symmetrical forces vibrations of a circular plate, in particular.

Besides theoretical considerations of the analysis of the field of acoustic radiation from superficial sources with a “guessed” distribution of vibration velocity (which approximately satisfies the boundary conditions related with the shape of the source), this field was also theoretically analysed. Here the cause is taken into consideration assuming that the distribution of the force inducing vibrations of the source is known.

A detailed description of parameters which characterize a circular membrane as a sound source or receiver, with a stress on the problem of the output impedance frequency characteristic, can be found in HAJASAKI's paper [1]. The acoustic impedance of radiation of a circular membrane excited to vibrate with the neglect of losses in the membrane and

the influence of the surroundings is known from the paper [5]. SZENDEROW [9] analysed sound radiation of an oscillating membrane without an acoustic baffle applying associated integral equations. The paper [8] analyzes the problem of radiation of an acoustic wave by a circular plate. However, the directional characteristic was only determined with the application of the classical Kirchhoff-Love plate theory under the assumption that the surface distribution of the factor forcing vibrations is known.

Expressions for acoustic power radiated by a circular plate, concerning individual forms of vibrations, are presented in the papers [6] and [7]. Yet, their application was limited to high frequencies. This problem was expanded in LEVINE's and LEPPINGTON's paper [3] by including a correction for the "oscillating" character of radiated acoustic power. Furthermore the effective damping coefficient was calculated for frequencies comparable with resonance frequencies, including losses in the plate and the relation between the wave radiated by the plate and its vibrations.

However, there is no expression so far for acoustic power radiated by a circular plate when the surface distribution of the factor forcing vibrations is known.

This paper undertakes this problem under the assumption that the plate is sufficiently thin and the forcing pressure is strong enough to neglect the influence of losses, including vibration damping by the acoustic field. Frequency characteristics of active power were determined for a known surface distribution of the pressure forcing vibrations. Elementary forms of expressions were achieved for special cases, i.e., for high frequencies of radiated wave and for a plate thickness sufficiently small with respect to its diameter. It was also shown that expressions obtained for limiting cases are already known from previous papers. The results of numerical calculations are presented in graphical form.

2. Assumptions of the analysis

Let us consider the case of an acoustic wave radiated in a fluid medium with low self-resistance (e.g., air) by a thin homogeneous circular plate ($r \leq a$, $z = 0$) with a plane, as a rigid acoustic baffle ($r > a$, $z = 0$) behind it complete fixing of the plate results in the following boundary conditions: the deflection of the plate $\eta(r)$ and the derivative $\partial\eta(r)/\partial r$ are equal to zero for $r = a$. We assume that the plate is subject to external pressure $\text{Re} \{ f(r) \exp(-i\omega t) \}$ for $0 \leq r < a$.

The theoretical analysis of such a system is based on the equation of vibrations given by LEVINE and LEPPINGTON [3]

$$(k_0^4 \nabla^4 - 1) v + 2\varepsilon_1 k_0 \varphi = -i/(M\omega) f \quad (1)$$

for $z = +0$. The quantity $\varphi(r, z) \exp(-i\omega t)$ is the acoustic potential which fulfills the Helmholtz equation $(\nabla^2 + k_0^2) \varphi = 0$, $k_0 = \omega/c$. From now on we will neglect the time factor $\exp(-i\omega t)$. The normal component of vibration velocity of the plates surface $v(r) = -i\omega\eta(r)$ and acoustic pressure generated by the plate $p(r) = i\rho_0\omega\varphi(r)$, where ρ_0 is the density in rest stage of the fluid medium. The wave number of the plate is defined with $k_p^4 = M\omega^2/B$, where M is the mass of the plate per unit surface,

$B = B_0(1 - i\varepsilon')$ is the plates flexural rigidity with internal losses in the plate included [4], ε' —measure of plates damping. The quantity $\varepsilon_1 = \rho_0/(Mk_0)$ is the measure of density in rest stage of the fluid medium to material density of the plate ratio.

We will limit our considerations to the case of acoustic power radiated by the plate to which the theory of bending of thin plates applies, accepting that the plates thickness h satisfies the inequality (e.g., [2]).

$$h \leq 0.1 D, \quad (2)$$

where $D = 2a$ is the diameter of the plate. In accordance with the assumptions, the plate is surrounded by a fluid medium with low self-resistance and the following condition is fulfilled:

$$\varepsilon_i k_0 = \rho_0/M \ll 1, \quad (3)$$

Hence, instead of Eq. (1) we have

$$(\nabla^4 - k^4) \eta(r) = f(r)/B_0, \quad (4)$$

where $k^2 = \omega\sqrt{M/B_0}$. The disregard of term $2\varepsilon_1 k_0 \varphi$ in Eq. (1) means that the influence of the acoustic wave radiated by both surfaces of the plate on the form of vibrations is disregarded.

Moreover, we accept that the amplitude of the factor inducing vibrations is as follows:

$$f(r) = \begin{cases} f_0 & \text{for } 0 < r < a_0, \\ 0 & \text{for } a_0 < r < a. \end{cases} \quad (5)$$

where $f_0 = \text{const}$. Accepted simplifications lead to a limitation of the range of application of the solution to Eq. (4) depending on the frequency of the factor inducing vibrations. The solution to Eq. (4) should not be applied to frequencies close or equal to resonance frequencies.

In practice such a type of vibration excitation can be realized with, for example, two flat circular electrodes with a radius $a_0 < a$, parallel to the surface of the plate [1]. The solution to Eq. (4) for a plate excited to vibrate by the factor (5) is as follows [8]:

$$\begin{aligned} \eta_1(r)/\eta_0 = 1 - \frac{\gamma_0}{2S(\gamma)} & \left\{ \frac{1}{\gamma} I_1(\gamma_0) + \frac{\pi}{2} I_1(\gamma) [J_1(\gamma_0)N_0(\gamma) + \right. \\ & \left. - J_0(\gamma)N_1(\gamma_0)] - \frac{\pi}{2} I_0(\gamma) [J_1(\gamma)N_1(\gamma_0) - J_1(\gamma_0)N_1(\gamma)] \right\} \times \\ & \times J_0(kr) + \frac{\gamma_0}{2S(\gamma)} \left\{ \frac{1}{\gamma} J_1(\gamma_0) + J_1(\gamma) [I_1(\gamma_0)K_0(\gamma) + I_0(\gamma)K_1(\gamma_0)] + \right. \\ & \left. - J_0(\gamma) [I_1(\gamma_0)K_1(\gamma) - I_1(\gamma)K_1(\gamma_0)] \right\} I_0(kr) \end{aligned} \quad (6)$$

for $0 < r < a_0$,

$$\eta_2(r)/\eta_0 = -\frac{\gamma_0}{2S(\gamma)} \left\{ \frac{1}{\gamma} I_1(\gamma_0) + \frac{\pi}{2} J_1(\gamma_0) \left[N_0(\gamma) I_1(\gamma) + \right. \right. \\ \left. \left. + N_1(\gamma) I_0(\gamma) \right] \right\} J_0(kr) - \frac{\gamma_0}{2S(\gamma)} \left\{ \frac{1}{\gamma} J_1(\gamma_0) + I_1(\gamma_0) \left[K_0(\gamma) J_1(\gamma) + \right. \right. \\ \left. \left. - K_1(\gamma) J_0(\gamma) \right] \right\} I_0(kr) + \frac{\gamma_0}{2} \left[I_1(\gamma_0) K_0(kr) + \frac{\pi}{2} J_1(\gamma_0) N_0(kr) \right] \quad (7)$$

for $a_0 < r < a$

where $J_n(x)$ is a Bessel function, $I_n(x)$ – modified Bessel function, $N_n(x)$ – Neumann function, $K_n(x)$ – cylindrical MacDonald function, all are of the n -order.

The following notation was introduced:

$$\gamma = ka, \quad \gamma_0 = ka_0, \quad S(\gamma) = J_0(\gamma) I_1(\gamma) + I_0(\gamma) J_1(\gamma) \quad (8)$$

and

$$\eta_0 = -\frac{f_0}{B_0 k^4}. \quad (9)$$

The relative amplitude of the transverse displacement of points on the plates surface can be expressed in a much simpler way in a special case when the whole surface of the plate is excited to vibrate with a factor different from zero. If we accept $a_0 = a$ ($\gamma_0 = \gamma$), then instead of the solution (6) and (7) we have

$$\eta_1(r)/\eta_0 = 1 - \frac{1}{S(\gamma)} \left[I_1(\gamma) J_0(kr) + J_1(\gamma) I_0(kr) \right] \quad (10)$$

and $\eta_2(r)/\eta_0 = 0$

2. Acoustic power

The calculation of active acoustic power radiated by the vibrating plate will be based on the definition

$$N = \frac{1}{2} \int_{\sigma} p(\bar{r}) v^*(\bar{r}) d\sigma \quad (11)$$

where p is the pressure radiated by the plate and v^* is a quantity conjugate with the complex quantity of vibration velocity v . In the case of a circular plate with its vibrations presented by the formulae (6) and (7), i.e., a circular source with an axially-symmetrical distribution of vibration velocity the Hankel representation (6) for acoustic power is applied:

$$N = \rho_0 c \pi k_0^2 \int_0^{\pi/2} M(\vartheta) M^*(\vartheta) \sin \vartheta d\vartheta, \quad (12)$$

where

$$M(\vartheta) = i\omega \left[\int_0^{\alpha_0} \eta_1(r) J_0(k_0 r \sin \vartheta) r dr + \int_{\alpha_0}^{\alpha} \eta_2(r) J_0(k_0 r \sin \vartheta) r dr \right] \quad (13)$$

is the characteristic function of the source. We calculate integrals from Eq. (13)

$$N = \rho_0 c \pi a^2 \varepsilon_0^4 \left(\frac{f_0 k_0 a}{M \omega} \right)^2 \int_0^{\pi/2} \left\{ \frac{1}{1 - \left(\frac{w}{\gamma} \right)^4} \left[\frac{J_1(\varepsilon_0 w)}{\varepsilon_0 w} + \right. \right. \\ \left. \left. - U(\varepsilon_0, \gamma) \frac{w}{\gamma} J_1(w) - W(\varepsilon_0, \gamma) J_0(w) \right] \right\}^2 \sin \vartheta d\vartheta, \quad (14)$$

where $\varepsilon_0 = a_0/a$, $W = k_0 a \sin \vartheta$ and

$$U = U(\varepsilon_0, \gamma) = \frac{1}{\varepsilon_0} \gamma S \left[J_1(\varepsilon_0 \gamma) I_0(\gamma) - I_1(\varepsilon_0 \gamma) J_0(\gamma) \right], \quad (15)$$

$$W = W(\varepsilon_0, \gamma) = \frac{1}{\varepsilon_0} \gamma S \left[J_1(\varepsilon_0 \gamma) I_1(\gamma) + I_1(\varepsilon_0 \gamma) J_1(\gamma) \right]. \quad (16)$$

It is convenient to use the notion of relative acoustic power $N/N^{(\infty)}$ in numerical calculations $N^{(\infty)}$ is the active power of the source for $k_0 = 2\pi/\lambda \rightarrow \infty$. If $k_0 \rightarrow \infty$ then $p(\bar{r}) = \rho c v(\bar{r})$. On the basis of the formula (11), we reach

$$N^{(\infty)} = \lim_{k_0 \rightarrow \infty} N = \frac{1}{2} \rho_0 c \int_{\sigma} v^2(\bar{r}) d\sigma. \quad (17)$$

In the case of vibrations of the plate (6) and (7) the quantity $N^{(\infty)}$ is equal to

$$N^{(\infty)} = \rho_0 c \pi a^2 \left(\frac{f_0}{M \omega} \right)^2 \frac{\varepsilon_0^2}{4S(\gamma)} \left\{ 2S(\gamma) + \varepsilon_0 S(\gamma_0) + \right. \\ \left. + \frac{\pi}{2} I_0(\gamma) T_1 \left[\gamma_0 J_0(\gamma_0) - 3J_1(\gamma_0) \right] - J_0(\gamma) T_2 \left[\gamma_0 I_0(\gamma_0) - 3I_1(\gamma_0) \right] + \right. \\ \left. + \frac{\pi}{2} I_1(\gamma) J_1(\gamma_0) \left[\gamma_0 T_3 - 3W_1 \right] + J_1(\gamma) I_1(\gamma_0) \left[\gamma_0 T_4 - 3W_2 \right] + \right. \\ \left. - \frac{6}{\gamma} I_1(\gamma_0) J_1(\gamma_0) + \frac{1}{S(\gamma)} \left[J_1(\gamma_0) I_0(\gamma) - I_1(\gamma_0) J_0(\gamma) \right]^2 \right\}, \quad (18)$$

where

$$W_2 = J_1(\gamma_0) N_0(\gamma) - J_0(\gamma) J_1(\gamma_0), \\ W_2 = I_1(\gamma_0) K_0(\gamma) + I_0(\gamma) K_1(\gamma_0), \\ T_1 = J_1(\gamma_0) N_1(\gamma) - J_1(\gamma) N_1(\gamma_0) \\ T_2 = I_1(\gamma_0) K_1(\gamma) - I_1(\gamma) K_1(\gamma_0), \\ T_3 = J_0(\gamma_0) N_0(\gamma) - J_0(\gamma) N_0(\gamma_0), \\ T_4 = I_0(\gamma_0) K_0(\gamma) - I_0(\gamma) K_0(\gamma_0). \quad (19)$$

The form of the quantity $N^{(\infty)}$ is more elementary when the whole surface of the plate is excited to vibrate with a factor different from zero. For $a_0 = a$, we have $W_1 = 2/(\pi\gamma)$, $W_z = 1/\gamma$, $T_1 = T_2 = T_3 = T_4 = 0$ and instead of Eq. (18) we have

$$N^{(\infty)} = \rho_0 c \pi a^2 \left(\frac{f_0}{M \omega} \right)^2 \beta, \quad (20)$$

where

$$\beta = 1 - \frac{J_1(\gamma) I_1(\gamma)}{S(\gamma)} \left[\frac{3}{\gamma} + \frac{J_0(\gamma) I_0(\gamma)}{S(\gamma)} \right]. \quad (20a)$$

4. Acoustic power for high frequencies

The relative acoustic power $\sigma_0 = N/N$ for the case of $a_0 = a$ ($\gamma_0 = \gamma$) is calculated on the basis of the relations (14) and (20). We substitute $\xi = \sin \vartheta$ and introduce the following notations

$$\alpha = k_0 a, \quad \delta = k/k_0 = \gamma/a, \quad (21)$$

$$W_0 = (2/S) J_1(\gamma) I_1(\gamma),$$

$$U_0 = (1/S) [J_1(\gamma) I_0(\gamma) - I_1(\gamma) J_0(\gamma)]. \quad (22)$$

We achieve

$$\sigma_0 = \delta^6 \beta^{-1} \int_0^1 \frac{\varepsilon}{\sqrt{1 - \xi^2}} \times \frac{\{ (\delta/\xi) J_1(\alpha \xi) - (\xi/\delta) U_0 J_1(\alpha \xi) - W_0 J_0(\alpha \xi) \}^2}{(\xi^4 - \delta^4)^2} d\xi. \quad (23)$$

The integral (23) is converted into a form making σ_0 analysis for high frequencies easier on the basis of the LEVINE and LEPPINGTON method [3]. We introduce the function of a complex variable

$$F(z) = [\delta/z - (z/\delta) U_0]^2 J_1(\alpha z) H_1^{(1)}(\alpha z) + \\ + 2(z/\delta) U_0 W_0 J_0(\alpha z) H_1^{(1)}(\alpha z) + W_0 [W_0 J_0(\alpha z) + \\ - 2(\delta/z) J_1(\alpha z)] H_0^{(1)}(\alpha z) \quad (24)$$

for

$$\operatorname{Re} F(\xi) = \{ [\delta/\xi - (\xi/\delta) U_0] J_1(\alpha \xi) - W_0 J_0(\alpha \xi) \}^2. \quad (25)$$

The calculation begins from a contour integral

$$\int_C \frac{z F(z) dz}{\sqrt{1 - z^2} (z^4 - \delta^4)^2} = 0. \quad (26)$$

The integral is calculated for contour C (Fig. 1) inside which the integrand is single-valued

and regular. We assume that $\delta < 1$ ($k_0 > k$). The contour integral is noted as follows

$$\int_0^1 + \int_1^\infty + \int_{R_\infty} + \int_\infty^0 = \frac{1}{2} \operatorname{Re} z(z = \delta) + \frac{1}{2} \operatorname{Re} z(z = i\delta) + \frac{1}{4} \operatorname{Re} z(z = 0). \quad (26a)$$

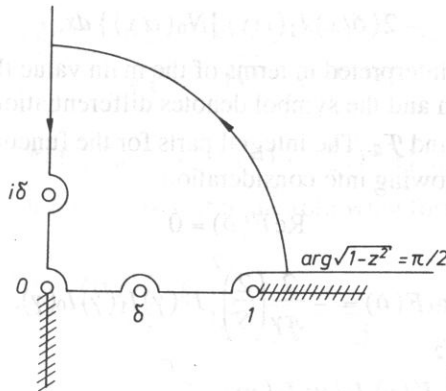


FIG. 1. Integration path (see [3]) for the expression (26)

Contributions to the value of the integral (26) from small semicircles around singular points with second order poles $z = \delta, +i\delta$ and $1/4$ arc of the small circle around the breakway point $z = 0$, which is a first order pole at the same time are calculated with the following auxiliary taken into consideration:

$$\begin{aligned} \mathcal{F}_1(z) &= \frac{zF(z)}{\sqrt{1-z^2}(z+\delta)^2(z^2+\delta^2)^2}, \\ \mathcal{F}_2(z) &= \frac{zF(z)}{\sqrt{1-z^2}(z+i\delta)^2(z^2-\delta^2)^2}, \\ \mathcal{F}_0(z) &= \frac{z^2F(z)}{\sqrt{1-z^2}(z^4-\delta^4)^2}. \end{aligned} \quad (27)$$

The contribution during integration over the big circle R_∞ disappears when its radius increases infinitely. If we also take into consideration the fact that $\operatorname{Re} F(i\tau) = 0$ for real values of τ , we obtain from the expression (26)

$$\begin{aligned} \operatorname{Re} \int_0^1 \frac{x F(x)}{\sqrt{1-x^2}(x^4-\delta^4)^2} dx &= \int_0^1 \frac{x}{\sqrt{1-x^2}} \times \\ &\times \frac{\{ [\delta/x - (x/\delta) U_0] J_1(\alpha x) - W_0 J_0(\alpha x) \}^2}{(x^4-\delta^4)^2} dx = \\ &= \operatorname{Re} \left\{ \pi i \left[\frac{1}{2} \mathcal{F}_0(0) + \mathcal{F}_1'(\delta) + \mathcal{F}_2'(i\delta) \right] \right\} + \end{aligned} \quad (28)$$

$$\begin{aligned}
& + \int_1^{\infty} \frac{x}{\sqrt{x^2 - 1} (x^4 - \delta^4)^2} \{ [\delta/x - (x/\delta) U_0]^2 J_1(\alpha x) N_1(\alpha x) + \\
& + 2(x/\delta) U_0 W_0 J_0(\alpha x) N_1(\alpha x) + W_0 [W_0 J_0(\alpha x) + \\
& - 2(\delta/x) J_1(\alpha x)] N_0(\alpha x) \} dx, \quad [\text{cont.}] (28)
\end{aligned}$$

where the first integral is interpreted in terms of the main value the second integral is its expansion to explicit form and the symbol denotes differentiation for an adequate argument of the functions \mathcal{F}_1 and \mathcal{F}_2 . The integral parts for the functions $\mathcal{F}'_1(\delta)$, $\mathcal{F}_2(i\delta)$ are found after taking the following into consideration:

$$\begin{aligned}
\operatorname{Re} F(\delta) &= 0 \\
\operatorname{Im} F(\delta) &= -\frac{2}{\pi\gamma} \left(\frac{2}{S}\right)^2 J_1^2(\gamma) I_1(\gamma) I_0(\gamma), \\
F(i\delta) &= \frac{2i}{\pi\gamma} \left(\frac{2}{S}\right)^2 I_1^2(\gamma) J_1(\gamma) J_0(\gamma), \\
\operatorname{Im} \delta F'(\delta) &= \frac{2}{\pi} \left(\frac{2}{S}\right)^2 \left\{ \frac{2}{\gamma} S J_1(\gamma) I_1(\gamma) - I_1^2(\gamma) [J_0^2(\gamma) + J_1^2(\gamma)] \right\}, \\
\operatorname{Re} \delta F'(i\delta) &= -\frac{2}{\pi} \left(\frac{2}{S}\right)^2 \left\{ \frac{2}{\gamma} S J_1(\gamma) I_1(\gamma) + J_1^2(\gamma) [I_0^2(\gamma) - I_1^2(\gamma)] \right\}, \quad (29)
\end{aligned}$$

while $\operatorname{Im} \mathcal{F}_0(0) = -\delta^{-6}$ is obtained immediately.

The integral from the formula (28) is calculated within the limits $(1, \infty)$ on the basis of known asymptotic expressions:

$$\begin{aligned}
J_1(\alpha x) N_1(\alpha x) &\approx -J_0(\alpha x) N_0(\alpha x) \approx (\pi \alpha x)^{-1} \cos 2\alpha x, \\
J_0(\alpha x) N_1(\alpha x) &\approx -(\pi \alpha x)^{-1} (1 + \sin 2\alpha x), \\
J_1(\alpha x) N_0(\alpha x) &\approx (\pi \alpha x)^{-1} (1 - \sin 2\alpha x), \quad (30)
\end{aligned}$$

for $\alpha \rightarrow \infty$, $x > 1$. Since the "non-oscillating" part of the integral is equal to

$$\begin{aligned}
& -(\pi \alpha)^{-1} \int_1^{\infty} \frac{2U_0 W_0 x/\delta + 2W_0 \delta/x}{\sqrt{x^2 - 1} (x^4 - \delta^4)^2} dx = \\
& = \frac{2J_1(\gamma) I_1(\gamma)}{\gamma S \delta^6} \left\{ -1 + \frac{1}{2\sqrt{1 - \delta^2}} + \frac{1}{2\sqrt{1 + \delta^2}} + \right. \\
& \left. - \frac{\delta^2}{4} \left[\frac{1}{2(1 - \delta^2)^{3/2}} - \frac{1}{2(1 + \delta^2)^{3/2}} \right] \right\}, \quad (31)
\end{aligned}$$

then when we apply the asymptotic calculation method to the "oscillating" part of the integral

$$\begin{aligned}
(\pi\alpha)^{-1} \int_1^\infty & \left\{ \frac{[(\delta/x)^2 + (x/\delta)^2 U_0^2 - 2U_0 - W_0^2] \cos 2\alpha x}{\sqrt{x^2 - 1} (x^4 - \delta^4)^2} + \right. \\
& \left. + \frac{[2(\delta/x) W_0 - 2(x/\delta) U_0 W_0] \sin 2\alpha x}{\sqrt{x^2 - 1} (x^4 - \delta^4)^2} \right\} dx, \quad (32)
\end{aligned}$$

and take the value $\text{Re} \{ \pi i [\frac{1}{2} \mathcal{F}_0(0) + \mathcal{F}_1'(\delta) + \mathcal{F}_2'(i\delta)] \}$ into consideration, we will finally reach a formula for relative power in the following form:

$$\begin{aligned}
\sigma_0 = & \beta^{-1} \left\{ \frac{1}{2} - \frac{J_1(\gamma) I_1(\gamma)}{\gamma S} \left(2 + \frac{1}{2\sqrt{1-\delta^2}} + \frac{1}{2\sqrt{1+\delta^2}} + \right. \right. \\
& + \frac{1}{S^2} \left[\frac{I_1^2(\gamma) [J_0^2(\gamma) + J_1^2(\gamma)]}{2\sqrt{1-\delta^2}} + \frac{J_1^2(\gamma) [I_0^2(\gamma) - I_1^2(\gamma)]}{2\sqrt{1+\delta^2}} \right] + \\
& + \frac{\delta^4}{\pi^{1/2} \alpha^{3/2} (1-\delta^4)^2} \left\{ \left[\frac{1}{2} (1+\delta^4) - \frac{2J_1(\gamma) I_1(\gamma)}{S^2} (J_0(\gamma) I_0(\gamma) + \delta^2 J_1(\gamma) I_1(\gamma)) + \right. \right. \\
& \left. \left. - \frac{\delta^2}{S} (J_1(\gamma) I_0(\gamma) - I_1(\gamma) J_0(\gamma)) \right] \cos(2\alpha + \pi/4) + \right. \\
& \left. \left. + 2 \frac{\delta}{S} \left[\delta^2 - \frac{J_1(\gamma) I_1(\gamma)}{S} (J_1(\gamma) I_0(\gamma) - I_1(\gamma) J_0(\gamma)) \right] \sin(2\alpha + \pi/4) \right\} \right\} \quad (33)
\end{aligned}$$

with the error $O(\delta^4 \alpha^{-3/2})$.

For the case of frequency of a factor which forces the plate to vibrate equal to the frequency of free vibrations, that is for

$$\delta = \delta_n, \quad \gamma = \gamma_n, \quad a_n = \frac{J_1(\gamma_n)}{J_0(\gamma_n)}, \quad S(\gamma_n) = 0 \quad (34)$$

we obtain the formula

$$\begin{aligned}
\sigma_n = \lim_{k \rightarrow k_n} \sigma_0(k) = & \frac{1}{\alpha} \frac{(1+a_n)^2}{(1-\delta_n^2)^{1/2}} + \frac{1}{2} \frac{(1-a_n)^2}{(1+\delta_n^2)^{1/2}} + \\
& \frac{2S_n^4}{\pi^{1/2} \alpha^{3/2} (1-\delta_n^4)^2} \{ (1-a_n^2 \delta_n^2) \cos(2\alpha + \pi/4) + 2a_n \delta_n \sin(2\alpha + \pi/4) \}. \quad (35)
\end{aligned}$$

identical with this published in [3].

5. Acoustic power in specific case

For $(k_0/k)^4 = (a/\gamma)^4 \ll 1$ a simplification in the formula (14) was accepted

$$\left[1 - (k_0/k)^4 \sin^4 \vartheta \right]^{-2} \approx 1. \quad (36)$$

The condition $(k_0/k)^4 \ll 1$ can also be substituted with another one, namely

$$\left(\frac{h}{2a} \right)^2 \left(\frac{\omega}{\omega_1} \right) \ll \frac{3\rho(1-\nu^2)}{E} \left(\frac{c}{\gamma_1} \right)^2, \quad (37)$$

where γ_1 is the root of the frequency equation $S(\gamma_1) = 0$, corresponding with the pulsation ω_1 , ρ is the volumetric density of the material of the plate, E – Young modulus, ν – Poissons ratio. As opposed to the inequality $(k/k_0)^4 \ll 1$ the inequality (37) contains an explicit dependence between the quantities $h/2a$, ω/ω_1 and the so-called “material constants”. Accepting $a_0 = a$, we have

$$\sigma_0 = (\alpha/\gamma)^2 \beta^{-1} \int_0^{\pi/2} \left[\frac{\gamma J_1(\alpha \sin \vartheta)}{\alpha \sin \vartheta} - \frac{\alpha}{\gamma} U_0 \sin \vartheta J_1(\alpha \sin \vartheta) + \right. \quad (38) \\ \left. - W_0 J_0(\alpha \sin \vartheta) \right]^2 \sin \vartheta d\vartheta.$$

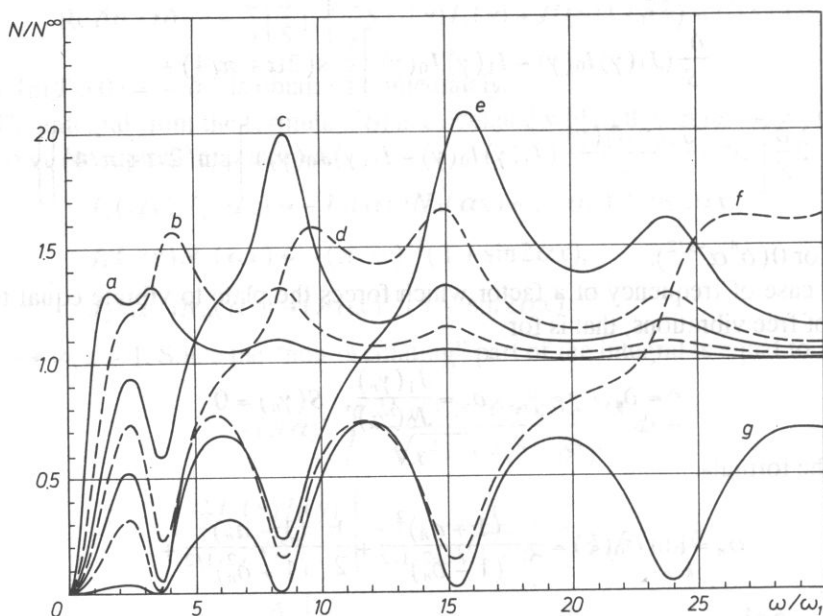


FIG. 2. Acoustic power radiated by a circular plate in terms of pulsation for different values of the parameter b_0 . $a_0/a = 1$ was accepted.

a – 0.25; b – 0.16; c – 0.12 d – 0.1;
c – 0.08; f – 0.06; g – 0.02.

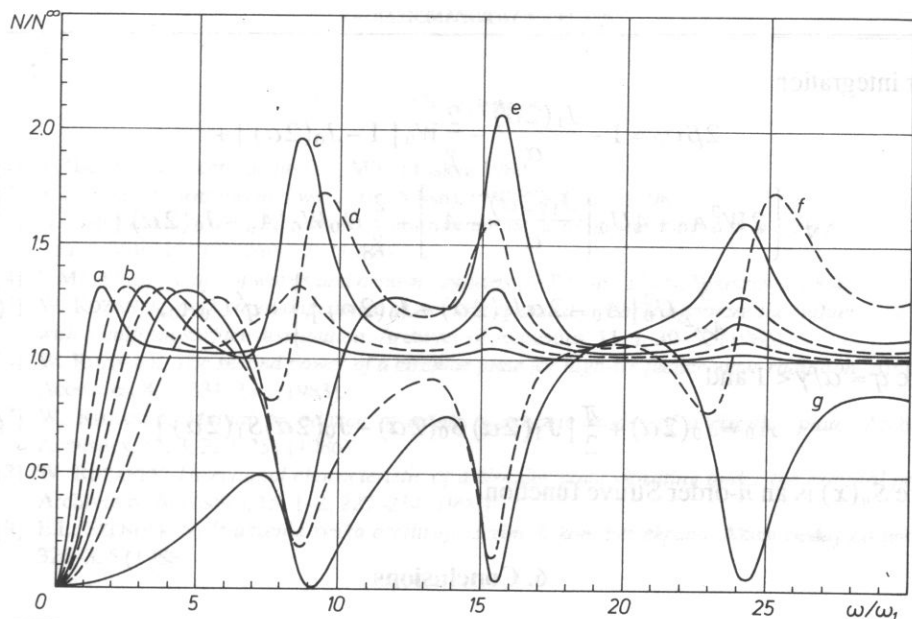


FIG. 3. Acoustic power radiated by a circular plate in terms of pulsation for different values of the parameter b_0 . $a_0/a = 0.5995$ was accepted.

a - 0.25; b - 0.16; c - 0.12; d - 0.1;
c - 0.08; f - 0.06; g - 0.02.

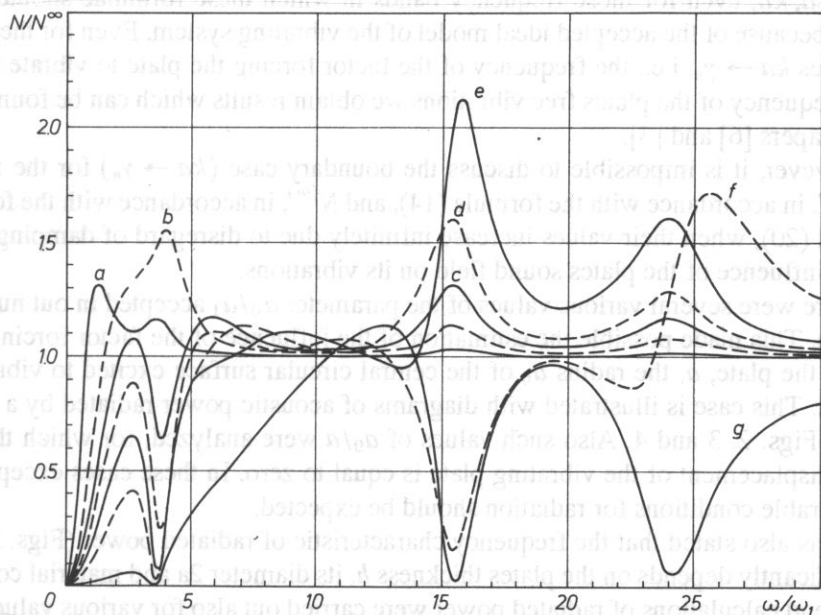


FIG. 4. Acoustic power radiated by a circular plate in terms of pulsation for different values of the parameter b_0 . $a_0/a = 0.7373$ was accepted.

a - 0.3; b - 0.16; c - 0.12; d - 0.1;
c - 0.08; f - 0.06; g - 0.02.

After integration

$$2\beta\sigma_0 = 1 - \frac{J_1(2\alpha)}{\alpha} - \frac{2}{\gamma} W_0 [1 - J_0(2\alpha)] + \\ + q^2 \left\{ 2W_0^2 A_0 + 4U_0 \left[\frac{J_1(2\alpha)}{\alpha} - A_0 \right] + \frac{2}{\gamma} U_0 W_0 [A_0 - J_0(2\alpha)] + \right. \\ \left. + \frac{3}{4\gamma^2} U_0^2 [A_0 - 2\alpha J_1(2\alpha) - J_0(2\alpha)] \right\} + q^4 U_0^2 A_0, \quad (39)$$

where $q = \alpha/\gamma < 1$ and

$$A_0 = J_0(2\alpha) + \frac{\pi}{2} [J_1(2\alpha) S_0(2\alpha) - J_0(2\alpha) S_1(2\alpha)], \quad (40)$$

where $S_n(x)$ is an n -order Struve function.

6. Conclusions

Our theoretical analysis has resulted in an expression for acoustic radiated by a circular plate, including the factor forcing the plate to vibrate.

The performed calculations indicate that the relative radiation power $N/N^{(\infty)}$, in accordance with the formulae (23) and (33), accepts finite values for all values of the parameter $k_0 a$, ka , even for those frequency bands in which these formulae should not be applied because of the accepted ideal model of the vibrating system. Even for the boundary values $ka \rightarrow \gamma_n$, i.e., the frequency of the factor forcing the plate to vibrate is equal to the frequency of the plates free vibrations we obtain results which can be found in the earlier papers [6] and [3].

However, it is impossible to discuss the boundary case ($ka \rightarrow \gamma_n$) for the radiated power N , in accordance with the formula (14), and $N^{(\infty)}$, in accordance with the formulae (18) and (20), when their values increase infinitely due to disregard of damping effects and the influence of the plates sound field on its vibrations.

There were several various values of the parameter a_0/a_1 accepted in our numerical example. This made possible the estimation of the influence of the factor forcing vibrations of the plate, a , the radius a_0 of the central circular surface excited to vibrate was changed. This case is illustrated with diagrams of acoustic power radiated by a circular plate in Figs. 2, 3 and 4. Also such values of a_0/a were analyzed, for which the volumetric displacement of the vibrating plate is equal to zero. In these cases exceptionally unfavourable conditions for radiation should be expected.

It was also stated that the frequency characteristic of radiated power (Figs. 2, 3 and 4) significantly depends on the plates thickness h , its diameter $2a$ and material constants. To this end calculations of radiated power were carried out also for various values of the following dimensionless parameter

$$b_0 = k_0 a / (ka)^2 = (h/2a) \sqrt{E/[3\rho c^2(1-\nu^2)]},$$

including the material constants, and is proportional to the quantity $h/2a$.

References

- [1] T. HAJASAKA, *Electroacoustics*, „Mir” Moskva 1982.
- [2] S. KALISKI, *Vibrations and waves* (in Polish), PWN, Warszawa 1985.
- [3] H. LEVINE and F.G. LEPPINGTON, *A note on the acoustic power output of a circular plate*, Journ. Sound. Vib., **121** (2), 269–275 (1988).
- [4] I. MALECKI, *Theory of waves and acoustic systems* (in Polish), PWN, Warszawa 1964.
- [5] W. RDZANEK, *Acoustical impedance of circular membrane vibrating under the influence of a force with a uniform surface distribution*. Archives of Acoustics, **11**, 1, 39–52 (1986).
- [6] W. RDZANEK, *The second power of a circular plate for high-frequency wave radiation*, Archives of Acoustics, **8**, 4, 331–340 (1983).
- [7] W. RDZANEK, *Mutual impedance of axially-symmetric modes of a circular plate*, Archives of Acoustics, **11**, 3, 329–251 (1986).
- [8] W. RDZANEK, *Directional characteristic of a circular plate vibrating under the external pressure*, Archives of Acoustics, **15**, 1–2, 227–234 (1990).
- [9] E.L. SZENDEROV, *Izłuczenie zvuka oscilirujuszczim diskom bez ekrana*, Akusticeskij Žurnal, **34**, 2, 326–335 (1988).

Received December 1, 1990, English version June 27, 1991

C H R O N I C L E

The 38th Open Seminar on Acoustics OSA'91 was held in Kiekrz n. Poznań on September 17th-20th 1991. The seminar was organized jointly by the Institute of Acoustics Adam Mickiewicz University, the Poznań Branch of the Polish Acoustical Society, the TONSIL Loudspeaker Factory in Września, and the Institute of Fundamental Problems of Technology at the Polish Academy of Sciences. The seminar attracted 110 participants, including 7 foreign guests. 86 papers were read on nearly all field of acoustics, i.e. acoustics of speech and music, psychoacoustics, electroacoustics, medical acoustics, environmental acoustics, solid body acoustics and molecular acoustics.

Participants of the seminar took part in a round table discussion on the latest trends in noise monitoring and measurement.

U. Joras

**4th Symposium on Sound Engineering and Mastering
Gdańsk, 17-19 June, 1991**

Six years ago, the participants of the 1st Sound Engineering Symposium in Gdańsk decided to organize similar symposia biannually. Consequently, in 1987, the Chopin's Academy of Music in Warsaw entertained the 2nd one, while in 1989, the Institute of Mechanics and Vibroacoustics of the Technical University of Mining and Metallurgy in Cracow played host to the 3rd one. Now, again in Gdańsk, the 4th Symposium closed a first periodic round of those useful meetings of musicians and engineers working on mutual interdisciplinary problems.

The debates of the 4th Symposium, held under the Patronage of the Rector of the Technical University of Gdańsk, took place there in the auditoria of the Shipbuilding Institute. The total number of presentations was 35, i.e. an introductory lecture, 23 contributed papers, and 11 laboratory demonstrations presented within a session "Practicum". The 23 papers and 10 communications have been published in the Symposium Proceedings edited and printed, partly in Polish, partly in English, by the TUG Sound Engineering Department and distributed among the participants prior to the debates. The total number of registrated participants was 90, including 3 guests from abroad; more unregistrated persons attended particular presentations, mainly during the Practicum session.

On the second day of Symposium, a special session was devoted to foundation and inauguration of activity of the Polish Section of the Audio Engineering Society. This initiative of the organizers was welcome by the participants, which results in a formal Organizatory Meeting of the Polish AES Section (see separate report).

The second day afternoon, participants were brought by bus to visit the Old City of Gdańsk, and, in particular, to see an interesting exposition of the newly opened Maritime Museum, situated within three mediaeval harbour granaries, recently rebuild beautifully after the total war destruction.

The final session completed the Symposium with a general fruitful discussion; among other conclusions the participants demanded a broadening of the didactic activities of the TUG Sound Engineering

Department in order to allow students from other universities of the Gdańsk to study that interdisciplinary important and useful domain.

Participation fee, as well as, accomodation and boarding costs for the participants could be calculated very cheap in comparison to the current prices, thanks to a grant obtained from the Ministry of Education, and to the sponsoring aid of the TUG Rector. Organizers acknowledge it with gratitude, and express thanks for that help on behalf of all Symposium participants.

Chairman of the Organisation Committee
Doc dr inż. Marianna Sankiewicz

The Polish Section of the Audio Engineering Society Organizatory Meeting in Gdańsk – 18. 6. 1991

The meeting was convoked on the second day of the Fourth Symposium on Sound Engineering and Mastering, held in Gdańsk. It was an initiative of the Symposium organizers, among which were four previously active AES members, who prepared the meeting having entered in direct contact with AES Europe Region Board.

The meeting started at noon, in the Auditorium of Ocean-technique Building at Gdańsk Technica. University. 69 persons participated in the meeting, among them Mr T. SHELTON, AES Vice-President (Europe Region). Debates were presided by DSc. A. CZYZEWSKI (Gdańsk) and Prof. M. ROLAND-MIESZKOWSKI (Halifax), both AES members.

An introduction in the aims of the meeting was given by A. CZYZEWSKI. Then, T. SHELTON informed about AES activities, as well as, about main Society laws, members duties and privileges. He presented also organisatory requirements concerning foundation of a new AES Section and the Polish Section in particular.

As all participants accepted the conditions and expressed their willingness to enter the Audio Engineering Society, so elections of the Polish Section Board became possible. The electoral part of the meeting was presided by M. ROLAND-CIESZKOWSKI, who asked for candidatures to the post of the Section Chairman. Four candidates were proposed by the participants. After secret voting and scrutiny Mrs. M. SANKIEWICZ has been elected as Chairman of the new founded Polish Section of the AES. She thanked the participants for their confidence and then she presented her proposal for a composition of the Section Board, adequate to the cope with hard organizatory tasks due to the initial period of activity. Her proposal having been accepted unanimously, the following colleagues have been elected by acclamation:

A. CZYZEWSKI (Gdańsk) – as Secretary, B. KOSTEK (Gdańsk) – as Treasurer, A. BRZOSKA (Warszawa), A. MIŚKIEWICZ (Warszawa), K. RUDNO-RUDZIŃSKI (Wrocław), J. ADAMCZYK (Kraków), E. HOJAN (Poznań), A. ŚLIWIŃSKI (Gdańsk), G. BUDZYŃSKI (Gdańsk) – as Members.

T. SHELTON congratulated the elected colleagues and wished them many organizatory successes. He expressed hope to meet Polish colleagues soon at the opportunity of the 92nd AES Convention in Vienna. He told also that the AES President R. K. FURNESS who intended to come fot this meeting, yet could not participate, will visit Polish Section at first opportunity.

M. ROLAND-CIESZKOWSKI thanked all participants for the fruitful result of the meeting. He expressed special gratitude for T. SHELTON for coming to Gdańsk and his active support to the initiators. Thus, thanks to cooperation of many people interested in audio engineering development in Poland, the Polish Section of AES as the first among the countries of the former East-European bloc has been called into existence.

Alphabetic list of the Polish AES Section founders:

J. Adamczyk, A. Brzoska, G. Budzyński, J. Cichmiński, H. Ciołkosz-Łupinowa, K. Cisowski, M. Czabajski, A. Czyżewski, A. Dobrucki, A. Dyro, M. Fengler, A. Gołaś, J. Gudel, E. Hojan, B. Iwanicka, M. Iwanowski, B. Janta-Półczyński, M. Kamińska, W. Kapczyński, W. Kasiński, P. Kleczkowski, B. Kostek, Z. Krawczyk, W. Kucharski, B. Kulesza, B. Libura, W. Makowski, M. Markuszewicz, S. Moroz, P. Mróz, B. Okoń-Makowska, T. Osiński, K. Pawlak, T. Pietrzykowski, P. Podgórski, J. Regent, A. Rehman, K. Rudno-Rudziński, D. Ruser, W. Rvszczowski, M. Sankiewicz, Z. Sobieszczański, C. Suproń, K. Szlifirski, M.

Szydłowski, M. Szyszkiewicz, A. Śliwiński, K. Środecki, A. Świdorski, M. Tajchert, J. Targoński, A. Tarka, Z. Wagner, K. Walczak, M. Waraksa, J. Waśniewski, Z. Wąsowicz, Z. Weyna, J. Wierzbicki, A. Witkowski, K. Wojtowicz, N. Wołk-Łaniewski, R. Wozniak, Z. Zając, W. Zająkała, S. Zieliński, B. Żółtogórski.

Chairman of the Polish AES Section
Doc dr inż *Marianna Sankiewicz*

[Address of the AES Polish Section Board:

Sound Engineering Department

Technical University

80-952 Gdańsk

Phones: (058) 471301 or (058) 472444]

92nd AES CONVENTION – 24–27. 03. 1992 – VIENNA

Polish AES Section Report

The Audio Engineering Society spring convention is the most important European event in the field of sound engineering and of related domains. For the first time in the history of the AES, Vienna was site of the Convention, continuing the tradition of former AES Convention sites: London, Hamburg, Montreux, Paris. In the opinion of the AES President, Mr. Roger FURNESS, a major factor in choosing Vienna for the 92nd Convention was the proximity of this city to eastern European countries. The idea which led to that choice was to bring East and West together. The decision was undertaken long before the Berlin Wall came down. Vienna was expected to be the first real opportunity for audio-engineers of the West to come together with those of the former Eastern Bloc. Exchange of information, mutual discussions and new contacts built-up in Vienna should contribute to further development and progress in the domain of audio-engineering.

The 92nd Convention was held in the modern Austria Center, Vienna, located on the left bank of the Danube, in the middle of a large island between Old Danube and New Danube rivers. The Center has a capacity for up to 9500 participants, and its fourteen large halls and auditoria are arranged with the greatest possible versatility and equipped with most advanced convention technology, including sophisticated appliance for film and video projections. Every hall has four or more booths for simultaneous translations, aided by an infrared transmission system. There are spacious exhibitions areas equipped with removable partition walls, with adjacent offices, foyers, buffets, restaurants etc.

The Center location is very convenient from a transport point of view. It is only eight minutes away from the Vienna downtown by subway, while a highway links it directly with a road network. There is a built-in car-parking facility for 1200 cars.

On the day of the Convention opening ceremony the impressive main entrance to the Austria-Center was decorated with flags of all countries whose Sections belong to the AES.

For the first time the Polish flag was there among the 24 one, as the Polish Section was founded in 1991, already after the previous European Convention. The opening ceremony took place in the Entrance Hall on Tuesday, March 24, at 9³⁰ a.m. During the ceremony an AES Fanfare was performed for the first time, composed for this occasion by the Austrian composer Rene Clemencic. The President of the AES Mr. Roger FURNESS and the Convention Chairman Mr. Ewald KERSCHBAUM opened the Convention. The program contained debates divided into 26 sessions, which, during three and half days of Convention, ran in three or sometime four parallel sections, and into three workshops, as well as, two seminar sessions.

The total number of contributed papers was 138. Authors' index contained 202 names. Those figures exceeded in about 50% the average number of the papers submitted to previous European AES Conventions. The contributions concerned almost all branches of audio-engineering: Music & Musical Acoustics; Architectural Acoustic; Audio History Presentation & Restoration; Computer Aided Audio Production; Digital Recording & Reproduction; Measurement Techniques & Instrumentation; Psychoacoustics; Digital Signal Processing; Sound Reinforcement; Additional & Special Topics; Transducers; New Techniques in Transmission. Workshops were devoted to problems of Re-Recording with optical Pick-Ups, of Tape Life – Tape

Care, and of Wireless Microphones. One seminar was on New Audio Media, while another one on the Sound of the Orchestra. That seminar consisted of an interesting lecture given by Prof. Jurgen MEYER, from PTB Braunschweig, followed by a short concert performed by the symphonic orchestra of the Technical University, Vienna, conducted partly by Prof. MEYER presenting examples to illustrate his lecture, and partly by the regular conductor Ottokar PROCHÁZKA, who ravished the audience with a typical Vienna music: Strauss' "An der schönen blauen Donau".

The AES Preprints containing texts of the contributed papers were available on the Convention opening. However, for the first time their price was not included into Convention fee.

Parallel to sessions devoted to papers presentations and discussions, exhibition activities ran in a huge area divided into stands and booths of various audio-industry enterprises, disc-producers, recording dealers, sound and vision studio technique companies, etc. Above 245 companies exhibited their most advanced products, giving opportunity to visitors to get familiar with the newest systems and techniques on the field of audio-engineering and related topics. It is impossible to report here the richness of exhibition and possibilities offered to customers. E. g. big mixing consoles automated with sophisticated computer systems including tape machines and other control room equipment were accessible to everyone who wanted to check their functioning. Technical information, publications, data, prospects, etc., were disseminated richly among interested guests. Special issues were edited daily containing actual information on subsequent Convention days. It may be added as a curiosity that only two companies from the former socialist countries were present: Czechoslovak "Tesla" from Bratislava exhibited mixing consoles, while Russian "Kunstkamera" represented a new private owned recording studio in Moscow.

Participation of Polish acousticians and sound-engineers was for the first time in the AES Conventions history so numerous: 30 members and 2 student-members were present. This was possible not only due to the proximity of Convention site but also thanks to favourable fee payment conditions offered to Polish participants. Those conditions were in advance agreed by the Polish Section Board with the AES Authorities so, that a reduced fee was payable in Polish currency. Therefore, Conference personal badges allowing free entrance to all debates and exhibition areas were distributed among Polish participants during their separate organizational meeting held on the first Convention day, in the main hall.

Three representatives of the Polish AES Section board, i.e. Mrs. M. SANKIEWICZ (Chairman), Mr. A. CZYZEWSKI (Secretary) and Mrs. B. KOSTEK (Treasurer) attended an AES European Section Committee meeting, which was held at 1 pm, on March 25, in the first floor restaurant-hall. The AES Vice-President Mr. Gerhard STEINKE, presiding over the European AES Region, welcomed all Sections representatives, especially warmly those from new founded Sections within the former Eastern-Bloc countries. He invited section chairmen to express their opinions relative to various aspects of AES activities. Among other, Mrs. SANKIEWICZ, speaking on behalf of the Polish Section, thanked the AES Authorities for their organizational assistance at Polish Section foundation; she expressed hope that one of the future AES Conventions could be organized in Gdańsk.

The most important contribution of the Polish Section to Convention debates were papers written by Polish authors or coauthors. There were four such papers, the first two read during the morning session on Music and Musical Acoustic, on March the 25:

"Acoustic Investigation of the Carillons in Poland" written by M. SANKIEWICZ, A. KACZMAREK and G. BUDZYŃSKI from Gdańsk Technical University, was presented by G. BUDZYŃSKI. Starting with the historical background of the topic, he continued with the investigations carried out recently in the laboratories of the Sound Engineering Department of the Gdańsk Technical University, on three carillons, and discussed the results.

"Computer Modelling of the Pipe Organ Valve Action" written by B. KOSTEK and A. CZYZEWSKI from Gdańsk Technical University, (Preprint No. 3266), was presented by B. KOSTEK. She introduced the audience to the topic of the pipe organ control systems. She described a pipe organ instrument, built recently in Bielsko-Biała (Southern Poland), she explained functions of its computer control system, and presented new hardware solutions applied to the system design, as well as appropriate experiments carried out. The paper aroused a vivid interest among several organ builders participating in that session.

The third paper of that session: "Isolation of Rhythmic Patterns in Musical Signals" by G. KALLIRIS and

G. PAPANIKOLAOU from the University of Thessaloniki (Preprint No. 3267), read by G. KALLIRIS and presented by both authors, was especially interesting to Polish participants, as an opportunity to meet their Greek coworkers and to discuss common problems of interest for both parties. This meeting was agreed in advance among partners of the scientific cooperation on the field of acoustics and sound engineering, carried on by the Gdańsk Technical University, by the Aristotle University of Thessaloniki, Greece, by the Aalborg University, Denmark, and the Dalhousie University in Halifax, Canada.

The next Polish paper was read during the afternoon session on Architectural Acoustics, on March the 26. The paper entitled "Signal Simulation Based on Convolution of Room Impulse Response" (Preprint No. 33287), written by A. GOŁAŚ, H. ŁOPACZ and H. WIERZBICKI from the Academy of Mining and Metallurgy, Cracow, was presented by A. GOŁAŚ. He described a theoretical approach to predicting sound signal transmission through various rooms and gave some results of experimental applications.

The fourth paper was read during the session on Psychoacoustics, on the last Convention day, the 27. The paper resulted of the above mentioned cooperation, under the title: "Investigation of the Loud-Music-Exposure Hearing Loss" (Preprint No. 3312), was written by G. WHITEHEAD and M. ROLAND-MIESZKOWSKI, from the Dalhousie University, by G. PAPANIKOLAOU from the Aristotle University of Thessaloniki and by G. BUDZYŃSKI from Gdańsk Technical University, who presented the paper. The described facts of aggravating hearing loss in young people due to listening too loud music were alarming to session participants. As they concluded that organization of preventive action was necessary and urgent, so a discussion started on possible ways of introducing it in practice.

Several other papers read during the Convention debates are worth to be mentioned. First of all, papers written by our Danish colleagues from Aalborg University and from Perceptive Acoustics A/S Aalborg. The first one "Head-Related Transfer Functions: Measurements on 24 Human Subjects" by D. HAMMERSHØJ, H. MØLLER, M. SØRENSEN, K. LARSEN (Preprint No. 3289), and the second one "Transfer Characteristics of the Headphones" by H. MØLLER, D. HAMMERSHØJ, C. JENSEN, J. HUNDENBØLL (Preprint No. 3290). Both papers were devoted to the perpetual difficulties in proper sound reproduction due to inherent differences of speaker- vs. headphone-systems.

A numerous audience and a vivid interest was evoked among participants by Mr. W. WOSZCZYK with his paper entitled "Microphone Arrays Optimized for Musik Recording" (Preprint No. 3255). After a prolonged discussion and many questions addressed to the lecturer in the hall, it was a great pleasure for Polish participants to meet Mr. WOSZCZYK separately and have with him a nice chat in Polish. He graduated in the sixties in Warsaw Technical University in electroacoustics and went to America. There he made his degree and a brilliant career in audio engineering in Canada, where he is with the McGill University, Montreal. Recently Mr. WOSZCZYK was elected AES Governor and Chairman of the AES Membership Committee. The Polish AES Section hopes to have many future contacts with Mr. Woszczyk.

Another item of the Polish Section activity may be quoted here. A mini-exhibition of latest issues of the "Archives of Acoustics", offered by its Editors, was arranged on a Convention press stand, in order to promote the Polish quarterly among acousticians of the world.

To complete this report a few sentences ought to be devoted to many events accompanying the Convention. Awards were handed for those who made valuable contribution to the AES, during an evening reception at the Palais Ferstel in Vienna, on March the 25. The Awards presentation was preceded by a short concert of the Vienna Boys Choir. The evening continued with dinner, wine and Vienna style music.

Several Technical Tours were organized for Convention participants. The Tours were aimed to visit interesting institutions and industrial plants in Vienna, as e.g.: the Austrian Broadcasting Corporation TV-Centre, the Siemens factory, the AKG factory, Bösendorfer piano manufacture, Vienna State Opera, Wiener Musikvereinsaal, etc.

A rich social programme with many guided tours was also organized. It is, however, obvious that all those accompanying events were almost inaccessible for those who wanted to attend as many sessions as possible and to visit numerous interesting stands at the exhibitions. Seeing so much within three days is an exhausting task, especially for visitors coming from Poland mostly by car, and accommodated far away from the Austria-Center, because of obvious economic reasons.

Nevertheless, for all Polish participants the Convention was a successful experience. It was also an

organizational achievement of the young Polish AES Section. As Berlin was decided for the next AES Convention site, so the Polish Section would like repeat such experience in Spring 1993.

Chairman of the Polish AES Section
Doc dr inż Marianna Sankiewicz

NOISE-93

THE INTERNATIONAL NOISE AND VIBRATION CONTROL CONFERENCE will be held in St. Petersburg, Russia on May 31 – June 3, 1993.

Two hundred word abstracts should be submitted to: Malcolm J. Crocker, Co-chairman NOISE-93, Mechanical Engineering Department, 202 Ross Hall, Auburn University, AL 36849-5341, USA or Fax 205-844-3307 by October 31, 1992 at the latest. Final manuscripts are due by November 30, 1992.

NOISE-93 is being organized by the St. Petersburg Mechanics Institute in cooperation with the Acoustical Society of the Russian Federation, the Acoustical Society of America and similar societies or institutes in Brazil, China, Finland, Germany, India, Italy, Japan, the Netherlands and the United Kingdom.

The co-chairs of NOISE-93 are Professors Nickolai I. Ivanov (St. Petersburg, Russia) and Malcolm J. Crocker (Auburn, AL, USA).

Papers may be presented in English or Russian. There will be simultaneous translation. Books of Proceedings will be available also in both languages at the Conference and the written papers will be translated by the organizers. There will be a parallel cultural program involving visits in Hermitage, palaces and ballet, or other similar events.

A total of about 500 participants are expected, including 300 from Russia and 200 from 30 other countries.

The registration fee for the Conference is \$290.00 which includes the Books of Proceedings, a reception, and 3 cultural events. Meals for 4 days can be purchased for an additional sum of \$120.00.

For further information contact Dr. Malcolm J. Crocker, Co-chairman NOISE-93, Mechanical Engineering Department, 202 Ross Hall, Auburn University, AL 36849-5341, USA (Tel.: 205-844-3301 or Fax: 205-844-3307).